UCRL-19060

cy. 2

RECEIVED
LAWRENCE
RADIATION LABORATORY

OCT 29 1969

LIBRARY AND
DOCUMENTS SECTION

ENHANCEMENT OF DUCTILITY IN HIGH STRENGTH STEELS

Dieter Fahr

(Ph. D. Thesis)

September 1969

AEC Contract No. W-7405-eng-48

TWO-WEEK LOAN COPY

This is a Library Circulating Copy
which may be borrowed for two weeks.
For a personal retention copy, call
Tech. Info. Division, Ext. 5545

LAWRENCE RADIATION LABORATORY
UNIVERSITY of CALIFORNIA BERKELEY

UCRL-19060
cy. 2

DISCLAIMER

This document was prepared as an account of work sponsored by the United States Government. While this document is believed to contain correct information, neither the United States Government nor any agency thereof, nor the Regents of the University of California, nor any of their employees, makes any warranty, express or implied, or assumes any legal responsibility for the accuracy, completeness, or usefulness of any information, apparatus, product, or process disclosed, or represents that its use would not infringe privately owned rights. Reference herein to any specific commercial product, process, or service by its trade name, trademark, manufacturer, or otherwise, does not necessarily constitute or imply its endorsement, recommendation, or favoring by the United States Government or any agency thereof, or the Regents of the University of California. The views and opinions of authors expressed herein do not necessarily state or reflect those of the United States Government or any agency thereof or the Regents of the University of California.

UNIVERSITY OF CALIFORNIA

Lawrence Radiation Laboratory
Berkeley, California

March 16, 1970

ERRATA

To: All recipients of UCRL-19060

From: Technical Information Division

Subject: UCRL-19060, "Enhancement of Ductility in High Strength Steels" (Ph. D. thesis) Dieter Fahr, IMRD and College of Engineering, September 1969

Please make the following corrections to subject report.

In Fig. 28 caption the (a) and (b) should read:

(a) Tempered for 80 minutes at 450°C; ×250

(b) No additional tempering; 250×

Fig. 30 caption should read:

(a) 80% reduction in thickness; ×70

(b) 60% reduction in thickness; ×70

(c) 40% reduction in thickness; ×70

(d) 20% reduction in thickness; ×70

TABLE OF CONTENTS

ABSTRACT v

I. INTRODUCTION 1

II. EXPERIMENTAL PROCEDURE 7

A. Material Preparation 7

B. Mechanical Testing 8

C. Magnetic Testing 9

D. Optical Microscopy 9

III. EXPERIMENTAL RESULTS AND DISCUSSION 10

A. The Effects of Varying Mn and C Contents on the Tensile Properties of a Metastable Austenitic Stainless Steel After 80% Reduction in Thickness at 450°C. 10

1. Variation of C Contents at Given Mn Contents 10

a. Room Temperature Tests 10

i. Alloys Containing 1% Mn 10

ii. Alloys Containing 2% Mn 13

iii. Alloys Containing 3% Mn 15

b. Dry Ice Tests 17

i. Alloys Containing 1% Mn 17

ii. Alloys Containing 2% Mn 18

iii. Alloys Containing 3% Mn 21

2. Variation of Mn Contents at Given C Contents 23

a. Room Temperature Tests 23

i. Alloys Containing 0.2% C 23

ii. Alloys Containing 0.4% C 24

iii. Alloys Containing 0.5% C 25

b. Dry Ice Tests 25

i. Alloys Containing 0.2% C 25

ii. Alloys Containing 0.4% C 25

iii. Alloys Containing 0.5% C 26

B. The Effects of Varying Reductions in Thickness at 450°C on the Tensile Properties of a Metastable Austenitic Stainless Steel 27

1. Alloys With 2% Mn and C Contents Varying From 0 to 0.5% 27

a. Room Temperature Tests 27

b. Dry Ice Tests 38

2. Alloys With 1% Mn and C Contents Varying From 0.2 to 0.5% 44

a. Room Temperature Tests 44

b. Dry Ice Tests 47

3. Alloys With 3% Mn and C Contents Varying From 0.2 to 0.5% 50

a. Room Temperature Tests 50

b. Dry Ice Tests 56

C. The Effects of 80% Reduction in Thickness at Varying Rolling Temperatures on the Tensile Properties of a Metastable Austenitic Stainless Steel 59

1. Alloys With 2% Mn and C Contents Varying From 0 to 0.5% 59

a. Room Temperature Tests 59

b. Dry Ice Tests 65

2. Alloys With 1% Mn and C Contents Varying From 0.2 to 0.5% 68

a. Room Temperature Tests 68

b. Dry Ice Tests 70

3. Alloys With 3% Mn and C Contents Varying From 0.2 to 0.5% 71

a. Room Temperature Tests 71

b. Dry Ice Tests 73

D. The Effects of Test Temperature Variations Between RT and -196°C on the Yield Strength of a Metastable Austenitic Stainless Steel 75

1. Alloys With 2% Mn and C Contents Varying From 0.2 to 0.5% 75

2. Alloys With 0.2% C and Mn Contents Varying From 1 to 3% 77

E. The Effects of Alloy Composition 78

F. Stress-Induced Formation of Martensite 80

G. Optical Microscopy 81

IV. SUMMARY AND CONCLUSIONS 84

ACKNOWLEDGEMENTS 91

REFERENCES 92

TABLES 95

FIGURE CAPTIONS 112

FIGURES 121

ENHANCEMENT OF DUCTILITY IN HIGH-STRENGTH STEELS

Dieter Fahr

Inorganic Materials Research Division, Lawrence Radiation Laboratory,
Department of Materials Science and Engineering, College of Engineering,
University of California, Berkeley, California

ABSTRACT

The conditions under which high strength and high ductility can be attained were studied in metastable austenitic steels. The stability of the austenite was shown to be the most important variable. It affected the tensile properties through the isothermal formation of martensite induced by elastic stresses and/or plastic strain. The results from 14 different alloys showed that low austenite stability resulted in high work hardening rates, high tensile strengths and low elongation values. Low austenite stability also caused the yield strength to decrease due to the stress induced formation of martensite. When the austenite was very stable, plastic deformation was initiated by slip and its work hardening rate was too low to prevent necking at small strains. A specific amount of strain induced martensite led to an "optimum" work hardening rate, resulting in maximum elongation. The effects of varying C and Mn contents, different test and rolling temperatures, rolling time and various reductions in thickness on the austenite stability were investigated. The amount of plastic deformation at a temperature at which no phase transformation can be induced, i.e. above the M_d temperature, had a negligible effect on the yield strength when the austenite was very unstable, its effect increased, however, as the austenite stability increased. The best combination of strength and ductility was attained when the austenite was stable enough for slip to initiate yielding but still sufficiently unstable so that

martensite could form during straining. To meet these requirements the alloy composition had to be such that the test temperature was between the M_s and the M_d temperatures, and processing of the steel had to be carried out close to or above M_d. Yield strengths exceeding 200,000 psi and elongation values approaching 40% were measured for a number of the alloys.

Serrations appeared in the stress strain curves when slip and the formation of martensite competed with one another as modes of deformation. No serrations were observed when one or the other mode predominated.

I. INTRODUCTION

The demand for high strength structural materials has led to the development of steels with strengths exceeding 400,000 psi. The usefulness of such ultra high strength steels is, however, severely limited by their low ductility. A certain degree of ductility is essential to alleviate local stress concentrations and thus to prevent catastrophic failure.

Efforts to improve the strength and toughness of steel have traditionally centered on modifications in composition or heat treatment. In recent years there has been considerable interest in thermomechanical treatments as a means of improving properties. Thermomechanical treatments can be defined as treatments involving plastic deformation during the heat-treating cycle in such a way as to modify the normal processes that occur during heat treatment, and thereby to obtain improved mechanical properties. There are several types of thermomechanical treatment, depending on where in the heat treating cycle the plastic deformation is introduced and on what the subsequent treatment is.

Kula (1) classified thermomechanical treatments according to the position of the deformation in the heat treatment cycle, i.e. the microstructure that is deformed, and the final microstructure that is formed:

Class I. Deformation <u>before</u> austenite transformation: Formation of martensite in strain-hardened austenite upon subsequent cooling.

This thermomechanical treatment was initially described by Harvey (2) and Lips and Van Zuilen (3), and led to the so-called ausforming steels. The austenite is deformed below the recrystallization temperature and above the M_d-temperature in the unstable austenite range, usually in the bay region between the pearlite and bainite noses of the TTT-diagram,

and then quenched to below M_s to transform to martensite.

M_s is defined as the temperature at which martensite starts forming spontaneously on cooling, while M_d is the temperature above which no martensitic transformation can be induced by plastic deformation.

Class II. Deformation <u>during</u> austenite transformation: Formation of martensite during deformation of metastable austenite.

This treatment is generally carried out at temperatures in the vicinity of M_s so that austenite transforms to martensite during deformation. Most frequently this is done on stainless steels which have M_s-temperatures below room temperature. The portion of the austenite that transforms depends on the temperature of deformation and the amount of straining. Various combinations of strength and ductility or toughness can be obtained (4-7).

Class III. Deformation <u>after</u> austenite transformation: Strain-hardening of austenite transformation products.

Within this broad class are treatments ranging from strain-aging of mild steel to the production of high-strength steel wire by patenting. The structures that are deformed may be pearlite, bainite, and tempered or untempered martensite. Deformation may be carried out at room temperature or at elevated temperatures and may or may not be followed by a reaging treatment (8).

A good combination of strength and ductility can be attained without plastic deformation in carbonless high nickel alloy steels (9). These so-called maraging steels derive their strength from very fine intermetallic precipitates that form upon aging of the Fe-Ni martensite.

It should be pointed out that all the above treatments require a martensitic transformation in order to produce high yield strengths in

the respective alloys.

Since plastic flow occurs by dislocation movement, obstacles to the motion or generation of dislocations, such as elements in solid solution, interface boundaries, precipitate particles, or the stress fields of other dislocations, will increase the strength. On the other hand, high ductility is obtained when dislocations can move freely.

In spite of these two opposing effects it has been observed that high strength steels are generally not inherently brittle, but that the low ductility is due to a local plastic instability caused by the inability of the material to work harden during a tensile test at a high enough rate to compensate for the increase in stress due to a reduction in cross sectional area.

The rate of work hardening is a function of dislocations interacting with each other and with other obstacles to their motion, such as precipitate particles.

The number of precipitates and other obstacles except dislocations does not change during a tensile test, and thus there is essentially no mechanism to increase the strain hardening drastically if a sudden increase in stress occurs due to necking. In high strength steels, the dislocation density is usually high and additional plastic flow does not add substantially to the density.

Within the past few years attempts have been made to increase the work hardening rate of high strength steels in order to prevent early failure of the tensile specimens at the site of incipient necking. One answer to this problem was to utilize a phase transformation. Such a phase transformation has to satisfy two requirements. First, the transformation product has to be stronger than the phase from which it forms

and, secondly, the formation of the new phase must occur during straining. The martensitic transformation in iron carbon alloys can be made to satisfy these requirements as recent studies (10) have shown. The result is greatly enhanced elongation.

The thermomechanical treatment applied is very similar to that used in the ausforming process. However, it does not involve a transformation to martensite during subsequent cooling.

The chemical composition must be adjusted in such a way that the testing or operating temperature lies between the M_s- and M_d-temperatures of the processed alloy. Since the alloys are austenitic at room temperature, the initial high yield strength (e.g. 200,000 psi) must be obtained by work hardening (80 to 90% reduction). The rolling has to be carried out at a temperature high enough for precipitation to occur but sufficiently low for an adequate increase in dislocation density. Moreover, the rolling temperature should lie above M_d and 450°C offers the best compromise for most steels in this class.

The strain induced martensite transformation has been recognized and studied by numerous investigators. Particularly relevant to the present study are two recent papers. Banerjee, Capenos and Hauser (11) were among the first to recognize the role of the transformation in delaying necking. Bressanelli and Moskowitz (12) made a comprehensive study of the individual and combined effects of composition, test temperature, and deformation rate on the tensile properties of metastable austenitic stainless steel. They clearly demonstrated the favorable effect strain induced martensite can have on the tensile elongation. Composition and test temperature directly affect the amount of martensite that forms during the test, whereas the deformation rate plays an indirect

role by influencing the specimen temperature.

The present work represents part of an effort to design alloys with high strength and good ducility. Since the mechanical properties of metastable steels depend very sensitively on the rate of martensite formation, there is a testing temperature at which optimum results can be obtained. The problem of the alloy designer is, therfore, to compose an alloy that will yield optimum mechanical properties in a temperature range in which the performance of the steel is most crucial.

Since Mn and C affect the M_s and M_d temperatures very strongly, 14 alloys with varying C and Mn contents were chosen. They were designed to improve the ductility in the temperature range between 24°C and -78°C. Variations in reduction in thickness as well as changes in rolling temperatures were investigated. The specimens were tested at four different temperatures between 100°C and -196°C.

It will be shown that the austenite stability is the most important factor which affects the yield strength, tensile strength, work hardening rate and elongation. The stability of the austenite, as predetermined by the chemical composition, is strongly influenced by the test and rolling temperatures, the rolling time and the reduction in thickness. Moreover, it will be shown that prolonged tempering can lead to interesting changes in work hardening rate.

Optimizing strength and ductility imposes strict restraints on the austenite stability. Not only does martensite form because of plastic straining, but it can also be induced to form by elastic stresses at temperatures above M_s (13). The effects of stress induced formation of martensite on the yield strength will be discussed. This investigation will also show that an increase in strain hardening rate as a result of

the formation of martensite increases tensile elongation only up to a certain optimum and then, when more martensite forms, ductility decreases.

Stress strain curves obtained in RT and dry ice tests will be discussed in detail.

Serrated stress strain curves in metastable austenitic stainless steels are definitely associated with the formation of martensite (12,14). Other investigators (15-17) have observed serrations in Armco iron, carbon steels, tin bronze and aluminum alloys, which formed as a result of dislocation-interstitial solute interactions (Cottrell atmosphere formation and Snock-Schoeck-Seeger stress induced ordering of interstitials).

Sometimes martensite formation does not cause serrations, and so an explanation of the different behaviors is offered.

Depending on the alloy composition and the conditions imposed during the test, martensite formation and austenite deformation can both be operative.

II. EXPERIMENTAL PROCEDURE

A. Material Preparation

The alloys (Table XVII) were prepared by induction melting "medium high purity" (99.9%) elements in an argon atmosphere and pouring the liquid into a water cooled copper mold. The resulting 20 lb ingots were then homogenized for 3 days at 1050°C and forged at 1100°C to 2.5" × 0.5" cross-section in order to break up the cast structure. The material was then further reduced to a thickness of 0.250" by rolling at 450°C (to avoid formation of martensite). This was followed by an austenitizing treatment of one hour at 1200°C in a helium atmosphere (to prevent decarburization of the surface).

The 0.250" thick samples to be reduced 80% to a final specimen thickness of 0.050" were, thus, ready for the selected thermomechanical treatments. For a final reduction in thickness of 60, 40 and 20%, respectively, the 0.250" thick material had to be reduced further (at 450°C) to the respective thicknesses of 0.125", 0.0833", and 0.0625". This was followed by another austenitizing treatment of one hour at 1200°C. The austenitic samples were then reduced 20, 40, 60 and 80% at 450°C and 80% at 250°C, 100°C and RT. Deformation was effected by rolling (heated rolls) and reheating the samples in an electric furnace between the passes. The samples rolled at RT (cold rolls) were water cooled between the passes.

450°C proved to be the optimum rolling temperature: at higher temperatures the final strength decreases rapidly; precipitation takes place at too low a rate at lower temperatures. Rolling at 250°C, 100°C, and RT results in varying amounts of martensite being formed during rolling.

80% reduction in thickness required between 1 and 2 hours, depending on whether the specimen remained austenitic or became martensitic. After rolling, the sheets were air cooled and then sand blasted to clean the surface.

B. Mechanical Testing

Samples were cut from the 0.050" thick sheets and ground to a rectangular shape (9/16" × 2-3/4") with a (46 grit) wheel. The tensile specimens were then ground with a finer (60 grit) wheel which determined the gage length (1") and the gage radius (1/8") (Fig. 1). The down feed was 0.001" per pass. Deionized cooling water with a rust preventing additive was used. The holes were drilled with a carbide drill.

Tensile tests were then carried out at four different temperatures on an Instron testing machine using a cross head speed of 0.04 in./min.

The RT tests were performed in air. For tests at 100°C, boiling distilled water heated by an immersion coil was used. Tests at -78 and -196°C were performed in a bath of dry ice in ethanol and in a liquid nitrogen bath, respectively. The engineering stress was calculated from the load-extension recording of the testing machine using the original cross section area. Gage marks allowed measuring the elongation of the fractured specimen under a travelling microscope with an accuracy of ±0.004 in. The fact that the two portions of the broken specimen cannot be rejoined completely was taken into account. The respective strain values were calculated from the load-extension graph dividing the final elongation value by the extension due to plastic deformation alone.

C. Magnetic Testing

The saturation induction of some specimens was measured in a "permeameter" to determine the relative increase of the amount of martensite due to quenching to sub-zero test temperatures. The equipment used has been described elsewhere (18). The transformation during processing had been qualitatively observed by means of a strong hand magnet. It was assumed that specimens which were non-magnetic were entirely austenitic. The highest amount of martensite as determined with the above equipment was approximately 50%; these 50% martensite specimens were strongly magnetic.

D. Optical Microscopy

The specimens were electropolished in a solution of 90% acetic and 10% perchloric acid at 0°C (20 volts). A solution of 5.0 gm cupric chloride, 100 ml hydrochloric acid, 100 ml methyl alcohol, and 100 ml distilled water was used for etching. (Mechanical polishing should be avoided since it can nucleate martensite.) A Carl Zeiss Optical Microscope was used for observation and photography.

III. EXPERIMENTAL RESULTS AND DISCUSSION

A. The Effects of Varying Mn and C Contents on the Tensile Properties of a Metastable Austenitic Stainless Steel After 80% Reduction in Thickness at 450°C

In a metastable austenitic steel of following composition: 9 Cr, 8 Ni, X Mn, Y C, balance Fe, the manganese content was varied from 1 to 3% while the carbon content increased from 0. to 0.5%. The alloys were tested at four different temperatures: room temperature, -78°C, -196°C, and 100°C.

1. Variation of C Contents at Given Mn Contents

a) Room Temperature Tests

i. Alloys Containing 1% Mn . Figure 2a shows engineering stress-strain curves of alloys with following carbon contents: 0.2, 0.3, 0.4 and 0.5%. Carbon and manganese are the most potent of the elements in suppressing the M_s, and, thus, the M_d temperature. However, 1% Mn and 0.2% C are too little to prevent the transformation from austenite to martensite as a result of cooling from the austenitizing temperature (1200°C) to room temperature (M_s > RT). The alloy was already partly martensitic before the final thermomechanical treatment. The stress-strain curve of this alloy, therefore, was markedly different from the curves of the alloys with higher carbon contents. There was no yield point or Luder's strain. Comparison with the 100°C tests (Table VII) shows that the measured yield strength did not represent the yield strength of the original matrix (~50% martensite, ~50% austenite), but rather it represents the onsets of a stress-induced transformation of the retained austenite to martensite. Serrations in the stress-strain curve, which are usually associated with a strain-induced phase transformation, were not observed.

With 0.3% C the critical temperature was lowered so much that the alloy remained austenitic after cooling from 1200°C to RT (M_s < RT). Plastic deformation again began with the stress-induced formation of martensite (Fig. 3a and 3d, Table VIII). Serrations which appeared in the Luder's strain portion of the stress strain curve indicated that the phase transformation was also assisted by strain. The "yield strength" of this (0.3% C) alloy was lower than for the previous one (0.2% C), as was expected, because the alloy was essentially austenitic, whereas the alloy containing 0.2% C was partly (~50%) martensitic.

With 0.4% C the austenite was even more stable, and the alloy remained austenitic after processing. Plastic deformation was again initiated by the stress-induced formation of martensite (Fig. 3a and 3d). Many serrations and only a small increase in stress seemed to indicate that strain also plays an important role in the formation of martensite in the Luder's strain portion of the stress-strain curve. The following steeper portion of the stress-strain curve was very smooth (no serrations) and, since martensite continued to form in this region (18), and the stress increases rapidly per unit strain, it can be assumed that the martensite formed in this region was stress induced. The association of a smooth curve with a stress-induced phase transformation, compared to a serrated curve for a strain-induced phase transformation, seems to be justifiable on the basis of following facts: the onset of plastic deformation which is definitely due to a stress-induced formation of martensite, always results in a very smooth deviation from the straight line of the elastic portion of the stress-strain curve; no serrations whatsoever were observed -- the smooth portion of the curves were always where the stress increase per unit strain was greatest. On the other hand,

the curve is serrated where there is hardly any stress increase with increasing strain. The stress-strain curve of the alloy containing 0.4% C (Table IX) demonstrates this very nicely. Plastic deformation started with the stress induced formation of martensite, then in the Luder's strain portion, slip in the austenite was mainly - if not entirely - responsible for the phase transformation. Thereafter martensite formed as the stress increased and, finally, in the almost horizontal last portion of the stress-strain curve, serrations appeared again. There was almost no stress increase in this region, hence it can be assumed that this last formation of martensite was mainly strain-induced. The importance of the strain lies in the fact that on plastic straining of the material, peaks of stress above the average stress occur. These locally higher stresses can form critical martensite nuclei, and thus induce the phase transformation.

A typical and very steep portion of the stress-strain curve at the end of the Luder's strain seems to represent the transition from mainly strain-induced to predominately stress-induced formation of martensite. The stress-strain curve is very steep immediately beyond the Luder's strain. Hence the deformation is primarily elastic during this very short steep portion. Plastic deformation then appears to set in as a result of the stress induced formation of martensite, and not as a result of slip in the austenite. During the deformation and transformation within the Luder's strain portion, the easy nucleation sites are exhausted and the remaining austenite becomes more stable (mechanical stabilization). Then, as soon as a certain critical stress is reached again, the stress induced formation of martensite sets in, resulting in a marked change of slope of the curve.

The short but very steep portion of the stress-strain curve reappears in many other stress-strain curves where there is a clearly definably Luder's strain.

The "yield strength" is higher in the 0.4% C steel than in the 0.3% C alloy. This is attributed to the higher carbon content. Also, the amount of Luder's strain seemed to increase with increasing carbon content. Moreover, the work-hardening rate at higher carbon contents (0.4% C compared to 0.3% C) was lower. This can be explained by the greater stability of the austenite as a result of a higher carbon content; less martensite formed per unit strain than in the less stable austenite. More austenite remained to be transformed and necking was therefore suppressed until a later stage during the test. The high elongation value (more than twice as high as in the 0.3% C alloy) seemed to indicate this.

With 0.5% C the austenite was stabilized so much that the alloy was completely austenitic after processing. The austenite stability was high enough to prevent a stress induced phase transformation and the measured yield strength represented the yield strength of the austenite (Table X). Some initial strain seemed to be required before the strain-induced phase transformation could take place in this alloy. The amount of martensite formed, however, was too small to prevent necking, and early failure of the specimen occurred. The yield strength was higher than in all the other alloys because of the higher carbon content. An increase of 0.1% C resulted in an increase in yield strength of approximately 20,000 psi.

ii. <u>Alloys Containing 2% Mn.</u> Stress-strain curves of alloys with the following carbon contents are shown in Fig. 2b: 0, 0.1, 0.2, 0.3,

0.4 and 0.5% C.

The alloy containing 0% C (Table I) was ferritic at room temperature and had a stress-strain curve that was markedly different from the stress strain curves of the alloys containing carbon. Its yield strength was higher than the "yield strengths" of the alloys containing 0.1 through 0.4% C.

With 0.1% C partial transformation to martensite occurred on cooling from 1200°C to RT ($M_f < RT < M_s$). The retained austenite was very unstable and transformed readily when deformed (Table II). This high degree of instability of the austenite resulted in a low "yield strength" (onset of transformation) and a high work hardening rate.

With 0.2% C the stability of the austenite increased, and the M_s and M_d temperatures were suppressed to below RT and 450°C, respectively. The alloy was completely austenitic after processing. At RT, however, stress induced formation of martensite initiated plastic deformation (Table III). The higher carbon content resulted in a higher "yield point" as compared with the 0.1% C alloy (higher stability of the austenite). Since the work hardening rate during the RT-test depended on the amount of martensite formed per unit strain, it was expected that higher carbon contents, with their stabilizing effect on the austenite, would result in lower strain hardening rates. This was found to be true for the alloys with 0.2, 0.3, 0.4 and 0.5% C.

As the carbon content increased, the "yield points" and Luder's strains increased and the work hardening rates decreased.

With 0.5% C the formation of stress induced martensite was prevented (Table VI) and the resulting yield strength was the normal yield strength of the austenite. Although the M_d temperature was still above RT, the

highly stabilized austenite did not allow a sufficient amount of martensite to form to prevent necking at this stress level (~230,000 psi). Some martensite formed, as was verified by magnetic measurements, and as indicated by the horizontal portion of the stress-strain curve (Fig. 2b).

Stress-induced martensite formation initiated plastic deformation in the alloys containing 0.1, 0.2, 0.3 and 0.4% C (Tables II, III, IV and V). This is shown clearly in Figs. 4a and 4d. At higher carbon contents only strain induced martensite formed, but not at a sufficiently high rate to improve ductility. It seems that a certain minimum amount of strain must be sustained by the austenite itself before a significant amount of strain-induced martensite can form.

iii. Alloys Containing 3% Mn. In Fig. 2c the stress-strain curves of alloys with 0.2, 0.3, 0.4 and 0.5% C are shown. The stabilizing effect of Mn on the austenite is clearly evident. The alloy containing 0.2% C was essentially austenitic after processing and was the only one in which plastic deformation was initiated by a stress-induced formation of martensite, (Figs. 5a and 5d, Table XI). This is evidenced in the stress-strain curves. The alloys having higher carbon contents exhibited similar yield points and the difference between upper and lower yield points ranged between 8000 and 10,000 psi, whereas in the 0.2% C alloy the difference amounted to only 4000 psi and the "yield point," as such, has a different appearance. Moreover, the difference in yield strength between the 0.2 and 0.3% C alloys was as large as between the 0.3 and 0.5% C alloys (30,000 psi), indicating that stress-induced formation of martensite results in lowering the "yield strength" of the 0.2% C alloy.

The work hardening rate was relatively low and thus it was not surprising that many serrations appeared in the portion of the stress-

strain curve following the Luder's strain. This seemed to indicate that the formation of martensite in that portion of the stress-strain curve was at least partly strain induced. Once more it can be seen that the Luder's strain portion of the stress-strain curve was followed by a very steep but short portion, which was referred to earlier as a region where little plastic deformation took place. In the subsequent smooth portion the formation of martensite was stress induced. As the slope changed, serrations appeared which were due mainly to strain induced bursts of transformation. Figures 5a and 5d show that there is no stress-induced formation of martensite initiating plastic deformation for alloys containing more than 0.2% C (Tables XII, XIII, and XIV).

With 0.3% C the M_s and M_d temperatures were lowered below RT and 450°C, respectively, so that the alloy was completely austenitic after processing. The work hardening rate was higher than that of the austenite, resulting in a very high elongation value. Enough austenite was retained at large strains to transform to martensite at such a rate that necking was prevented.

With 0.4% C the critical temperatures were suppressed even more. Although the M_d was still above RT, the rate of martensite formation was decreased to the point where necking could not be prevented beyond a certain strain (still within the Luder's strain).

With 0.5% C the M_d temperature was lowered to approximately RT, with the result that the specimen failed at the site of incipient necking. The work hardening rate of the austenite per se was too low at this stress level (~230,000 psi) to compensate for any localized increase in stress due to necking.

b. Dry Ice Tests

i. Alloys Containing 1% Mn. Lowering the test temperature to -78°C decreased the stability of the austenite with respect to its transformation to martensite even more. As Figs. 3b and 3d show, the onset of yielding occurred at even lower stress levels than at 100°C and RT. The difference in "yield strength" between RT and -78°C is clearly visible in Fig. 3c, and it can be seen that in all four alloys (0.2, 0.3, 0.4 and 0.5% C) plastic deformation started when stress-induced martensite formed. The amount of martensite formed per unit strain was much larger, and thus the strain hardening rate was increased drastically (Fig. 2d). A negligible amount of martensite formed while cooling the specimens from room temperature to -78°C (an increase in saturation induction of less than 0.5% was measured for the least stable alloy).

The 0.2% C alloy, which was already partly martensitic (~50%), exhibited the same type of stress-strain curve as at RT. The "yield strength" was decreased because of the lower stability of the retained austenite. The work hardening rate was much higher than at RT, resulting in lower elongation.

In the 0.3% C alloy, and in the 0.4% C alloy, the largest drop in "yield strength" was observed. The work hardening rate was extremely high and the shape of the curve was different from the stress-strain curve of the RT test. There was no indication of a Luder's strain and there were no serrations.

In the 0.4% C alloy, because of its higher carbon content, a higher yield strength and a lower work hardening rate were found. Moreover, there was some indication of a Luder's strain. Otherwise the same changes occurred at -78°C, compared to the RT tests as was the case for the

0.3% C alloy. No serrations occurred because the transformation took place so readily.

In the 0.5% C alloy, only a negligible amount of martensite formed at the onset of yielding at RT. At -78°C, however, stress-induced martensite initiated plastic deformation. A clearly definable Luder's strain region followed. Also, the very steep transition between the horizontal and the steep portion of the stress strain curve is in evidence. Since this alloy is the most stable of all of the 1% Mn alloys, its "yield strength" dropped very little, as compared to the RT-test. Moreover, its rate of martensite formation was lowest, resulting in the lowest work hardening rate, the highest elongation values, and longest Luder's strain. The changes due to varying carbon contents paralleled those observed in the room temperature tests. They were the direct result of varying stability of the austenite.

ii. Alloys Containing 2% Mn. Figures 4b and 4d clearly indicate that alloys with a carbon content between 0.1 and 0.4% C form stress-induced martensite at -78°C before the yield strength of the room temperature material is reached. That the alloy containing 0.5% C starts yielding as a result of a stress-induced phase transformation too, cannot be seen immediately by comparing the dry ice test with the 100°C test, because the measured "yield strength" at -78°C has a higher value than at 100°C, which could be due to the normal temperature dependence of the yield stress. However, the increase in strength seems to be too small to account for the temperature difference. Figure 4c clearly shows that lowering the temperature to -78°C does not result in an expected increase in yield strength beyond the RT test value, but rather it leads to a lower stress level at which plastic deformation sets in.

This can only be due to stress-induced formation of martensite. The decreased stability of the austenite (at -78°C) leads to a higher rate of martensite formation which, in turn, results in a drastically increased work hardening rate (Fig. 2e) compared to the corresponding room temperature test.

For the 0% C alloys the stress strain curve remained essentially unchanged (the alloy was already ferritic at RT).

The 0.1% C alloy was already partly martensitic at RT and so the same type of stress strain curve was obtained at -78°C, except that the work hardening rate was substantially higher. There was no further drop in "yield strength" due to stress-induced formation of martensite, as compared to RT. The "yield strength" values were about equal, indicating that some additional martensite formed when a specimen was cooled to -78°C. The resulting increase in strength at the lower temperature compensated for the greater ease with which martensite formed.

The 0.2% and 0.3% C alloys had the largest drop in "yield strength" due to stress-induced formation of martensite. They were essentially austenitic before the tests, and the austenite became very unstable at -78°C. The work hardening rate of these two alloys was essentially the same (also in the RT tests). This was due to the fact, that the actual carbon content of the "0.2% C" alloy was closer to 0.3% C than to 0.2% C, so that the difference in carbon content between the two alloys was only about 0.05%. (Table XVII)

The slightly higher carbon content, nevertheless, led to a higher "yield strength," larger Luder's strain and higher ultimate tensile strength. Moreover, some signs of instability appeared in the Luder's strain portion of the stress-strain curve of the 0.3% C alloy, whereas

this was not the case for the 0.2% C alloy. The greater ease with which martensite formed in the lower carbon alloy may have been responsible for this, as mentioned previously. Signs of instability were found at higher carbon contents (Fig. 2e).

The 0.4% C alloy exhibited a tremendous increase in work hardening rate, compared to the RT tests. The "yield strength" drop was smaller than for the preceding two alloys because of the increased stability of the austenite. Also, the dependence of the Luder's strain on the stability of the austenite is clearly demonstrated. The Luder's strain at -78°C (Fig. 2e) was only half as large as at RT (Fig. 2b). The ultimate tensile strength was higher than in the lower carbon alloys.

In the 0.5% C alloy the stress-induced formation of martensite lowered the "yield point" by about 12,000 psi, compared to its RT value (Table VI). While the rate of formation of martensite at RT was too low to compensate for the increase in stress due to necking, more martensite than necessary for high elongation values formed during the dry ice test. The Luder's strain was larger than for all the other (lower carbon) alloys, and, as expected, the work hardening rate was the lowest. Although the 0.5% C alloy had the highest elongation value, optimum ductility could be expected at temperatures between RT and -78°C. The very steep portion of the stress-strain curve following the Luder's strain is very much in evidence again. In all the dry-ice test curves signs of instability are found only in the Luder's strain portion of the curves, whereas at RT, serrations appear also in the steeper section following the Luder's strain. There is evidence that stress-induced martensite forms continuously with increasing stress, while strain-induced martensite forms intermittently resulting in bursts of martensite which, in turn, cause the

serrations. Strain, either as the result of the formation of martensite or of the slip mode of deformation is assumed to affect the stress conditions so that local peaks of stress may be formed, activating some martensite embryos (4). In other words, strain-induced stress peaks (stress peaks, higher than the average stress in the material measured over the cross-section of the specimen), led to formation of martensite which is referred to as strain-induced.

iii. Alloys Containing 3% Mn. Figure 2f shows the stress-strain curves of the alloys containing 0.2, 0.3, 0.4 and 0.5% C. A comparison with the 100°C tests (Figs. 5b and 5d) indicates that plastic deformation seems to be initiated by stress-induced formation of martensite in the first three alloys. The 0.5% C alloy, however, was stable with respect to a phase transformation-induced onset of yielding at 100°C and RT, but became unstable at -78°C. There was a drop of about 7000 psi in "yield point" compared to RT. Thus, all alloys started deforming as a result of stress-induced formation of martensite (Figs. 5c and 5d). As in the dry ice tests of the alloys containing less manganese, the work hardening rate was markedly increased, leading to higher ultimate tensile strengths; the Luder's strain was decreased. Due to the higher rate of formation of martensite, the elongation values dropped for the alloys that formed a sufficient amount of martensite at RT and increased for the more stable alloys whose work hardening rate was too low at RT (Fig. 2c). Again, no serrations were observed beyond the Luder's strain portion of the stress-strain curve, (Fig. 2f).

The 0.2% C alloy showed the largest drop in "yield point" due to its low austenite stability at -78°C, its work hardening rate was the highest for the same reason (Table XI).

The 0.3% C alloy exhibited a clearly defined Luder's strain with a marked, very steep transition to the steeper portion of the stress strain curve (Fig. 2f).

In the 0.4% C alloy, the increased formation of martensite resulted in an elongation value twice as large as in the RT tests (Table XIII).

In the 0.5% C alloy, the tremendous contribution of the Luder's strain to the total strain resulted in a 10 fold increase in elongation for this alloy at -78°C compared to RT (Table XIV). The very sharp change in slope after the steep transition portion following the Luder's strain can be explained by a renewed onset of plastic deformation. As previously indicated, the very steep portion is probably due mainly to elastic deformation. The sudden change in slope is to be expected as soon as the stress reaches a high enough value to induce further formation of martensite. Since no serrations occurred, deformation of martensite can be looked upon as the predominant mode of plastic deformation. Slip in the austenite still may have taken place locally as a result of the formation of martensite. Serrations occurred when the formation of martensite became more difficult, i.e. when there was more competition between the general slip mode of deformation and the formation of martensite. Martensite formed as a result of stress concentrations produced by the slip in the austenite.

Figure 6a shows that the Luder's strain increased approximately linearly with increasing carbon content.

2. Variation of Mn-Contents at Given C-Contents

a. Room Temperature Tests

i. Alloys Containing 0.2% C. Figure 7a shows the marked effect of managenese on the austenite stability. 1% Mn was too little to suppress the M_s temperature to below RT. Approximately 50% of the austenite transformed to martensite on cooling from 1200°C to RT. The retained austenite, however, was very unstable with respect to deformation and started yielding as a result of stress-induced formation of martensite at a stress-level about 60,000 psi lower than at 100°C (Table VII). The shape of the stress-strain curve was clearly different from the essentially austenitic alloys containing 2 and 3% Mn. There was no "yield point" and no Luder's strain, nor were there any serrations.

The 2% Mn alloy was sufficiently stabilized so that no transformation took place upon cooling from 1200°C to RT. The drop in yield strength due to stress-induced formation of martensite was about 40,000 psi (Table III)(compared to 60,000 psi for 1% Mn). The higher stability of the austenite due to an increase in managenese was also revealed in a lower work hardening rate and a higher elongation value, both being due to a lower rate of martensite formation. Serrations appeared, especially in the second half of the stress-strain curve when the formation of martensite became more difficult.

The stress-strain curve for the 3% Mn alloy showed a marked Luder's strain region, a lower work hardening rate and a higher elongation value than the 2% Mn alloy. The increased stability of the austenite was further indicated by the higher "yield strength." Although plastic deformation was still initiated by stress-induced formation of martensite, the difference in "yield strength" between the RT and the 100°C test was only

about 10,000 psi (Table XI). Serrations are in evidence in the Luder's strain portion of the stress-strain curve as well as in the following steeper region. The sharp transition at the end of the Luder's strain is clearly visible and followed by a small smooth portion of the curve before serrations indicate the increased influence of strain on the formation of martensite. The fact that serrations appear earlier in the test than in the preceding (2% Mn) alloy is due to the higher austenite stability (formation of martensite is more difficult).

ii. Alloys Containing 0.4% C. As a results of the higher carbon content (0.4% C compared to 0.2% C) the 1% Mn alloy was essentially austenitic before the test, but it started forming stress-induced martensite when pulled. The "yield strength" at RT was about 40,000 psi below that at 100°C (Table IX). The 1% Mn alloy had the lowest "yield point" of the 3 alloys shown in Fig. 7b, but ended up with the highest ultimate tensile strength. This was expected, because it was the least stable of the three alloys.

Increasing the manganese content to 2% led to a Luder's strain twice as long as in the 1% Mn alloy (Fig. 7b). The increased stability of the austenite affected the mechanical behavior and properties in the way previously discussed. Yielding was still initiated by a very small amount of stress induced martensite ("yield strengths" at RT and 100°C were equal);(Table V).

The 3% Mn alloy was stabilized so much that the rate of martensite formation was too low to compensate for the increase in stress due to a decreasing cross sectional area. The specimen failed after a certain amount of strain (still in the Luder's strain region). The measured yield point represented the stress at which the austenite started yielding

(Table XIII). The yield point itself had a different appearance (Fig. 7b).

iii. Alloys Containing 0.5% C. The 1% Mn alloy still started deforming plastically as a result of stress-induced formation of martensite. The rate at which this hard martensite forms were, however, too low to lead to high elongation values (Fig. 7c, Table X).

Figure 7c shows that the austenite of the 2% Mn alloys was not completely stable with respect to deformation. Small amounts of martensite formed, as indicated by the horizontal portion following the yield point (of the austenite) (Table VI). This was also verified by magnetic measurements.

The 3% Mn alloy, and the one containing 4% Mn, were so stable (M_d < RT) that the specimens failed at the site of incipient necking.

b. Dry Ice Tests

i. Alloys Containing 0.2% C. All three alloys started yielding as a result of stress-induced formation of martensite. Due to the decreased stability of the austenite, the work hardening rate was increased drastically, leading to different stress-strain curves for the alloys containing 2 and 3% Mn. The type of the stress-strain curve of the 1% Mn alloy did not change (as compared to the RT-curve) because the alloy was already 50% martensite before the test. The Luder's strain portion of the other two alloys (2 and 3% Mn) was reduced and their ultimate tensile strength increased significantly (Tables III and XI). Figure 7d exhibits the effect of manganese on the stability of the austenite very clearly.

ii. Alloys Containing 0.4% C. In contrast to the two austenitic (2 and 3% Mn) alloys containing 0.2% C, where the "yield points" were closer together at -78°C than at RT, (Figs. 7a, and 7d; Tables III and XI)

the alloys containing 0.4% C had their "yield points" at more separated stress levels at -78°C than at RT (Figs. 7b and 7e). This did not change for both cases at -196°C (Tables V and XIII). All three alloys started yielding due to stress induced formation of martensite. The "yield strength" values at -78°C as compared to RT decreased according to the relative austenite stability of the alloys: ~50,000 psi for the 1% Mn alloy , ~25,000 psi for the alloy containing 2% Mn, and ~15,000 psi for the alloy with 3% Mn, (Tables V, X and XIII). The 3% Mn alloy, which did not form enough martensite at RT, had the highest elongation value at -78°C. Figure 7e illustrates the effect of varying Mn contents on the "yield strength," ultimate tensile strength, the work hardening rate, the Luder's strain and the total elongation. All these quantities are interrelated and depend actually on the degree of stability of the austenite. Figure 6b shows that the Luder's strain increased linearly with increasing manganese content (increasing stability of the austenite).

iii. Alloys Containing 0.5% C. Plastic deformation started in all alloys except the 4% Mn alloy as a result of the stress-induced formation of martensite (note the different appearance of the "4% Mn" yield point in Fig. 7f). The usual changes in the stress-strain curves occurred due to the decreased stability of the austenite at lower temperatures. The alloys containing 1 and 2% Mn exhibited a smaller difference in work-hardening rate and Luder's strain than one would expect on the basis of the other results (0.2 and 0.4% C). This is due to the fact that the 1% Mn alloy contained about 1% more Cr and about 0.03% more C than the 2% Mn alloy, according to the chemical analysis (Table XVII). Since both chromium and carbon increase the austenite stability with respect to plastic deformation, the effect of the 1% Mn difference was almost

compensated for.

The alloy containing 4% Mn was close to the optimum test temperature at -78°C (Table XV). It seems as if the total strain can be looked upon as Luder's strain, which would agree well with the fact that the Luder's strain and elongation increase with increasing austenite stability (obtained by additions of C and Mn). This relationship holds up to a certain value of elongation.

B. The Effects of Varying Reductions in Thickness at 450°C on the Tensile Properties of a Metastable Austenitic Stainless Steel

1. Alloys With 2% Mn and C Contents Varying From 0 to 0.5%

a. Room Temperature Tests

The 0.0% C alloy was completely ferritic after cooling from the austenitizing temperature (1200°C) to RT. Since no carbides could form during rolling at 450°C, and because no phase transformation could take place during the test, the difference in stress strain curves (Fig. 8a) was due only to the varying reductions in thickness (Table I). All specimens failed at the site of incipient necking.

In the 0.1% C alloy the austenite was more stable, resulting in only a partial transformation to martensite on cooling from 1200°C to RT. The retained austenite was very unstable with respect to elastic stresses and plastic deformation. Stress-induced formation of martensite initiated yielding and led to markedly lower "yield strength," compared to the alloy without carbon where no phase transformation took place. There was a very small difference in "yield strengths" for the various amounts of prior deformation (Fig. 8b; Table II). This indicated that for a low austenite stability the "yield strength" cannot be raised drastically by large amounts of prior deformation at temperatures above

M_d. An increase in reduction in thickness from 20% to 80% results in an increase in "yield strength" of only 30,000 psi.

Thermomechanical treatment seems to affect the mechanical properties of highly unstable austenite more by its effect on the stability of the austenite rather than by the change in dislocation density and the microstructure per se.

The effects of thermomechanical treatment on the stability of austenite are manifold. Small amounts of prior plastic deformation have been found to stimulate the formation of martensite, whereas large reductions in thickness increase the stability of the austenite. If this effect had played a dominant role in the above alloy, a larger difference in "yield strengths" would be expected. On the other hand, larger reductions in thickness require more time, i.e. the material being rolled is held for a longer time at a given temperature (450°C), allowing more time for diffusion and precipitation. Moreover, a greater amount of plastic deformation provides for more nucleation sites for the carbide precipitates. Precipitation of carbides leads to a depletion of alloying elements in the matrix which in turn renders the austenite less stable. This last effect would tend to bring the respective "yield strengths" closer together.

(A reduction in thickness of 80% required three times as much time as a reduction of 60% for this alloy (partly martensitic). Samples reduced by 60, 40 and 20% were held for the same time at the rolling temperature.) Although Fig. 8b indicates that the latter effect seems to be predominate, the respective magnitude of both effects depends on the degree of austenite instability and was not investigated.

The low stability of the austenite was further underlined by the

relatively high work hardening rate compared to alloys containing more carbon (Figs. 8c through 8f). The work hardening rate of the specimen reduced by 60% was greatest, followed by that of the specimen reduced by 40%. The specimens reduced by 80 and 20% exhibited similar work hardening rates. This indicated that there must be a maximum with respect to the stimulation of the formation of martensite due to prior deformation between 80 and 20% reduction in thickness (for this alloy).

Serrations appeared in the last portion of the stress strain curve much earlier, i.e. at lower strains, for the specimens reduced by 60, 40 and 20% than for the specimen reduced by 80%. This could not be due to different stress levels, since there was practically no difference in stress between the specimens reduced by 60 and 80%, at that strain. Thus, it had to be due to the difference in prior deformation or due to the longer time the 80% sample was held at 450°C. In order to investigate this, a specimen with 60% reduction in thickness was held at 450°C for 80 minutes so that its total time at 450°C (2 hrs) was exactly the same as needed to reduce a sample 80% at 450°C. The following results were obtained: Stress induced formation of martensite initiated plastic deformation at the same stress level as for the untempered specimen. The work hardening rate was, however, dramatically increased and corresponded to the work hardening rate of the untempered specimen at -78°C. The increased work hardening rate resulted in a higher tensile stress (260,000 vs 240,000 psi) and a lower elongation value (11.2 vs 16.3%). The microstructures of the tempered and the untempered specimens are shown in Figs. 28a and b. No serrations whatsoever appeared in the stress-strain curve, indicating that serrations are directly related to the stability of the austenite which can be strongly affected by thermo-

mechanical treatments.

The above results show that extremely high work hardening rates can be obtained at RT if proper thermomechanical treatments are employed. The fact that the high work hardening rates obtained at -78°C (in this alloy system) can be procured at RT has the additional advantage that at RT there will not be the drop in "yield strength" characteristic of the lower temperatures.

By varying the time of tempering a wide range of work hardening rates could be achieved with only one alloy (having the same thermomechanical history).

The presence of 0.2% C prevented the formation of martensite on cooling to RT (M_s < RT). At room temperature, however, the austenite was so unstable that plastic deformation started as a result of the stress induced formation of martensite (Table III). The higher stability of the austenite in this alloy compared to the 0.1% C alloy was apparent in the marked difference in "yield strengths" between the specimens that underwent a reduction in thickness of 20, 40 and 60%. The difference was about 30,000 psi, respectively, (Fig. 8c). Another indication for the increased stability as a result of higher C content was the lower work hardening rate. The most interesting feature in Fig. 8c is that the "yield strength" of the specimen reduced by 80% is lower than that of the specimen reduced by 60%. This is especially striking because there was a clear effect of the amount of prior deformation on the "yield strength" up to 60% reduction in thickness. The deviation in the 80% reduced specimen must be due to the fact that a reduction in thickness of 80% required twice as much time (1 hr vs. 30 min) as that of 60%. For previously stated reasons this results in a lower alloying element content of the matrix (less Cr,

Mn and C) and thus a less stable austenite. Despite a higher amount of prior deformation, less stress was required to initiate the phase transformation. Because martensite formed more readily, the work hardening rate was much higher. This resulted in a significantly higher tensile strength for the 80% than for the 60% reduced specimen.

The difference in strain hardening rate was mainly due to the larger amount of martensite forming per unit strain and not due to a larger amount (longer time at 450°C) and finer distribution (higher reduction in thickness) of carbide precipitates. This will be shown with the help of the results from a higher carbon alloy.

The strain hardening rate was decreased in the following sequence, 80, 20, 40 and 60% reduction in thickness. Since the samples reduced by 20, 40 and 60% were held for the same length of time at 450°C, increasing amounts of plastic deformation seem to increase the stability of the austenite. Higher stability of the austenite resulted in lower strain hardening rates independent of which way the austenite stability had been enhanced.

As a result of its inhomogeneous nature, plastic deformation tends to "subdivide" the grains into smaller units and, thus, effectively provides a finer "grain size." A fine grain size, however, decreases the average size of a martensite plate formed from a given embryo (4). The volume of martensite per activated embryo is therefore expected to decrease with increasing plastic deformation.

This mechanical stabilization of the austenite could well be the dominating effect, overriding the influence of more intensive precipitation due to a greater number of nucleation sites formed as a result of larger amounts of plastic deformation. (Depletion of the matrix of

alloying elements renders austenite less stable, this leads to a higher strain hardening rate.)

All stress-strain curves in Fig. 8c exhibit serrations. For the sample with the smallest amount of prior deformation (20%) the curve is first smooth, then after a certain strain serrations appeared in increasing frequency and amplitude. The same behavior was displayed by the sample that was reduced 40% in thickness except that serrations appeared near the beginning of the test. 60% reduction in thickness resulted in very many serrations at the beginning of the test. Thereafter the frequency decreased, whereas the amplitude of the serration increased. The stress strain curve of the most severely deformed specimen (80%) showed some signs of instability at the beginning, but then became smooth as the strain hardening rate increased due to ready formation of martensite. After all the easy nucleation sites had become exhausted, serrations occurred in the last portion of the stress-strain curve.

The larger serrations have to occur at the end of the test when the stress is higher. Higher stress results in a larger amount of martensite (19). Martensite causes the volume to increase and this causes a momentary load drop. The drop in load is the larger the more martensite forms per burst. Large serrations are always separated from one another by a certain amount of strain. The accompanying work hardening provides the necessary higher stress for a martensite embryo to become a critical nucleus. If there are no small serrations visible between large ones near the end of the test, it can be assumed that no transformation takes place between these bursts. This would agree with the observation made regarding the strain hardening rate of the sample with 60% reduction in thickness (Fig. 8c). Its work hardening rate was the lowest. Although

large serrations are due to the formation of a large amount of martensite, the serrations were widely separated and thus less martensite formed on the average than in the samples that had been reduced 20 and 40%, which exhibited twice or three times the numbers of serrations. These latter samples had a higher work hardening rate than the former due to formation of more martensite per unit strain.

The stress-strain curves for the 0.3% C alloy shown in Fig. 8d are similar to those given in Fig. 8c. The reason for this is that the compositions of these two alloys were not too different with respect to the austenite stability. Chemical analysis showed that the carbon content of this (0.3% C) alloy was only about 0.05% higher than in the preceding (0.2% C) alloy, and that the effect of the higher carbon content was partly neutralized by a lower Cr content (9.8% vs. 10.7%) (Table XVII). Nonetheless, the stability of the austenite was slightly increased, as can be seen from the lower strain hardening rate of the materials with 80 and 20% reduction in thickness (Fig. 8d) compared to the corresponding samples of the preceding (0.2% C) alloy (Fig. 8c). Moreover, the "yield point" of the material with 80% prior deformation was higher than the "yield strength" of the specimen with 60% prior deformation, which was not the case in the preceding alloy. This is another indication of a small increase in austenite stability. Plastic deformation started as a result of stress-induced formation of martensite at stress levels that hardly differed from those of the preceding alloys (Table IV).

Only the sample with 80% prior deformation exhibited a marked yield point. The stress-strain curves of the other samples showed a smooth portion before serrations appeared. This smooth portion was most likely due to stress-induced formation of martensite (using up the sites of easy nucleation). The extent of the smooth portion increased with

decreasing amounts of prior deformation. It should not be implied that a smooth curve always indicates a stress-induced formation of martensite, but rather that if martensite forms it is most likely stress-induced. If one compares for instance the stress-strain curves of samples with 20% prior deformation of this alloy (0.3% C) and of the preceding alloy (0.2% C) in Fig. 8d and 8c, respectively, it seems evident that the larger extent of the smooth portion of the curve for the higher carbon alloy is due to a greater contribution of the slip mode of deformation in the austenite to the total deformation. This seemed to be confirmed in the following alloy (0.4% C), where the stress-strain curve of the sample with 20% reduction in thickness did not show any sharp serration (Fig. 8e). (The increased stability of the austenite caused slip to be the predominate mode of deformation.) Moreover, the markedly lower strain hardening rate in the 0.3% C alloy compared to the 0.3% C alloy indicated that less martensite formed.

The specimens with a prior reduction in thickness of 40 and 60% did not show any change in work hardening rate compared to the lower carbon alloy (0.2% C). Since all four specimens to be compared (40%, 60% in Figs. 8c and 8d) had been held for the same length of time (30 min) at 450°C, the higher carbon content (greater supersaturation) may have led to a larger amount of carbide precipitation. Even if more carbon (than in the lower carbon alloy) had been retained in solution, a greater amount of fine precipitates would have removed some of the alloying elements (Cr, Mn) and thus may have cancelled the effect of a slightly increased carbon content. Although the strain hardening rate of the specimen with 80% prior deformation was slightly lower than for the preceding alloy, it was markedly higher than for the specimens of the

same alloy subjected to smaller amount of reduction in thickness. The reason for this, as already explained previously, lies in the lower stability of the austenite due to more extensive alloy carbide precipitation (longer time at 450°C: 50 vs 30 min).

The stress-strain curves for the 0.4% C steel in Fig. 8e clearly show the marked increase in austenite stability as reflected in higher yield strengths and lower work hardening rates, compared with the two preceding alloys. The yield strengths of the samples with reductions in thickness of 20, 40 and 80% were increased by approximately 30,000 psi respectively over the values obtained for the 0.2 and 0.3% C alloys. The increase in yield strength of the specimen with 60% prior deformation was less than 10,000 psi and also its work hardening rate changed only slightly, as is expected, since both depended on the stability of the austenite. The smaller change in austenite stability for the sample with 60% reduction in thickness must be explained by the effect of thermomechanical treatment on the precipitation process, and thus on the stability of the austenite. Compared with the preceding alloys, the specimen reduced 60, 40 and 20% were held 10 minutes longer at 450°C (40 vs. 30 min), which may have had different effects for different amounts of prior deformation. Moreover, composition variations within an alloy are likely to have existed, although efforts had been made to keep variations at a minimum.

A comparison with tests at 100°C (Table V) indicates that plastic deformation at RT may still be initiated by a stress-induced formation of martensite. However, the stress level at which yielding started was very close to the expected yield strength of the austenite.

Besides the fact that the yield strengths of the samples reduced by 80 and by 60% had clearly separated stress levels (198,000 vs 166,000 psi), the most striking difference with respect to the two preceding alloys was that there was practically no difference in strain hardening rate between these two samples, whereas in the preceding alloys the strain hardening rate for the sample with 80% prior deformation was significantly higher than for all the other specimens having lesser amounts of reduction in thickness.

Since the present alloy (0.4% C) had a higher carbon content, and because a reduction in thickness of 80% at 450°C required the same time as for the preceding alloys, the higher work hardening rate for specimens of lower carbon alloys (0.2% and 0.3% C) subjected to the above thermo-mechanical treatment (80%, 450°C) must be due to a lower stability of the austenite and not due to precipitation hardening. (This could have been responsible for the difference in strain hardening rate between samples of 80 and 60% prior deformation. Almost twice as much time (at 450°C) was needed to reduce a specimen 80% as is required for a 60% reduction in thickness.)

The higher carbon content should have resulted in a higher work hardening rate if the work hardening rate of this alloy were significantly affected by precipitation hardening. This was not the case. Also, the strain hardening rate of this alloy was lower than those of lower carbon content.

As found for the other alloys, the stress strain curves exhibited serrations. The first occurrence of these serrations was shifted to larger strains with decreasing prior deformation (for samples held for the same time at 450°C). The sample with only 20% prior deformation

had a stress-strain curve without any sharp serrations; there were, however, some signs of instability toward the end of the test. The 40 and 60% reduction in thickness specimens had serrations. The amplitude of the serrations increased, while their frequency decreased, with increasing strain (for the reasons discussed previously).

The sample with 80% prior deformation had a stress strain curve with only a few instabilities in the Luder's strain region. Thereafter many sharp serrations appeared. The pattern was similar to those described above for samples of 40 and 60% reduction in thickness (Fig. 8e). Only the samples that have been reduced 80% showed a clearly definable Luder's strain region in their stress strain curves at RT.

Figure 8f, for the 0.5% C alloy, shows the stress strain curves characteristic of a highly stabilized austenite. The measured yield strength values represent the yield strength of the austenite. The M_d-temperature was slightly above RT ($RT < M_d < 100°C$), and thus some martensite formed during the test. The rate of martensite formation was, however, too low to prevent failure at the site of incipient necking. The elongation values decrease with increasing amount of prior deformation. (This holds only for the samples that had been held for the same time at 450°C.) 80% reduction in thickness at 450°C required about twice as much time as 60% reduction and there was more time for precipitation to occur. The resulting depletion of the matrix of alloying element rendered the austenite less stable. This led to a slightly improved ductility over the 60% reduced sample. The small amount of martensite which formed helped the material to recover after yielding, as indicated by the horizontal portion of the stress strain curve following the yield point, but it is not sufficient to sustain large strains. This was the only alloy (of this series) in

which the effect of prior deformation on the yield strength was not modified by a phase transformation (Fig. 9). Figure 10 shows that the effect of prior deformation was the greater the higher the carbon content (i.e., the higher the austenite stability).

b. Dry Ice Tests

Since the 0% C alloy was ferritic at RT, there was no phase transformation that could alter the shape or the type of the stress-strain curves (Fig. 11a). The yield strength values were higher than at room temperature, as was expected, on account of the temperature dependence of the dislocation mobility.

In the partly martensitic 0.1% C alloy, the retained austenite was so unstable that the amount of prior deformation did not seem to play a role as long as all specimens were held for the same time at 450°C. Internal stresses set up by non-uniform deformation during processing or while the specimens were being cut, in addition to non-uniaxial stresses originating from the applied load affected the yield strength tremendously. They aided in bringing about the transformation to martensite at a much lower externally measured (average) stress than anticipated.

The increased instability of the austenite at -78°C resulted in a lower stress necessary to initiate plastic deformation through the formation of martensite. The "yield strengths" measured for the specimens with a prior deformation of 60 and 40% were lower than for the specimen with only 20% reduction in thickness (Fig. 11b, Table II). While the yield strengths of the samples reduced 60 and 40% were about 30,000 to 40,000 psi lower at -78°C than at RT, the yield strengths for the other two samples (80 and 20% reduction in thickness) hardly changed as a result of the change in test temperature.

It is noted that the strain hardening rates of the samples reduced 80 and 20% were about equal at RT, and that the strain hardening rates of the other samples were higher and increased in following order according to the thermomechanical treatment: 40%, 450°C; 60%, 450°C.

Since the work hardening rate can be taken as a measure of the stability of the austenite in such an alloy system, it is not surprising that the samples with the higher stability at RT had a higher yield strength at -78°C than the less stable samples of the same alloy irrespective of the amount of prior deformation. The amount of prior deformation, however, was reflected in the tensile strength values (Fig. 11b).

The work hardening rate of all the samples was strongly increased as compared to RT. The rate decreased with respect to the pre-test treatment in the following order: 40%, 60%, 80% and 20% reduction in thickness at 450°C. At -78°C martensite formed so readily as the stress increased that no serrations appeared in the stress strain curves.

The stress strain curves for the 0.2% C alloy in Fig. 11c show a marked decrease in yield strengths and a drastic increase in work hardening rate as compared to those obtained at RT. The difference between the highest and lowest yield strength at RT (Fig. 8c) was about 70,000 psi, whereas this difference amounted to only about 30,000 psi at -78°C (Table III).

As previously mentioned, the effect of different thermomechanical treatments on the yield strength was enhanced as the stability of the austenite increased. In other words, the difference between the highest and lowest yield strength value at room temperature should be larger than for the same samples (of different thermomechanical treatments) at -78°C. If the austenite stability is increased by alloying, the difference in

yield strength for a given temperature should increase as the alloying element content is increased. This holds for the alloy system investigated.

In the alloy containing 0.2% C (Fig. 11c) the work hardening rates of the samples with 80 and 60% prior deformation were the highest (at -78°C), and about equal, followed by the work hardening rates of the specimens with 40 and 20% reduction in thickness. The stress level of the tensile strength depended on the austenite stability (higher when less stable), whereas the difference in tensile strength between the various samples due to different amounts of prior reduction in thickness seemed to be little affected by the stability of the austenite.

The stress-strain curves for the 0.3% C alloy in Fig. 11d show a strongly increased work hardening rate compared to the work hardening rates obtained in RT tests (Fig. 8d). The "yield strengths" were significantly decreased for the specimens with 80, 60 and 40% prior deformation, namely by about 40,000, 65,000 and 30,000 psi, respectively. The "yield strength" of the specimen with a reduction in thickness of only 20% did not change as compared to the RT "yield strength." The fact that the work hardening rate for a specimen with such a treatment was the lowest of all the specimens at RT (i.e. the austenite stability was highest), and that the saturation induction obtained from magnetic measurements increased 12% due to some formation of martensite during cooling to the test temperature (-78°C), seemed not to be a sufficient reason to account for the fact that there was no change in yield strength. Additional tests run with specimens of the same material and with the same thermomechanical treatment revealed that some yield strength values were as much as 25,000 psi lower at -78°C. This indicated how sensitively the mechanical properties depend on the austenite stability, and upon other factors which are

difficult to control like internal stresses, and small deviations in thickness and width of the gage section of the specimens, etc.

Although some test results indicated otherwise, the yield strength was generally shifted to markedly lower values as the test temperature was lowered from RT to -78°C. The difference in stress levels at which yielding occurred for the various thermomechanical treatments was strangely reversed by a change in test temperatures.

At RT the yield strengths of the specimens with a prior reduction in thickness of 20, 40 and 60% were clearly separated (difference of 35,000 to 40,000 psi) whereas the specimens with 80% prior deformation yielded at a stress level less than 10,000 psi higher than that of the 60% deformed specimen (Fig. 8d).

At -78°C just the reverse took place. The specimen with 80% prior deformation yielded at a stress about 35,000 psi higher than the specimen with 60% reduction in thickness. The yield strength of the latter specimen and the ones for the samples with 20 and 40% prior deformation were separated by only 5,000 psi, respectively (Fig. 11d). In general, the yield strength values for different thermomechanical treatments differ less the higher the instability of the austenite, as was pointed out earlier. The amount of martensite that forms during cooling to the respective test temperatures has a major influence on the yield strength. Magnetic measurements revealed that the amount of martensite that formed during cooling was not the same for different thermomechanical treatments. The specimen with 80% reduction in thickness was the least stable at RT, as verified by the relatively low yield point. More martensite formed during cooling to -78°C than in the other specimens. This higher pre-tent martensite content was, in part, responsible for the "yield strength"

difference.

The austenite of the specimen with 80% reduction in thickness remained the least stable of all, at least with respect to plastic deformation, as verified by the high work hardening rate (Fig. 11d). The work hardening rates of the specimens with other thermomechanical treatments were lower and decreased in following order: 60, 40 and 20% reduction in thickness at 450°C.

The question as to why the stress strain curves of the preceding alloy in Fig. 11c do not display the same pattern as in Fig. 11d, although their curves compared very nicely at RT in Fig. 8c and 8d, respectively, can be explained by the relative difference in the instability of the austenite due to different compositions. The difference in austenite stability between two alloys at RT may be less than at -78°C. At any rate, the effect of austenite stability difference on the mechanical properties will be altered by a change in temperature.

Fracture was not preceded by necking in specimens with only 20 and 40% prior deformation, and there were no serrations in the stress strain curves before the maximum load was reached. This indicates that there may be a critical amount of prior deformation above which more martensite nuclei can be made available by plastic deformation during the test.

The stress strain curves for the 0.4% C steel in Fig. 11e show the expected changes resulting from a decrease in test temperature as compared to the RT results, i.e. higher work hardening rates, lower yield strengths, lower elongation values, and a smaller difference between the highest and lowest yield strength (reduced effect of prior deformation).

The specimen with 80% reduction in thickness had a markedly higher yield point than the specimens with different thermomechanical treatments.

This was also observed in the preceding alloy and was due to the fact that the specimen with 60% reduction in thickness experienced by far the highest decrease in yield strength due to a lower testing temperature (-78°C compared to RT, Table V). This kind of behavior was found with all alloys from 0.1 through 0.4% C. The alloy containing no carbon was already fully transformed to ferrite and in the alloy with 0.5% C the austenite was too stable to allow such drastic changes.

The maximum difference in yield strength between RT and -78°C was obtained for the alloy containing 0.3% C. The drop in yield strength for the specimens with 60% prior deformation was on the average 20,000 psi greater than for the specimens of other thermomechanical treatments. This particular amount of prior deformation must affect the stability of the austenite with respect to the stress-induced formation of martensite, either through the dislocation network as such or by its effect on the precipitation process.

In this (0.4% C) alloy the yield strength values for 60 and 40% reduction in thickness were identical. The difference in thermomechanical treatment became, however, evident in the work hardening rates and tensile strength values. Specimens with 80 and 60% prior deformation exhibited the highest work hardening rates. The work hardening rates resulting from the other treatments decreased as the amount of prior deformation decreased. The specimens with only 20 and 40% prior deformation failed without prior necking, as in the preceding two alloys. There were no sharp serrations, although some signs of instability could be observed in the Luder's strain portions of the stress strain curves.

The stress strain curves for the 0.5% C steel in Fig. 11f clearly show the lower stability of the austenite in the specimen that had undergone

an 80% reduction in thickness at 450°C as compared to specimens with a smaller amount of prior deformation. The reason for this, as already explained for the RT tests results, is the much longer time the 80% specimen was held at 450°C (75 vs 35 min).

The lower stability was indicated by the smaller Luder's strain region and the higher work hardening rate as compared to the specimen with 60% prior deformation. Moreover, the specimen with 80% reduction in thickness was the only one that had a lower yield point at -78°C than at RT (Table VI). The higher elongation values for the 60 and 80% specimens, as compared to the specimens with less prior deformation (Fig. 11f), indicated that more martensite formed per unit strain in the specimens with the larger amounts of prior deformation.

This was expected on the basis of the results of the preceding alloys in which the highest work hardening rates were found for the specimens with 80% and 60% prior deformation.

Although the specimens with 40 and 20% reduction in thickness sustained larger strains than at room temperature they failed long before the end of the expected Luder's strain portion of the stress-strain curve was reached, as the specimen of the same treatment in the preceding alloys fractured before necking occurred.

Other than some signs of instability in the Luder's strain portion of the stress strain curve, there were no sharp serrations.

2. Alloys With 1% Mn and C Contents Varying From 0.2 to 0.5%

a) Room Temperature Tests

Since the 0.2% C alloy was already partly transformed (~50% martensite) after cooling from 1200°C to RT, the measured yield strength values were relatively high (Fig. 12a). Plastic deformation was initiated by a stress-

induced formation of martensite (Table VII). The low stability of the retained austenite minimized the effect of prior deformation. The maximum and minimum yield strength were separated by only about 30,000 psi. This difference in yield strength due to prior plastic deformation increased with increasing austenite stability to above 100,000 psi (Fig. 10).

Although the specimens with 60 and 80% prior deformation had about the same "yield strengths," the work hardening rates were quite different. The austenite in the 80% specimen was less stable because the alloying content of the matrix had been diminished during a more extensive precipitation process (about twice as long at 450°C as the 60% specimen).

The work hardening rates decreased with decreasing amount of prior deformation.

In the stress strain curve with the lowest work hardening rate (20%, 450°C) a few small serrations appeared. The formation of martensite became more difficult and no serrations occurred in the other curves.

The 0.3% C alloy was sufficiently stabilized so that it remained austenitic after cooling from 1200°C. The resulting stress-strain curves (Fig. 12b), were thus markedly different from the ones for the preceding alloy.

The "yield strength" values were on the average about 80,000 psi lower than for the 0.2% C alloy. The effect of prior reduction in thickness became more obvious: greater changes in "yield strength" values and work-hardening rates were observed. Many small serrations occurred during the entire test of the specimens with 20 and 40% prior deformation. In the specimens with larger amounts of prior deformation serrations appeared only in the Luder's strain portion of the stress-strain curve, thereafter

the strain hardening rate was too high, indicating that martensite formed very readily. The strain hardening rates for the specimens with 80 and 60% reduction in thickness were approximately the same. This was presumed to be due to the much smaller difference in time for the two treatments (70 vs 50 min at 450°C). It usually takes about twice as much time to reduce a specimen 80% as is required for a 60% reduction in thickness at 450°C.

Figure 12c shows a phenomenon in the 0.4% C alloy that had previously been observed in an alloy containing 2% Mn (which had a comparable austenite stability). While the "yield strengths" of the specimen with 20, 40 and 60% prior deformation were clearly separated, the yield strength of the specimen with a prior reduction in thickness of 80% was almost the same as the one for a 60% reduced specimen (Table IX). Since the 80% specimen was held at 450°C for 100 min as compared to 45 min for the "60%" specimen, the stability of the austenite decreased as a result of a diminished alloying content of the matrix due to prolonged precipitation.

The austenite stability increased with decreasing amounts of prior deformation, as indicated by the respective work hardening rates.

There was a clear effect of the amount of prior deformation on the stability of the austenite, and thus on the rate of formation of martensite in this alloy. There was a certain amount of prior plastic deformation between 40 and 60% which affected the rate of martensite formation in such a way that maximum elongation values were obtained (Fig. 12c). Too little martensite seemed to have formed in the specimens with 20 and 40% reduction in thickness to suppress necking.

No serrations appeared in the stress strain curve for the specimen with 20% reduction in thickness. This agreed with previous observations

that serrations disappeared for this thermomechanical treatment (20%, 450°C) as the stability of the austenite increased.

Remarks on the serrations as they appeared on the other curves, on their frequencies and on their amplitudes have been made elsewhere.

The 0.5% carbon content increased the stability of the austenite so much that the stress measured at the onset of plastic deformation (which was due to stress-induced formation of martensite) approached the yield strength of the austenite (Table X).

Different amounts of prior deformation had their greatest effect on the "yield strength" when the tendency for a phase transformation to occur was least (Fig. 10).

The increase in volume due to the formation of martensite was the greater, the higher the carbon content. The drop in load when the martensite formed in bursts was thus increased. The serrations in the stress strain curve of the specimen with 80% reduction in thickness (Fig. 12d) indicated a burst-like formation of martensite at relatively low strains. Close observation of the stress-strain curve of the specimen with 60% prior deformation showed that fracture was preceded by a large drop in load due to a transformation burst.

b) Dry Ice Tests

The stress-strain curves of the 0.2% C alloy (Fig. 13a) clearly showed the effect of a lower test temperature on the mechanical behavior. The lower stability of the austenite resulted in a lower stress being needed to induce the formation of martensite, a higher work hardening rate and lower elongation values, as compared to the RT tests (Table VII). There were no serrations.

The fact that the specimens were partly martensitic (~50%) was

reflected in the relatively high "yield strength." The minimum "yield strength" value was about 25,000 psi higher than the highest "yield strength" in the next following alloy (0.3% C) which was essentially austenitic.

Although cooling the 0.3% C alloy from 1200°C to RT did not result in a phase transformation, the austenite was extremely unstable with respect to plastic deformation at -78°C (Fig. 13b). The specimens started yielding as a result of a stress induced formation of martensite at a stress level about 50,000 psi lower than at RT (Table VIII). It was this lower "yield strength" and the enormous work hardening rate which made it difficult to obtain fracture of the specimens within the gage sections. The stress at which most specimens failed, was three to fives times as high as the corresponding "yield strength." All specimens including many reruns broke at the holes where the load was applied to the specimen through a pin.

The gage section of the specimen work hardened so strongly under uniaxial tension that a stress level was reached during the test at which the material around the hole started yielding. The resulting bi- or even tri-axial stresses resulted in a high stress concentration around the hole and thus led to brittle fracture in this region of the specimen. Moreover, the additional stresses may well affect the formation of martensite in such a way that a lower work hardening rate is obtained than under uniaxial stress.

This problem could not be overcome with the type of specimen used (Fig. 1).

The tensile stress obtained by dividing the maximum load by the cross sectional area did not represent the actual ultimate tensile stress of the material, because the specimen did not fail in the gage section (Table VIII).

The less stable the austenite, the more was the onset of transformation affected by factors that could not readily be controlled, like internal stresses, their distribution, surface irregularities, and changes in cross sectional area.

Specimens out of the same batch of material which underwent the same thermomechanical treatment exhibited "yield strength" difference of up to 40% in this particular alloy.

The stress-strain curves for the 0.4% C alloy in Fig. 13c, show a phenomenon that had already been observed in alloys containing 2% Mn, namely that the "yield strength" of the alloy with 60% prior deformation experienced a far greater decrease than all the other specimens, compared to the "yield strength" measured in room temperature tests. As for the 2% Mn, 0.2% C alloy (Fig. 11c) the "yield strength" was lowered so much that the specimen with 40% prior deformation yielded at a higher stress level. The high work hardening rate for the 60% specimen confirmed the enormous decrease in austenite stability. For the remaining specimens, the strain hardening rates decreased in the following order of reduction in thickness: 80, 40, and 20%.

The observation that specimens with only 20 and 40% reduction in thickness fractured without prior necking had been made earlier for alloys containing 2% Mn. The specimens with 60 and 80% prior deformation reach a maximum in the stress-strain curve before they failed. There were no serrations.

The stress-strain curves for the 0.5% C alloy in Fig. 13d are much different from all the preceding ones in this series. This was due to the higher carbon content, which according to chemical analysis was more than 0.15% higher than in the preceding alloy (Table XVII). The higher

austenite stability was evidenced in the lower work hardening rates and the higher yield strength values. While the yield strengths of the specimens with only 20 and 40% reduction in thickness increased slightly, as compared to the RT tests, the yield strengths of the specimens with 60 and 80% prior deformation decreased, the latter more than the former. This had been observed before (Fig. 11f), and it agrees well with the relative austenitic stability as determined from room temperature tests.

There was a marked Luder's strain in the stress curves of the 60 and 80% specimens during which signs of instability (smooth serrations) were observed.

The work hardening rate increased with increasing amounts of prior deformation.

3. Alloys With 3% Mn and C Contents Varying From 0.2 to 0.5%

a) Room Temperature Tests

The 0.2% C alloy remained essentially austenitic after processing. It transformed very readily, however, when deformed at RT (450°C < M_d < RT). The stress strain curves in Fig. 14a show that the amount of prior deformation and the time at 450°C required for the reduction in thickness affected the precipitation process and thus the austenite stability, very critically.

The higher stability of the austenite as compared to the corresponding 2% Mn alloy (Fig. 8c) was reflected in the lower work hardening rate of the specimen with 80% reduction in thickness. The work hardening rate was lower, although the sample was held for a longer time at 450°C (70 vs 60 min).

The greater loss of alloying elements due to a more extensive precipitation led to a lower austenite stability and thus to a markedly

higher strain hardening rate for the specimens with 80% prior deformation, as compared to specimens with 60% reduction in thickness. Specimens having 80% reduction in thickness usually required twice as much time as was needed to reduce a sample 60% at 450°C. This time factor was believed to be mainly responsible for the more extensive precipitation.

Figure 14a shows, however, that the specimen with 60% reduction in thickness, and not the one with 80% prior deformation, had the highest strain hardening rate. This strain hardening rate was even higher than that of the corresponding specimen of the 2% Mn alloy, which on account of its composition, was less stable and should have had a higher work hardening rate if the processing and testing conditions had been constant. This was, however, not the case: 60% reduction in this alloy required almost twice as much time as for the 2% Mn alloy (55 vs 30 min), and a higher work hardening rate due to a lower stability of the austenitic matrix was expected.

The time factor gains in importance as the amount of prior deformation increases. More nucleation sites are provided by additional deformation and thus precipitation takes place more rapidly. Moreover, the specimen with 60% reduction in thickness was dynamically "strain aged" for a much longer time than the specimens with a smaller amount of prior deformation, which were held for the same time (55 min) at 450°C. After the specimens with 20 and 40% prior deformation were reduced to their final thickness, they were essentially tempered till the 60% sample was fully reduced.

All this was reflected in the decreasing strain hardening rate with decreasing amounts of prior deformation. The specimen with 20% reduction in thickness, for instance, had a lower strain hardening rate than the

corresponding sample of the 2% Mn alloy, in spite of its much longer time at 450°C.

The fact that the specimen with 60% reduction in thickness was the least stable was further underlined by the suppressed "yield point." The question why the specimen with 80% prior deformation did not have a higher strain hardening rate than the specimen with 60% reduction in thickness still had to be answered. The austenite in the former specimen should have been less stable chemically, considering the aforementioned effects of processing time and amount of deformation on the precipitation process.

However, the difference in processing time in this case was only 15 min (70 vs 55 min). In other alloys where the strain hardening rate of the specimen with 80% reduction in thickness was significantly higher than that of the specimen with 60% prior deformation, the time difference amounted to a factor of two.

The main reason, however, for the fact that the actual instability of the austenite revealed during the test could not be increased indefinitely by increasing the processing time and amounts of plastic deformation was that there was a mechanical stabilization. The effect of this stabilization prevailed over a possible further decrease of the austenite stability on mere composition considerations as the amount of prior deformation increased.

Several factors contributed to this mechanical stabilization. The higher the dislocation density, the more difficult becomes the generation and motion of additional dislocations. Formation of martensite in iron-carbon alloys is associated with an increase in volume. This volume increase has to be accommodated by either slip or twinning. Low carbon contents and high temperatures favor the slip mode of deformation, whereas

the probability of twinning is increased when the carbon content is high and the deformation temperature is low. No twins formed at RT. Another factor was that the grain size of the austenite was effectively decreased by large amounts of plastic deformation. The resulting cell structure reduced the amount of martensite formed per nucleus, and thus led to a lower total amount of martensite.

On the other hand, small amounts of plastic deformation are known to stimulate the formation of martensite (5). Local stress concentrations are believed to be martensite nucleation sites. In the widely accepted reaction path theory (20,21) it is postulated that strain embryos exist in the austenite that provide part of the activation energy for the nucleation process. These embryos are visualized to be regions of localized strain in which the atoms in the austenite lattice are displaced part way along the path to their ultimate positions in the martensite.

Considering merely the two opposing mechanical effects, one expects a maximum stimulation of the martensite formation somewhere between small and very large amounts of prior deformation. The exact position of such a maximum will be determined by chemical factors such as the composition of the alloy matrix and processes affecting it, like precipitation. A change in test temperature usually renders a specimen of one treatment more unstable (or stable) than that of another treatment. In other words it seems to be impossible to establish general rules as to how much prior deformation at a given temperature will be necessary for a maximum amount of martensite to form, since this will change as the composition and other factors change.

All stress strain curves in Fig. 14a show serrations. In the specimen with 20% prior deformation they appear only after some initial strain, and there is no "yield point."

In the steeper portion of the stress-strain curve of the specimen with 60% reduction in thickness one observes that the serrations are much smaller (smaller amplitudes) than in the immediately preceding Luder's strain or the following (flatter) portion of the curve. This tendency of the serrations to decrease in amplitude as the slope of the stress-strain curve increases, agrees well with earlier observations. Above a certain critical slope the stress-strain curve is smooth and below this slope serrations appear. Stress induced formation of martensite initiated yielding for all thermomechanical treatments of this alloy (Table XI).

In the 0.3% C alloy the increasing effect of prior deformation on the yield strength values of a metastable austenitic steel as the stability of the austenite increases is clearly documented in Fig. 14b (compared with Fig. 14a). The austenite had become so stable that the measured yield strength was actually the yield strength of the austenite. The appearance of the yield point of the specimen with 80% prior deformation indicated that there was no phase transformation taking place as yielding began. No yield point appeared in the stress-strain curves of the specimens with different thermomechanical treatments. Beside the difference in reduction in thickness, the specimen with 80% prior deformation was held for 75 min at 450°C as compared to 45 min for the other specimens.

The austenite of the specimen with 80% reduction in thickness was thus rendered less stable chemically, which resulted in a higher elongation

value. The austenite became more strain rate sensitive, i.e. martensite formed more readily at sites of incipient necking and thus contributed effectively to the higher elongation values. The larger number of serrations demonstrated this. The first larger serration in the stress-strain curve of the specimen with 80% reduction in thickness was characteristic of this type of alloy, and such a burst of transformation often caused premature failure.

The actual magnitude of such serrations is a function of the elasticity of the testing machine. The Instron tensile testing machine used is not very stiff.

Since the work hardening rate was already so low that it approached the optimum value desired for maximum elongation, any further stabilization of the austenite would have resulted in lower elongation values.

The 0.4% C alloy (Fig. 14c) showed that the stability of the austenite had been increased to the point where martensite formed at too low a rate to effectively prevent necking at larger strains. The elongation values decreased with increasing amounts of prior deformation for the specimens held for the same length of time at 450°C (20, 40 and 60% reduction in thickness). The specimen with 80% reduction in thickness was dynamically "strain aged" for a longer time and the austenite thus became less stable. This lower austenite stability resulted in a higher elongation value than in the specimen with 60% prior deformation (Table XIII).

As in the preceding alloy, only the 80% specimen exhibited a yield point in its stress strain curve.

There were no serrations. Serrations seemed to appear when the competition between the slip mode of deformation and the formation of martensite as a mode of deformation was greatest, i.e. when they contributed more or less equally to the total deformation. The stress strain curves, however, had a smooth appearance when either of the flow

processes predominated, i.e. when martensite formed very readily, the work hardening rate was very high and the curve was smooth, or the curve was smooth when the work hardening rate was very low (when deformation occurred mainly by slip in the austenite).

The austenite in the 0.5% C alloy was even more stable and the elongation values were correspondingly lower (Fig. 14d) than in the preceding alloy (Fig. 14c). A comparison of Figs. 14b, c, and d shows how relatively small variations in carbon content affect the austenite stability, and thus the transformation induced plasticity of the alloys. The M_d temperature must still have been above RT for the specimen with 80% prior deformation, as can be seen by the temporary recovery after yielding (Fig. 14d). The amount of martensite, that formed during the test was, however, so little that it did not result in improved ductility. The other specimens behaved as if no phase transformation had taken place. The higher the strength, the lower the ductility (Table XIV).

b) Dry Ice Tests

Lowering the test temperature for the 0.2% C alloy from RT to -78°C changed the stress strain curves completely. The decreased austenite stability led to an average "yield strength" drop of 30,000 psi and a much higher work hardening rate which, in turn, reduced the elongation values (Fig. 15a; Table XI). The specimens with 20 and 40% reduction in thickness fractured at the holes.

In the specimens with 60 and 80% prior deformation fracture was preceded by necking.

The higher austenite stability of the 0.3% C alloy compared to the 0.2% C alloy (Fig. 15a) manifested itself not only in the higher yield strengths and lower work hardening rates but also in the completely

different shape of the stress strain curves (Fig. 15b).

The specimens with 40, 60 and 80% prior deformation exhibited a well defined Luder's strain portion in their stress strain curves. The difference in work hardening rate due to different thermomechanical treatments was evident. The work hardening rate decreased with decreasing amounts of prior deformation. The higher austenite stability, as reflected in the lower work hardening rates of the specimens with 20 and 40% reduction in thickness, resulted in an increase in yield strength at -78°C compared to RT, whereas the relatively lower austenite stability of the specimens with 60 and 80% reduction in thickness caused a decrease in "yield strength" with decreasing temperature (Table XII).

The amounts of increase or decrease in yield strength depended on the difference in austenite stability, i.e. the greater the change in austenite stability, the larger the increase or decrease in yield strength.

Necking preceded fracture in the specimens with 60 and 80% prior deformation.

For the 0.4% C steel, the higher yield strength values and the lower work hardening rates as well as longer Luder's strains (Fig. 15c) are signs for the higher stability of this alloy, as compared to the preceding alloy (Fig. 15b). The respective work hardening rates relate to the different thermomechanical treatments in the same way as in the previous case.

Necking preceded fracture only in the specimen with 80% reduction in thickness. The other specimens failed before the maximum in their stress-strain curves was reached. As in the preceding alloy the "yield strength" of the specimens with 20 and 40% reduction in thickness increased, whereas it decreased for the other, more heavily worked specimens as

the test temperature was lowered to -78°C.

While in the alloys of lower austenite stability an increase in work hardening rate due to a lower test temperature resulted in reduced elongation values, the ductility in this alloy was improved significantly by an increase in work hardening rate due to a decrease in test temperature (Table XIII). The reason for this was that the austenite stability at RT was too high and thus the work hardening rate was below the so-called "optimum" work hardening rate for maximum elongation. Lowering the test temperature from RT to -78°C raised the work hardening rate to above the optimum, but closer to it.

In the lower carbon alloys the work hardening rates at RT were above or very close to the optimum. An increase in work hardening rate, therefore, resulted in a departure from the optimum. This became even more obvious in the following alloy.

For the 0.5% C alloy, the further increased stability led to still higher yield strength and Luder's strain values and to lower work hardening rates (Fig. 15d). Moreover, the specimen with 80% reduction in thickness remained the only one whose yield strength decreased due to a change in test temperature from RT to -78°C. All the other specimens experienced an increase in yield strength which was larger the lower the amount of prior deformation (= the higher the austenite stability). In none of the specimens was fracture preceded by necking.

The less stable the austenite was at -78°C, the more specimens necked down before failing (see Figs. 15b, c, and d). In Fig. 15a all specimens should have necked down before fracture, except that the specimens with 20 and 40% prior deformation failed at the holes.

The elongation values at -78°C compared to RT changed according to the relative austenite stability. For the specimens with 80, 60 and 40% reduction in thickness it increased by the following factors, respectively: 10, 12, and 2. The specimen with 20% prior deformation elongated less at -78°C than at RT.

In the specimen with 40% reduction in thickness the austenite stability was sufficiently affected by the test temperature decrease so that the resulting transformation raised the work hardening rate closer to the optimum. In the specimens with 80 and 60% prior deformation the work hardening rate was raised to above, but very close to, the optimum work hardening rate.

Since the specimen with 60% reduction in thickness had the lower work hardening rate of the two, it is not surprising that its elongation value was higher. It was expected that a specimen with a reduction in thickness between 60 and 40% at 450°C would yield optimum elongation values under the given tests conditions.

C. The Effects of 80% Reduction in Thickness at Varying Rolling Temperatures on the Tensile Properties of a Metastable Austenitic Stainless Steel

1. Alloys With 2% Mn and C Contents Varying From 0 to 0.5%

a) Room Temperature Tests

The 0.0% C alloy was ferritic after cooling from 1200°C to RT. Assuming that this alloy was carbon free, it is difficult to explain the relative yield strength of the different specimens (Fig. 16a). One would expect that a specimen rolled at RT would have the highest yield strength, but it yielded at a lower stress than all the other specimens. Variation in reduction in thickness or in handling during the specimen

preparation should have had the same effect in tests at different temperatures. However, the yield strengths of the specimens rolled at 250 and 450°C were highest in the RT and 100°C tests, whereas the specimens rolled at RT and 100°C had a higher yield strength when tested at -78 and -196°C (Table I). This difference suggested that there might have been some carbon in the alloy (through the iron used), and possibly more than was found by chemical analysis (0.008% C). If some carbon were present, then there was a possibility of carbide precipitation, which would have affected the yield strength. Moreover, not all austenite may have transformed to the body centered phase, and the amount of ferrite may have been increased after the composition of the matrix has been altered by rolling at 450 and 250°C, respectively. This could explain why the specimens rolled at 450 and 250°C exhibited a higher yield strength than the specimens rolled at 100°C and RT, when tested at RT and 100°C, because all specimens were at RT before the tests. For the tests at -78°C and -196°C, there should not have been any difference in the amount of body centered phase between the specimens rolled at different temperature, because cooling the specimens to the respective tests temperatures would have transformed the retained austenite. The expected difference in yield strength should have been due only to the different dislocation density resulting from rolling at different temperatures. The yield strength was found to be lower the higher the rolling temperatures, when tested at -78 and -196°C.

The 0.1% C alloy was partly martensitic after cooling from 1200°C to RT. The retained austenite was so unstable that the difference in rolling temperature between RT and 450°C resulted in a difference in yield strength of 200,000 psi (Table II). Tempering of the martensite

and a change in matrix composition due to the precipitation also contribute to this difference.

The rolling temperature not only affected diffusion, and thus precipitation and the tempering of the martensite, but also the amount of additional martensite that formed as a result of plastic deformation.

The stress strain curves in Fig. 16b clearly show the effect of different rolling temperatures. While the specimen rolled at RT failed in a brittle manner (untempered martensite), the other specimens started deforming plastically as a result of stress-induced formation of martensite.

The effect of the rolling temperature on the stability of the retained austenite, and thus on the work hardening rate, was evident. The work hardening rate increased with increasing rolling temperatures, indicating the effect of precipitation on the matrix composition.

In the specimen rolled at 250°C the competition between slip and formation of martensite as possible modes of deformation seemed to be greatest. The increasing amplitude and decreasing frequency (distance between serrations increased) underline the greater difficulty with which martensite formed toward the end of the test. In addition to the fact that the nucleation of a sufficient amount of martensite became more difficult, the formation of martensite was hampered by an increase of the specimen temperature (12) during the test.

The strain hardening rate of the specimen rolled at 450°C was the highest. The ready formation of martensite resulted in a smooth stress-strain curve (formation of martensite was the predominant mode of deformation).

The higher stability of the 0.2% C alloy reduced the amount of martensite formed during processing and prevented martensite formation

during cooling from 1200°C to RT. This was reflected in the much lower fracture strength of the specimen rolled at RT.

The stress strain curves of all the other specimens (Fig. 16c) showed serrations. The work hardening rates and "yield strengths" were affected by the rolling temperatures in the same way as in the preceding alloy.

Plastic deformation started as a result of stress-induced formation of martensite in all specimens except the one rolled at RT (Table III).

While in the preceding alloy the specimen rolled at 450°C did not exhibit any serrations in its stress strain curve (Fig. 16b), serrations occurred in the stress strain curve of the corresponding specimen of this alloy (Fig. 16c), but only during the second half of the test. This was due to the higher stability of the austenite which made it more difficult to form martensite after the easy nucleation sites had been used up.

In the next following alloy the stress strain curve of the specimen rolled at 100°C was smooth, compared to the others (Fig. 16d), because the stability of the austenite had increased so much that the formation of martensite became very difficult and slip was the predominant mode of deformation.

Whenever one mode of deformation was prevalent, the stress strain curve became smooth, but as soon as slip and formation of martensite started to compete with one another as modes of deformation, the stress strain curve became serrated.

On comparing the effects of varying amounts of prior deformation at 450°C, the time factor played a significant role. The time for which specimens were held at different temperatures while being reduced 80%

was less important because of the exponential temperature dependence of diffusion and precipitation processes. The maximum time required to reduce a specimen 80% at a given temperature was about twice the minimum time (or less) for the same reduction at another temperature.

Doubling the rolling time at 450°C was equivalent to a temperature increase of approximately 20°C with respect to its effect on the precipitation process. The different rolling temperatures were widely enough separated so that the time factor could be completely neglected for qualitative comparisons.

As previously pointed out, there was only a very slight, but still noticeable increase, in austenite stability as compared to the preceding (0.2% C) alloy (the increase in carbon content is smaller than indicated and a decrease in chromium content almost cancelled the effect of the carbon increase; Table XVII).

The increase in austenite stability was reflected in the higher yield strength values and the slightly lower work hardening rates (Fig. 16d, Table IV). The relatively larger increase in yield strength in the specimen rolled at 100°C was due to the fact that the onset of yielding was not initiated by a stress-induced formation of martensite as it was in the specimens rolled at 250 and 450°C.

The slightly increased strength of the specimen rolled at RT may have been due to the increased hardness of the martensite. Martensite still formed very readily at RT, and since the specimen is not tempered, it failed by brittle fracture. The strong effect of higher rolling temperatures on the austenite was evident. The specimen rolled at 450°C always had the lowest yield strength and the highest tensile strength, provided the other specimens were essentially austenitic before the test too.

While the stress strain curve for the specimen rolled at 100°C was relatively smooth, the curves of the specimens rolled at 250°C and 450°C respectively, were heavily serrated (Fig. 16d). It should be noted, however, that the serrations in the curve of the specimen rolled at 250°C were much larger, i.e. of a greater amplitude, than the ones caused by the specimen rolled at 450°C. The greater amplitude usually indicated a more difficult formation of martensite. This agrees well with the relative austenite stability of the two specimens, as reflected in their yield strengths and work hardening rates. Since rolling at 450°C resulted in the lowest austenite stability of all the specimens to be compared, it was not surprising that martensite formed more readily and thus the serrations were smaller. Comparison with the corresponding curve of the preceding alloy (80%, 450°C) in Fig. 16c showed that the first portion of the stress strain curve was smooth because of the still lower austenite stability of that specimen.

As the austenite stability was increased even more (in the 0.4% C alloy) the difference in yield strength values between the specimens rolled at different temperatures decreased (Fig. 17b and d). Less martensite formed during rolling at room temperature, and plastic deformation was not initiated by a stress-induced formation of martensite in the specimens rolled at 100, 250 and 450°C (Table V). The specimen rolled at RT failed by brittle fracture (untempered martensite).

The stress-strain curves of the other specimens (Fig. 16e) exhibited higher yield points and lower work hardening rates. On account of the higher stability of the austenite, the slip mode of deformation gained in importance. This was reflected in the smoother appearance of the stress strain curves. The lower the relative austenite stability due

to different rolling temperatures, the earlier sharp serrations occurred. In other words, serrations appeared at smaller strains, the easier martensites formed. Moreover, it can be observed again that the amplitude of the serrations increased with increasing austenite stability.

The high austenite stability of the 0.5% C alloy reduced the yield strength of the specimen rolled at RT to its lowest value, compared to the corresponding specimens of the preceding alloys. The amount of martensite that formed during rolling was so little that the specimen failed in a ductile manner.

The yield points of the other specimens (Fig. 16f) reached their highest values on account of the high austenite stability.

All specimens fractured soon after yielding, with the exception of the specimen rolled at 450°C which had the lowest austenite stability among the specimens of this alloy. This slightly lower austenite stability permitted some martensite to form during the RT tests so that the specimen could continue to stretch more after yielding. This was reflected in the horizontal portion of the stress strain curve. The rate of martensite formation was, however, too low for the specimen to sustain large strains.

b) Dry Ice Tests

The small amount of carbon found in the 0.0% C alloy had an effect on the yield strength in RT and 100°C tests, but at -78°C and -196°C all specimens had the same amount of ferrite and thus the difference in yield strengths as a result of different rolling temperatures was due only to the difference in dislocation density (Table I, Fig. 18a). No transformation took place during the tests.

Since the 0.1% C alloy had transformed partly on cooling from 1200°C to RT, more martensite formed when the specimens were cooled to -78°C.

This was verified by magnetic measurements, and manifested itself in the fact that the yield strength values for the specimens rolled at 100, 250 and 450°C were practically unchanged, as compared to the room temperature tests (Table II), although the retained austenite became even more unstable with respect to deformation. The work hardening rate was strongly increased as a result of the lower test temperature (Fig. 18b) and changed with the rolling temperatures, as in the room temperature tests. The austenite stability was the lower the higher the rolling temperature.

The higher strength of the specimen rolled at RT when tested at -78°C was due to the test temperature difference only. No phase transformation took place, whereas in the other specimens plastic deformation started as a result of the stress-induced formation of martensite.

The "yield strength" values in the 0.2% C alloy were lower than in the 0.1% C alloy, although the austenite had become more stable. The work hardening rates were lower and there was a well defined Luder's strain portion in the stress strain curves (Fig. 18c). The lower yield strengths were due to a smaller amount of pre-test martensite. Stress-induced formation of martensite initiated plastic deformation. The tensile strengths of the specimens rolled at 100, 250 and 450°C exceeded the fracture strength of the specimen rolled at RT, which failed by brittle fracture due to its high amount of untempered martensite (Table III).

The slight increase in austenite stability in the 0.3% C alloy, as compared to the preceding alloy, was reflected in larger Luder's strains, lower work hardening rates and higher yield strength values (Fig. 18d). Everything else said for the preceding (0.2% C) alloy still applied.

For the 0.4% C alloy, a further increase in "yield strength" values

and Luder's strains and a decrease in work hardening rates occurred. The Luder's strain portion became longer and wavier as the austenite stability increased (Fig. 18e). Sharp serrations, as found in RT tests, were not observed. Moreover, in all the lower carbon alloy of this series, necking preceded fracture in the specimens rolled at 100, 250 and 450°C. In this alloy fracture occurred at the maximum of the stress strain curve before necking set in. This effect that necking occurred before fracture at -78°C depended on the austenite stability and had already been observed in specimens with varying amounts of prior deformation.

The 0.5% C alloy provided the only specimen rolled at RT that deformed plastically at RT and at -78°C. The fact that the retained austenite in the other alloys did not transform at all at -78°C (in spite of high stresses) indicated that the amount of untempered martensite played an important role in governing the type of fracture, independent of a thermodynamically possible phase transformation. Figure 18f shows how much the austenite stability within a given alloy can be changed by varying the rolling temperature. Rolling at 450°C resulted in the lowest austenite stability. This was clearly demonstrated by the lowest yield point, the lowest Luder's strain and the highest work hardening rate.

Compared to the room temperature tests, the "yield strengths" were hardly increased, indicating that yielding was assisted by the formation of martensite.

The elongation values were significantly higher than at RT where the rate of martensite formation was too low.

2. Alloys With 1% Mn and C Contents Varying From 0.2 to 0.5%

a) Room Temperature Tests

In the 0.2% C alloy, approximately 50% of the austenite transformed to martensite when this alloy was cooled from 1200°C to RT. Since the retained austenite was very unstable with respect to plastic deformation more martensite formed during rolling. The yield strength, therefore, was strongly influenced by the amount of martensite formed before the test. The rolling temperature not only affected the amount of martensite that forms during rolling and the relative austenite stability, but also played a role in this alloy as a martensite tempering temperature.

The stability of the austenite remained higher the lower the rolling temperature. On the other hand, more martensite formed during rolling the lower the rolling temperature. The results of this strong influence of rolling temperature on the formation of martensite during the test can be seen in the stress strain curves shown in Fig. 19a.

The specimen rolled at RT had only a small amount of relatively stable austenite left, and thus not enough martensite formed during the test to prevent necking at this stress level (350,000 psi). The specimen fractured soon after yielding set in.

At 100°C, less martensite formed during rolling and some precipitation occurred (3 hrs at 100°C). There was more austenite of a lower stability available for transformation during the test. The austenite stability was affected chemically by the precipitation process and mechanically by the formation of martensite during rolling. Both effects decreased the austenite stability as the rolling temperature increased (more precipitation, less martensite). The specimen rolled at 100°C formed enough martensite during the test to recover after the initial

yielding (horizontal portion of the stress strain curve). The work hardening rate, however, was not sufficient to sustain large strains.

As the rolling temperature was increased further to 250 and 450°C, martensite formed more readily and higher elongation values were obtained.

Stress-induced formation of martensite initiated plastic deformation in the specimens rolled at 100, 250 and 450°C (Table VII). The significant change in austenite stability due to varying rolling temperatures was reflected in the work hardening rates (Fig. 19a).

The higher stability of the 0.3% C alloy resulted in lower "yield strength" values, since the amount of pre-test martensite was drastically decreased. Yielding was initiated by formation of martensite in all but the specimen rolled at RT (Table VIII).

The stress strain curves in Fig. 19b showed very clearly that the amplitude of the serrations increased as the formation of martensite became more difficult. In the specimen rolled at 450°C martensite formed very readily, while less martensite formed per unit strain in the specimen rolled at 100°C. This was documented by the different work hardening rates.

In the 0.4% C steel, as the austenite stability increased further, the formation of martensite became more difficult. This was reflected in the amplitude of the serrations seen in Fig. 19c. The serrations in the stress strain curves shown in Fig. 19c are obviously larger than the ones exhibited by the corresponding curves of the preceding alloy (Fig. 19b). Moreover, the relative difference in austenite stability due to different rolling temperatures was clearly demonstrated (Fig. 19c), not only by the difference in "yield strength" (Table IX) and work hardening rate, but also by the distinct size difference of the serrations. Each

of these quantities could be taken as an indicator for the relative stability of the austenite in this alloy.

The stress strain curves for the 0.5% C alloy in Fig. 19d clearly show that this alloy was too stable for maximum elongation values. The difference between the yield strength of a specimen rolled at RT and the one rolled at 450°C decreased with increasing austenite stability (Fig. 17a and d). Higher stresses were required to initiate yielding by the $\gamma \rightarrow \alpha'$ phase transformations in the latter, and less martensite formed during rolling of the former. The slopes of the stress strain curves still revealed the relative austenite stability. While the slope of the stress strain curve of the specimen rolled at 450°C was slightly positive, it decreased with decreasing rolling temperature and became slightly negative for the specimen rolled at RT. Too little martensite formed per unit strain to prevent failure at the site of incipient necking.

b) Dry Ice Test

The decreased austenite stability of the 0.2% C alloy at -78°C compared to RT resulted in an improved ductility for the specimen rolled at 100°C. The specimens rolled at 250 and 450°C had relatively high work hardening rates at RT and thus a further increase resulted in higher tensile strength but lower elongation values (Fig. 20a). Small cracks in the specimen rolled at RT caused it to fracture at the hole.

The decrease in test temperature for the 0.3% C steel brought about the usual changes in "yield strength" and strain hardening behavior. The low stress level at which martensite started forming and the high work hardening rate (Fig. 22b) caused the specimens rolled at 250 and 450°C to fail at the hole.

The increased austenite stability of the 0.4% C steel, as compared

to the preceding (0.3% C) alloy, resulted in higher "yield points" (Table IX), clearly defined Luder's strains, and a more distinct difference in work hardening rate due to the different rolling temperatures (Fig. 20c).

As the carbon content was further increased to 0.5%, the Luder's strain and "yield points" kept increasing and the work hardening rate decreased, with respect to the lower carbon alloys. The relative effects of the different rolling temperatures were very distinct. The highest rolling temperature resulted in the lowest "yield point" and highest tensile strength whereas the reverse was true for the lowest rolling temperature (Fig. 20d, Table X).

3. Alloys With 3% Mn and C Contents Varying From 0.2 to 0.5%

a) Room Temperature Tests

Changing the rolling temperature of the 0.2% C alloy from RT to 100°C resulted in a difference in yield strength of approximately 120,000 psi (Table XI). This difference was mainly due to the different amounts of martensite that formed during rolling. Rolling at 100°C left not only more austenite untransformed but also decreased its stability (through precipitation) which led to an even lower "yield strength."

Changes in rolling temperature above 100°C and thus above the M_d temperature, affected the tensile properties mainly through the resulting change in austenite stability.

Rolling at 100°C seemed to provide a work hardening rate that was very close to the optimum work hardening rate yielding maximum elongation values (Fig. 21a). The higher work hardening rates of the less stable specimens, rolled at 250 and 450°C, resulted in lower elongations.

Stress-induced formation of martensite, and not slip, was responsible for the onset of plastic deformation in the specimens rolled at 100, 250 and 450°C.

The increased austenite stability of the 0.3% C alloy, as compared to the preceding (0.2% C) alloy, resulted in less martensite being formed during rolling at RT, and thus in an effective drop in yield strength. For the specimens rolled at higher temperatures, the yield strength values increased due to the increased austenite stability (Table XII). The difference in yield strength between specimens rolled at RT and 450°C decreased more rapidly with increasing carbon content for alloys with 3% Mn than for alloys containing 2% Mn (Figs. 17b, c, and d). Yielding was caused by slip in the austenite, and not by stress-induced formation of martensite, in all specimens. (Note the different appearance of the yield points in Fig. 21b as compared to Fig. 21a.)

The relative change in austenite stability caused by the different rolling temperatures was very distinct. It was clearly reflected in the elongation values in Fig. 21b. The work hardening rates of the specimens rolled at 24, 100, and 250°C were definitely below the optimum value, which was closely approached by the specimen rolled at 450°C. While deformation in the specimens rolled at the lower temperatures occurred mainly by slip (smooth stress strain curves), formation of martensite competed with slip as a mode of deformation in the specimen rolled at 450°C (serrated stress strain curve).

The higher carbon content in the 0.4% C alloy increased the stability of the austenite so much that the specimens rolled at 24, 100 and 250°C did not recover after the initial yielding. Too little martensite formed per unit strain, although the M_d was above the test temperature ($100°C > M_d > RT$).

The effect of varying rolling temperatures was evident. Rolling at RT transformed some of the original austenite to martensite. This

small amount of martensite led to a distinctly higher yield strength (Fig. 21c, Table XII).

The change in austenite stability due to rolling at 100, 250 and 450°C was reflected in the elongation values (Fig. 21c). The higher the rolling temperature, the more martensite formed during the test. The specimen rolled at 450°C formed a sufficient amount of martensite to recover after the initial yielding.

Since the M_d temperature of the 0.5% C alloy was close to or at room temperature, no martensite formed during rolling. Rolling at 100, 250 and 450°C did, however, raise the M_d temperature to above the room temperature and thus made the formation of some martensite possible.

Although all specimens failed soon after yielding began, the stress strain curves in Fig. 21d shows that the tendency for a specimen to recover increased with increasing rolling temperatures.

b) Dry Ice Tests

Lowering the test temperature for the 0.2% C alloy resulted in an increase in strength of the specimen rolled at RT, while the "yield strengths" of the other specimens decreased by about 35,000 psi on account of the lower austenite stability (Table XI). The maximum difference in yield strength due to different rolling temperatures (24°C and 450°C) approached 200,000 psi.

Since the specimens rolled at 100, 250 and 450°C had work hardening rates close to the optimum at RT, lowering the test temperature to -78°C increased the work hardening rates and thus lower elongation values resulted.

The stress strain curves in Fig. 22a show clearly defined Luder's strains but no sharp serrations.

The "yield strength" values of all specimens of the 0.3% C alloy were lower at -78°C than at RT. The decrease in austenite stability was, however, much more apparent in the elongation values. At room temperature, only the specimen rolled at 450°C had a strain hardening rate close to the optimum strain hardening rate yielding maximum elongation. All the other specimens rolled at lower temperatures had lower strain hardening rates and thus less elongation (Fig. 21b). An increase in work hardening rate due to a lower test temperature meant a departure from the optimum value for the specimen rolled at 450°C, whereas the work hardening rates of all the other specimens were brought closer to that optimum.

Figure 22b shows the expected results. The elongation for the specimen rolled at 450°C was less at -78°C than at RT, whereas the elongation values of the other specimens increased. The increase with respect to the room temperature values was ten fold for the specimen rolled at RT, about four fold for the specimen rolled at 100°C, and the specimen rolled at 250°C almost doubled its room temperature value. The elongation of the specimen rolled at 450 C was only 2/3 of its room temperature value.

The work hardening rates of all 0.4% C alloy specimens were below the critical optimum value at RT. Since the relative work hardening rates of the specimens were higher the higher the rolling temperatures, the specimen rolled at 450°C had a value closest to the optimum and exhibited therefore, the greatest elongation (Fig. 21c).

The increase in work hardening rates due to the lower tests temperature (-78°C) shifted the work hardening rates of the specimens rolled at 100, 250 and 450°C closer to and above the optimum value in such a way that the greatest elongation was obtained for the specimen rolled at 100°C (Fig. 22c). The rate of the martensite formation was too low

in the specimen rolled at RT to yield high elongation values. Its work hardening rate remained below the optimum.

The higher austenite stability of the 0.5% C alloy compared to the preceding (0.4% C) alloy, decreased the work hardening rate of all the specimens so that they were shifted with respect to the optimum value. Figure 22d shows that the elongation of the specimen rolled at 250°C was increased while the specimen rolled at 100°C had less elongation than in the preceding alloy (Fig. 22c).

In comparison with the room temperature values (Fig. 21d), the elongation of all specimens was increased more than in any other alloy by lowering the test temperature to -78°C.

D. The Effects of Test Temperature Variations Between RT and -196°C on the Yield Strength of a Metastable Austenitic Stainless Steel

1. Alloys With 2% Mn and C Contents Varying From 0.2 and 0.5%

Figures 23a through 23d show how the yield strength varied with the test temperature at different carbon contents for all thermodynamical treatments applied.

The lower the carbon content the less stable was the austenite. The austenite stability affects the yield strength in three ways. First by the amount of martensite that forms during processing, secondly by the amount of martensite that forms during cooling to the test temperatures which lie below the rolling temperatures, and thirdly by the ease with which martensite formation can be induced by elastic stresses.

It is obvious that when a large amount of martensite forms during rolling, e.g. at RT, the effect of further transformation decreases as the amount of (transformable) austenite decreases.

For the specimens reduced 80% at RT there was only a very small decrease in yield strength due to the test temperature being changed,

because of these two opposing effects. The amount of austenite retained after processing is the smaller the less stable the austenite, and thus it becomes more difficult to compensate for the normal temperature dependence of the yield strength in non-transformable material (e.g. martensite) by a decrease in stress required to initiate the transformation of the retained austenite.

In the alloy containing 0.2% C (Fig. 23a) the "yield strength" decreased with decreasing temperatures for all thermomechanical treatments. At a carbon content of 0.5%, however, the austenite was so stable that a possible transformation due to elastic stresses could only modify the temperature dependent increase in strength as the test temperature was lowered (Fig. 23d).

The curves of specimens with the following thermomechanical treatments, 80%, 100°C; 80%, 250°C, 80%,450°C; and 60%, 450°C, showed a clear minimum in Figs. 23a, b, and c. This minimum was due to the fact that only relatively little martensite formed when the samples were cooled to -78°C, while the amount of pre-test martensite was increased measurably by lowering the temperature to -196°C.

Reducing specimens 40 and 20% at 450°C did not lower the austenite stability as much as for the other thermomechanical treatments (except 80% RT), so that the amount of martensite that formed at -196°C, although considerable, was not as large as for the above mentioned specimens.

The stress to induce the formation of martensite at -196°C was so much lower than at -78°C or RT, that its effect prevailed over that of the increased amount of martensite formed on cooling to that temperature (Fig. 24).

Figure 24 also shows that the relative increase in martensite due to quenching was much smaller for the 0.3% C alloy than for the above (0.2% C) alloy.

The fact that this resulted in even larger yield stress decreases with decreasing test temperatures seemed to indicate that the formation of martensite by quenching was not in the same way dependent on the austenite stability as was the stress-induced formation of martensite.

The drastic change in slope from Fig. 23c to Fig. 23d demonstrated once more how sensitively the austenite stability depended on the composition of an alloy. This was especially true for the specimens with 60, 40 and 20% reduction in thickness.

2. Alloys With 0.2% C and Mn Contents Varying From 1 to 3%

The alloy containing only 1% Mn was already 50% martensitic at RT and formed more martensite on quenching to -78 and -196°C. The curves in Fig. 25a show a clear minimum. The yield strength values measured at -196°C were higher than those at RT.

As the Mn content was increased (2% Mn) less martensite formed before the actual test. This resulted in flatter minima and lower yield strength levels (Fig. 25b) for the respective thermomechanical treatments. The yield strength values at RT were higher than at -196°C.

More manganese (3% Mn) increased the austenite stability and thus raised the yield strength values (Fig. 25c).

The yield strength of the specimens with 20 and 40% reduction at 450°C did not keep decreasing with decreasing temperature, as in the 2% Mn alloy, but increased slightly at -196°C as compared to -78°C. This was not due to a largely increased amount of martensite (Fig. 25d) as a result of quenching, but rather due to a smaller decrease in stress

(higher austenite stability) necessary to induce the $\gamma - \alpha'$ phase transformation as compared to the 2% Mn alloy. This decrease in stress at -196°C was more than compensated for by the temperature dependent increase in strength of the material, which was too stable to transform or could not undergo a phase transformation.

Figure 25d shows the difference in saturation induction between RT and -78°C and between RT and -196°C. The stabilizing effect of manganese is apparent.

E. The Effects of Alloy Composition

The effect of the alloy composition on the austenite stability is further outlined in the Figs. 26a, b, and c for specimens with 20% reduction in thickness at 450°C.

Figure 26a shows the alloy with 0.2% C with the highest yield strength values at all temperatures because of its large amount of pre-test martensite. The yield strength dropped as the carbon content increased to 0.3% because less martensite formed before the test, with a further increase in carbon the yield strength increased as the stability of the austenite increased and higher stresses were required to bring about the $\gamma - \alpha'$ transformation.

Alloys with 2% Mn and varying carbon content are shown in Fig. 26b. The normal, temperature dependent increase in yield strength is given by the alloy without carbon (no transformation; ferritic). Some austenite was retained in the alloy with 0.1% C. Part of this austenite transformed on loading and thus caused a lower yield strength as compared to the 0% C alloy. The yield strength values dropped further with alloys containing 0.2 and 0.3% C because of the decreasing amount of pre-test martensite. Then the yield strength increased again as the carbon content increased,

rendering the austenite more stable and thus making the $\gamma - \alpha'$ phase transformation more difficult.

In Fig. 26c, 3% Mn had stabilized the austenite so much that the alloy with 0.2% C showed the lowest yield strength values. The variation in the amount of martensite present before the test did not play a role with respect to the yield stress levels. An increase in carbon beyond 0.2% resulted immediately in an increase of the yield strength values on account of the increased austenite stability. (This was in contrast to the alloys with less manganese.)

The effect of increasing Mn content at 0.2 and 0.4% C is shown in Figs. 27a and b for specimens reduced 20% at 450°C. At 0.2% C the amount of martensite in the 1% Mn alloy (Fig. 27a) was about 50%, whereas only 5% martensite was present before pulling at -196°C in the 2% Mn alloy. This difference was mainly responsible for the much lower yield strength values of the 2% Mn alloy. The yield strength increased again as the austenite stability increased for the 3% Mn alloy.

At 0.4% C (Fig. 27b) the increase in carbon content, as compared to Fig. 27a, reduced the amount of pre-test martensite so much that it did not play an important role anymore in affecting the yield strength. The increasing stability of the austenite with increasing Mn-content was, however, very obvious, especially between 2 and 3% Mn where the slope in the curves of Fig. 27b changed from a positive to a negative one, reflecting again the normal temperature dependence of the yield strength in alloys that do not undergo any, or only very little, phase transformation.

F. Stress-Induced Formation of Martensite

A stress-induced phase transformation was responsible for the unusual decrease in yield strength at lower temperatures. In order to prove that elastic stresses induce the formation of martensite, three specimens were tested at -78°C up to their respective yield strengths and then unloaded. The specimens were then tested to failure at RT. Specimens of alloy no. 692-9 (1% Mn, 0.2% C) with following thermomechanical treatments 80%, 250°C; 40% 450°C, and 20%, 450°C were chosen because their yield strength vs test temperature curves (Fig. 25a) exhibited the largest variation in yield strength with temperature.

The results (Table XVI) prove that a decrease in austenite stability due to a lower test temperature resulted in lower stresses required to bring about $\gamma - \alpha'$ phase transformation. The difference in yield strength between -78°C and RT varied from 30,000 to 50,000 psi, depending on the thermomechanical treatment.

The "yield strengths" measured at -78°C were slightly higher than the ones obtained in the regular dry ice tests (Tables VII and XVI) because they represent the strength at the moment of unloading which took place at a strain of about 0.4% or more (compared to the 0.2% strain-yield strength in the regular tests). The yield strength values at RT, after straining at -78°C did not change very much with respect to the results of the regular RT tests (Tables VII and XVI). The relative small increase in martensite (the alloy was already 50% martensitic) due to quenching to -78°C and straining at this temperature lowered the elongation values much more than it increased the yield strengths.

Another specimen (alloy no. 6811-15; 80%, 250°C, Table IX) was loaded at RT to a stress level 40,000 psi below its elastic limit at

this temperature. On quenching the specimen to -78°C the effects of thermal contraction of the specimen and the fixtures were registered on the load-extension graph, however, shortly after this rapid quench the stress level was the same as at RT, indicating that no phase transformation had taken place. This was verified by observation of the polished specimen surface and measurement of the gage length. At a stress level 30,000 psi below the elastic limit at RT, however, plastic deformation was initiated by the formation of martensite upon quenching to -78°C resulting in a stress drop of 35,000 psi and a permanent elongation of 0.11%. Figure 29 shows the polished specimen surface after martensite formed.

These experiments prove conclusively that the martensitic transformation can be initiated by elastic stresses at temperatures above M_s.

G. Optical Microscopy

Figure 28a shows the microstructure of a partly martensitic alloy (No. 6811-13) which had been reduced 60% at 450°C (40 min). Deformation markings can be seen in the retained austenite. Some precipitation took place during the rolling process outlining the grain boundaries and austenite-martensite interfaces. The stress-strain curve of this specimen is given in Fig. 8b.

Figure 28b shows the microstructure of a specimen with exactly the same thermomechanical treatment except that it had been tempered for 80 more minutes at 450°C (total time at 450°C: 2 hours). Additional precipitation took place in the austenite, the martensite and at the interfaces. The austenite stability was thus lowered and the resulting stress strain curve at RT resembled the one for the untempered specimen

at -78°C (Fig. 11b), with the exception that the yield strength remained the same in spite of the decreased austenite stability. This was due to the strengthening effect of the precipitates.

Figure 29a shows the surface of an electropolished specimen (alloy No. 6811-15, 80%, 250°C) after stress-induced formation of martensite. The specimen was loaded at RT to a predetermined stress level and then quenched to -78°C. Figures 29b and c show some features of the martensite as they appeared on the unetched surface. The tensile axis is indicated.

Figures 30a through d show the microstructures of specimens (alloy No. 689-15) with the following thermomechanical treatment: 20%, 450°C; 40%, 450°C; 60%, 450°C and 80%, 450°C. All samples were essentially austenitic. The samples with 20, 40 and 60% reduction in thickness had the same microstructure as the one with 80% prior deformation (Fig. 30d) before they were rolled down to the starting dimensions required to yield 20, 40 and 60% reduction and austenitized (1200°C, 1 hr.) again.

The effects of varying degrees of cold work on the recrystallized grain size are apparent. Moreover, it can be seen how much more the austenite grains align themselves in the rolling direction as the amount of final reduction increases. The rolling direction is indicated, and the respective stress strain curves can be found in Figs. 8d and 11d.

The effects of varying rolling temperatures on the microstructure of specimens with 80% reduction in thickness are seen in Figs. 31a through d. In Fig. 31a most of the grains are austenitic. The relatively large amount of precipitates at 450°C makes a distinction between austenite and martensite difficult. The amount of martensite should be negligibly small according to magnetic measurement. In Fig. 31b (250°C) a distinction between these two phases becomes easier. As the rolling

temperature decreased further to 100°C (Fig. 31c) and RT (Fig. 31d), the amount of martensite increased strongly and thus the original austenite grain boundaries disappeared more and more. The respective stress strain curves can be found in Figs. 16d and 18d.

The micrograph in Fig. 32 clearly shows that two modes of deformation were operative when an austenitic sample of alloy No. 689-15 was deformed at RT. An austenite grain with deformation markings is surrounded by martensite. It was mentioned previously that serrations occur in a stress strain curve when these two modes of deformation compete with one another.

The heavily serrated stress strain curves (Fig. 16d) of the specimens rolled at 250 and 450°C which were essentially austenitic before the room temperature test, seemed to prove this.

IV. SUMMARY AND CONCLUSIONS

The purpose of this investigation was to elucidate the conditions under which the γ - α' phase transformation can be utilized to improve the mechanical properties of metastable austenitic stainless steels.

The alloy system chosen evolved from a series of alloys designed to enhance the ductility of high strength steels by means of a deformation induced phase transformation.

It has been found that the austenite stability has by far the greatest effect on the mechanical properties investigated. Changes in chemical composition and test or processing temperatures strongly affect the stability of the austenite, which can be critically modified by thermo-mechanical treatments.

The stability of the austenite affects the yield strength, ultimate tensile strength, the work hardening rate, the Luder's strain and the total elongation.

Yielding is initiated by stress-induced formation of martensite when the austenite stability is low. The stress required to bring about this transformation decreases with decreasing austenite stability.

Easy formation of martensite leads to a high work hardening rate and thus to large ultimate tensile strengths and small elongation values.

There is usually no Luder's strain portion in the stress strain curve when the austenite is very unstable.

As the austenite stability increases, higher stresses are required to initiate the phase transformation (higher yield strength) and the work hardening rate decreases (less martensite forms per unit strain), which in turn results in higher elongation and Luder's strain values as well as in lower tensile strengths.

The formation of martensite, per se, does not result in a serrated stress strain curve. Serrations appear when the formation of martensite becomes more difficult as the austenite stability increases.

At -78°C the austenite stability of most of the alloys tested is so low that martensite forms very readily and the stress strain curves remain smooth after some signs of instability in the Luder's strain portion. When the austenite is very stable the stress strain curve is smooth too, since only very little or no martensite forms during testing. Somewhere between these extremes in austenite stability there is a maximum as to the formation of serrations and their amplitude.

It was shown that increasing the stability of a very unstable alloy by adding elements like C or Mn leads to the appearance of, first, small and then larger serrations in the stress strain curve; as the austenite is rendered even more stable the serrations become smaller again and finally disappear. The same can be observed by lowering the stability of a stable austenite.

Since the slope of a stress-strain curve (work hardening rate) depends on the stability of the austenite there is an upper and lower critical slope between which serrations appear in the stress strain curves.

There are two modes of deformation operative in the alloys investigated: slip and the formation of martensite. When the austenite stability is low, formation of martensite is the predominant mode of deformation resulting in a high work hardening rate and a smooth stress strain curve.

On the other hand, deformation occurs by slip in the austenite when very little or no martensite forms, i.e., when the work hardening rate of the alloy approaches the austenite work hardening rate.

Serrations appear when these two modes of deformation compete with one another.

A distinction is made between stress-and strain-induced formation of martensite, although the martensite embryo is looked upon as a stress embryo and the effect of strain, as a consequence of either the martensite or slip mode of deformation, is such that it results in stress peaks above the average stress level set up in the lattice.

Stress-induced formation of martensite usually takes place when the austenite stability is low. It initiates yielding at a relatively low stress level and thereafter the stress increases rapidly (high work hardening rate) so that embryos of less favorable orientation and less energy can be activated readily after the easy nucleation sites have been used up.

On the other hand, a higher austenite stability makes the formation of martensite more difficult and some deformation occurs by slip in the austenite. It is therefore not easy to provide the high stresses necessary to render additional embryos supercritical after the most energetic and most favorably oriented embryos have been consumed. Since the work hardening rate of the austenite is relatively low, it requires some strain to build up local internal stress peaks some of which may be high enough to nucleate some martensite before the average stress has reached the level necessary for martensite formation. This results in serrations and thus the association of a serrated stress strain curve with strain-induced formation of martensite is justified. Moreover, this explains why "stress-induced martensite" forms continuously while the "strain-induced martensite" forms intermittently resulting in bursts of transformation.

The build up of stresses during the slip process in the austenite

actually brings about the competition between formation of martensite and slip as modes of deformation.

For improved ductility due to formation of martensite the processing temperature always has to be above the testing temperature. In other words, the austenite (or retained austenite) must be less stable at the temperature at which it is expected to enhance ductility by its transformation, than at the processing temperature.

Changes in processing temperature can result in drastic changes of the tensile properties depending on whether or not rolling is carried out above or below the M_d-temperature.

The rolling temperatures affect the mechanical properties by the amount of martensite that forms, through tempering of martensite that may form during or before rolling on cooling from 1200°C to RT, and at higher temperatures through precipitation which effectively lowers the alloy content of the matrix and thus renders the retained austenite less stable, (i.e. it raises the M_s and M_d temperatures).

A similarly strong effect is that of the test temperatures on the tensile properties, especially on the elongation values. At 100°C the specimens are pulled above M_d and, thus, fail immediately after yielding sets in. As -196°C, the martensite that forms on cooling the specimens down to this temperature affects the elongation values adversely. The only temperatures at which the $\gamma - \alpha'$ phase transformation makes a significant contribution to the ductility are the dry ice and room temperatures.

Large elongation values are obtained when the work hardening rate is rather low, i.e. the austenite stability relatively high. There are always serrations in the stress strain curves of specimens with high

elongation values.

There is an optimum work hardening rate (or austenite stability) for maximum elongation. In such a case the total elongation can be considered to be equal to the Luder's strain.

A decrease in austenite stability (lower test temperature, fewer alloying elements) will yield higher elongation values for very stable alloys, whereas the opposite is true for unstable alloys.

Whenever a clearly definable Luder's strain portion can be observed in stress strain curves of metastable austenitic alloys, the ductility can be improved by increasing the austenite stability.

The amount of different reductions in thickness at temperatures above M_d has relatively little effect on the "yield strehgth" when the alloy is very unstable and transforms readily during the test (below M_d). The effect becomes, however, significant when the austenite stability increases to the point that no stress-induced formation of martensite can take place anymore.

The length of time specimens are held at 450°C while they are reduced by different amounts plays an important role with respect to the austenite stability as affected by precipitation. Additional tempering at 450°C after the rolling process is completed can result in drastic changes in work hardening rates.

The rolling time plays a negligible role when the effects of different rolling temperatures are compared. This is due to the much greater effect temperature has on diffusion and, thus on precipitation (exponential relationship).

The alloy composition has the strongest effect on the stability of the austenite. The addition of almost any element, with the possible

exception of Co, increases the austenite stability, i.e. suppresses the M_s and M_d temperatures.

Mn and C belong to the elements that affect these critical temperatures most strongly. Experiments show that increasing the stability of the austenite by adding the Mn instead of C yields better mechanical properties. This is due to the fact that carbon as the interstitial solute plays a much greater role in the formation of the martensite. High carbon contents lead to harder martensite. There is, however, no evidence that the hardness of the martensite is an important factor with respect to the effectiveness of the phase transformation regarding the prevention or delay of necking at high stress levels. Moreover, the amount of carbon that can be dissolved in the matrix is very limited.

Thus, it is suggested that a carbon content between 0.2 and 0.4% be taken for the design of a high strength metastable austenitic steel. The austenite stability should then be roughly adjusted by adding the proper amount of Mn. Cr is recommended for fine adjustments since its effect on the M_d temperature is smaller than that of Mn, and it has been found that Cr affects the mechanical properties very favorably.

For high strength and large elongation the austenite stability has to be high enough so that yielding occurs by slip and not by stress-induced formation of martensite. Moreover thermo-mechanical treatments are more effective when the austenite stability is relatively high. On the other hand, the rate of strain-induced martensite formation must be sufficient to prevent premature failure at the site of incipient necking.

Optimum results thus have very strict requirements as to the austenite stability which hardly can be met under normal production and processing conditions. Since the austenite stability itself is very sensitively

affected by small variations in composition, rolling temperature and time (precipitation), internal stresses, variation in specimen dimensions, etc., it is difficult to reproduce results exactly. This becomes more and more difficult as the austenite stability decreases.

ACKNOWLEDGEMENTS

The author wishes to express his appreciation to Professor Victor F. Zackay and Professor Earl R. Parker of the Department of Materials Science and Engineering, University of California, Berkeley, for their advice and constant encouragement.

Further thanks are due to Mrs. Gloria Pelatowski for her help in preparing the illustrations and Mrs. Pat Shand and Miss Jane Ball for their efforts and patience in typing the manuscript.

This work was supported by the United States Atomic Energy Commission through the Inorganic Materials Research Division of the Lawrence Radiation Laboratory.

REFERENCES

1. E. B. Kula, Strengthening of Steel by Thermomechanical Treatments, in Strengthening Mechanisms, Proceedings of the 12th Sagamore Army Materials Research Conference, Syracuse University Press (1966).

2. R. F. Harvey, Step Quenching, Hot Peening, Improve Lean Alloys, Iron Age 168 (Dec. 27, 1951), p. 70.

3. E. M. H. Lips and H. Van Zuilen, Improved Hardening Technique, Metal Prog. 66 (Aug. 1954) p. 103.

4. T. Angel, Formation of Martensite in Austenitic Stainless Steels, J. Iron and Steel Inst. 177 (May 1954) p. 165.

5. H. C. Fiedler, B. L. Averbach, and M. Cohen, The Effect of Deformation on the Martensitic Transformation in Stainless Steels, Trans. ASM 47 (1955) p. 267.

6. G. W. Powell, E. R. Marshall, and W. A. Backofen, Strain Hardening of Austenitic Stainless Steel, Trans. ASM 50, (1958) p. 478.

7. T. C. Shyne, F. W. Schaller, and V. F. Zackay, The Tensile and Yield Strength of Cr-Mn-N Steels at Low Temperature, Trans. ASM, 52 (1960) p. 848.

8. E. T. Stevenson and M. Cohen, The Effect of Prestraining and Retempering on AISI Type 4340, Trans. ASM 54 (1961) p. 72.

9. J. C. Hamaker, Jr. and D. H. Yates, New High Strength Steel Applications, Presented at the 1966 WESTEC Conference, March 1966, Los Angeles, Calif., ASM Technical Report No. W6-6.2.

10. V. F. Zackay, E. R. Parker, D. Fahr, and R. Busch, The Enhancement of Ductility in High-Strength Steels, ASM Trans. Quart. 60 (1967) p. 252.

11. B. R. Banerjee, J. M. Capenos, and J. J. Hauser, Fracture Mechanics of Extra Work Hardening Type 301 Stainless, in Application of Fracture Toughness Parameters to Structural Metals, Gordon and Breach (1966).

12. J. P. Bressanelli and A. Moskowitz, Effects of Strain Rate, Temperature, and Composition on Tensile Properties of Metastable Austenitic Stainless Steels, ASM Trans. Quart. 59 (1966) p. 223.

13. S. A. Kulin, M. Cohen, and B. L. Averbach, Effect of Applied Stress on the Martensite Transformation, Trans. AIME, J. Metals (June 1952) p. 661.

14. J. Baruch, A. Rosen and S. R. Bodner, Discontinuous Yielding of Metastable Austenitic Stainless Steel, Trans. JIM, Vol. 9 (1968) Supplement p. 448.

15. C. F. Elam, The Influence of Rate of Deformation on the Tensile Test with Special Reference to the Yield Point in Iron and Steel, Proc. Roy. Soc. A165, (1938) p. 568.

16. B. Russel, Repeated Yielding in Tin Bronze Alloys, Phil. Mag. 8 (1963) p. 615.

17. W. J. Bratina, J. T. McGrath, and D. Mills, Repeated Yielding in Quenched Fe-C Alloys, Trans. JIM, Vol. 9 (1968) Supplement p. 436.

18. B. de Miramon (M.S. Thesis) University of California, Berkeley, Sept. 1967.

19. E. Scheil, Uber die Umwandlung des Austenits in Martensit in Eisen-Nickel Legierungen unter Belastung, Ztsch. anorg. allgem. Chemie (1932) 207 p. 21.

20. M. Cohen, E. S. Machlin, and V. G. Paranjpe, Thermodynamics of the Martensitic Transformation. Thermodynamics in Physical

Metallurgy, Trans. ASM (1950) 42A p. 242.

21. E. S. Machlin and M. Cohen, The Isothermal Mode of the Martensitic Transformation, J. Metals, Trans. AIME (May 1952) p. 489.

TABLE I

ALLOY NO. 6811-14 9 Cr, 8 Ni, 2 Mn, 0 C, bal. Fe

TENSILE PROPERTIES

Test Temperatures	RT			-78°C			-196°C			100°C		
Thermo-Mechanical Treatment	Y.S. 10^3 Psi	U.T.S. 10^3 Psi	Elong. %	Y.S. 10^3 Psi	U.T.S. 10^3 Psi	Elong. %	Y.S. 10^3 Psi	U.T.S. 10^3 Psi	Elong. %	Y.S. 10^3 Psi	U.T.S. 10^3 Psi	Elong %
80%, RT	184	-	3.6	259	-	2.4	310	-	1.9	196	-	1.9
80%, 100°C	197	-	2.3	247	-	4.2	280	-	2.2	189	-	1.9
80%, 250°C	218	-	3.2	226	-	2.6	257	-	1.8	231	-	1.9
80%, 450°C	222	-	2.9	218	228	3.3	267	-	3.8	194	199	3.4
60%, 450°C	195	-	3.9	206	208	3.3	253	-	2.5	185	-	2.2
40%, 450°C	173	-	3.0	201	204	3.2	213	-	4.0	184	-	3.0
20%, 450°C	163	-	4.2	194	197	3.7	221	-	3.0	148	-	1.9

TABLE II

ALLOY NO. 6811-13 9 Cr, 8 Ni, 2 Mn, 0.1 C, bal. Fe

TENSILE PROPERTIES

Test Temperatures	RT			-78°C			-196°C			100°C		
Thermo-Mechanical Treatment	Y.S. 10^3 Psi	U.T.S. 10^3 Psi	Elong. %	Y.S. 10^3 Psi	U.T.S. 10^3 Psi	Elong. %	Y.S. 10^3 Psi	U.T.S. 10^3 Psi	Elong. %	Y.S. 10^3 Psi	U.T.S. 10^3 Psi	Elong %
80%, RT	328**	-	0	359**	-	0	376**	-	0	-	-	-
80%, 100°C	231	272	11.0	224	300	10.3	243	356	10.6	252	-	1.9
80%, 250°C	154	252	21.8	153	284	14.3	183	343	12.3	226	-	3.1
80%, 450°C	128	246	16.6	130	286	11.4	145	345	11.5	208	218	1.6
60%, 450°C	110	240	16.3	72	278	13.1	138	331	14.4	167	-	3.0
40%, 450°C	103	232	20.0	77	264	12.7	11	(257)*	(6.6)*	185	-	3.8
20%, 450°C	96	211	20.1	108	244	14.0	95	298	10.5	135	139	3.1

* Specimen broke at hole

** Fracture strength

TABLE III

ALLOY NO. 6811-12 9 Cr, 8 Ni, 2 Mn, 0.2 C, bal. Fe

TENSILE PROPERTIES

Test Temperatures	RT			-78°C			-196°C			100°C		
Thermo-Mechanical Treatment	Y.S. 10^3 Psi	U.T.S. 10^3 Psi	Elong. %	Y.S. 10^3 Psi	U.T.S. 10^3 Psi	Elong. %	Y.S. 10^3 Psi	U.T.S. 10^3 Psi	Elong. %	Y.S. 10^3 Psi	U.T.S. 10^3 Psi	Elong %
80%, RT	280**	-	0	266**	-	0	270	-	0.5	278**	-	0
80%, 100°C	190	256	28.2	151	299	16.1	174	255	9.2	216	-	1.9
80%, 250°C	172	237	22.3	135	307	16.5	151	285	9.7	200	-	1.9
80%, 450°C	153	253	23.3	121	306	16.0	147	(215)*	(8.2)*	190	-	1.9
60%, 450°C	158	218	29.6	108	292	15.6	106	(169)*	6.5	170	-	2.3
40%, 450°C	119	204	30.4	115	273	15.0	83	196	6.5	-	-	-
20%, 450°C	87	177	30.8	90	210	12.1	46	117	3.1	98	104	7.5

*Specimen broke at hole

**Fracture strength

TABLE IV

ALLOY NO. 689-15 9 Cr, 8 Ni, 2 Mn, 0.3 C, bal Fe

TENSILE PROPERTIES

Test Temperatures	RT			-78°C			-196°C			100°C		
Thermo-Mechanical Treatment	Y.S. 10^3 Psi	U.T.S. 10^3 Psi	Elong. %	Y.S. 10^3 Psi	U.T.S. 10^3 Psi	Elong. %	Y.S. 10^3 Psi	U.T.S. 10^3 Psi	Elong. %	Y.S. 10^3 Psi	U.T.S. 10^3 Psi	Elong %
80%, RT	286*	-	0	279	-	0.4	273*	-	0	251*	-	0
80%, 100°C	229	233	13.4	178	306	19.0	191	238	9.2	227	-	0.7
80%, 250°C	185	226	18.1	161	302	19.5	178	178	4.2	201	-	0.6
80%, 450°C	166	255	21.5	127	314	14.8	149	210	9.5	182	-	0.6
60%, 450°C	158	212	19.2	92	287	19.1	120	199	10.2	156	160	0.9
40%, 450°C	116	174	20.0	87	261	18.2	72	153	7.8	123	127	1.3
20%, 450°C	82	141	270	82	197	12.9	33	148	8.7	78	91	6.1

*Fracture strength

TABLE V

ALLOY NO. 689-16 9 Cr, 8 Ni, 2 Mn, 0.4 C, bal. Fe

TENSILE PROPERTIES

Test Temperatures	RT			-78°C			-196°C			100°C		
Thermo-Mechanical Treatment	Y.S. 10^3 Psi	U.T.S. 10^3 Psi	Elong. %	Y.S. 10^3 Psi	U.T.S. 10^3 Psi	Elong. %	Y.S. 10^3 Psi	U.T.S. 10^3 Psi	Elong. %	Y.S. 10^3 Psi	U.T.S. 10^3 Psi	Elong %
80%, RT	264*	-	0	263*	-	0	278*	-	0	268	-	1.5
80%, 100°C	236	238	22.4	200	300	18.2	218	220	4.1	225	-	0.7
80%, 250°C	219	238	25.1	180	310	17.0	201	-	5.0	215	-	0.7
80%, 450°C	197	251	25.8	172	318	17.4	191	-	0.9	200	202	0.6
60%, 450°C	166	223	30.6	125	299	19.1	181	-	5.8	171	173	0.7
40%, 450°C	145	170	20.9	124	278	18.3	114	163	7.4	143	146	0.7
20%, 450°C	108	134	23.8	95	244	17.3	77	137	6.7	110	112	0.6

*Fracture strength

TABLE VI

ALLOY NO. 686-21 9 Cr, 8 Ni, 2 Mn, 0.5 C, bal. Fe

TENSILE PROPERTIES

Test Temperatures	RT			-78°C			-196°C			100°C		
Thermo-Mechanical Treatment	Y.S. 10^3 Psi	U.T.S. 10^3 Psi	Elong. %	Y.S. 10^3 Psi	U.T.S. 10^3 Psi	Elong. %	Y.S. 10^3 Psi	U.T.S. 10^3 Psi	Elong. %	Y.S. 10^3 Psi	U.T.S. 10^3 Psi	Elong %
80%, RT	257	-	3.1	256	263	10.0	286*	-	0	243	248	1.5
80%, 100°C	250	-	1.7	258	268	17.8	279*	-	0	237	242	1.5
80%, 250°C	224	228	2.7	232	240	14.9	250*	-	0	219	225	2.3
80%, 450°C	222	235	3.5	223	314	18.0	237*	-	0	217	228	1.5
60%, 450°C	193	212	3.1	205	236	13.8	222*	-	0	196	199	1.5
40%, 450°C	161	176	4.2	184	187	4.9	215*	-	0	153	160	2.3
20%, 450°C	109	126	5.1	117	139	7.6	154	157	1.2	115	121	2.7

*Fracture strength

TABLE VII

ALLOY NO. 692-9 9 Cr, 8 Ni, 1 Mn, 0.2 C, bal. Fe

TENSILE PROPERTIES

Test Temperatures	RT			-78°C			-196°C			100°C		
Thermo-Mechanical Treatment	Y.S. 10^3 Psi	U.T.S. 10^3 Psi	Elong. %	Y.S. 10^3 Psi	U.T.S. 10^3 Psi	Elong. %	Y.S. 10^3 Psi	U.T.S. 10^3 Psi	Elong. %	Y.S. 10^3 Psi	U.T.S. 10^3 Psi	Elong %
80%, RT	350	-	1.3	(346)*	-	(0)*	-	-	-	-	-	-
80%, 100°C	308	-	2.8	289	335	7.2	365	-	2.0	-	-	-
80%, 250°C	256	275	12.9	211	300	9.3	292	356	10.5	-	-	-
80%, 450°C	212	276	13.4	187	306	9.7	274	369	10.8	274	-	3.0
60%, 450°C	210	251	13.8	174	283	10.3	242	327	12.1	-	-	-
40%, 450°C	194	240	13.5	140	271	8.3	210	324	11.6	-	-	-
20%, 450°C	180	216	18.3	126	261	11.4	195	271	7.2	-	-	-

*Specimen broke at hole

TABLE VIII

ALLOY NO. 692-7 9Cr, 8 Ni, 1 Mn, 0.3 C, bal. Fe

TENSILE PROPERTIES

Test Temperatures	RT			-78°C			-196°C			100°C		
Thermo-Mechanical Treatment	Y.S. 10^3 Psi	U.T.S. 10^3 Psi	Elong. %	Y.S. 10^3 Psi	U.T.S. 10^3 Psi	Elong. %	Y.S. 10^3 Psi	U.T.S. 10^3 Psi	Elong. %	Y.S. 10^3 Psi	U.T.S. 10^3 Psi	Elong %
80%, RT	317**	-	0	282	-	0.4	(208)*	-	(0)*	-	-	-
80%, 100°C	198	241	9.3	133	320	12.0	180	294	7.6	-	-	-
80%, 250°C	147	229	9.5	125	(281)*	(9.1)*	123	195	6.5	-	-	-
80%, 450°C	153	223	10.4	101	(279)*	(8.0)*	137	229	6.7	212	-	3.2
60%, 450°C	126	214	11.2	76	(217)*	(6.5)*	75	178	4.6	-	-	-
40%, 450°C	115	193	15.0	51	(194)*	(5.7)*	63	(158)*	(3.0)*	-	-	-
20%, 450°C	102	125	13.9	58	(202)*	(4.2)*	68	(161)*	(2.4)*	-	-	-

*Specimens broke at hole

**Fracture strength

TABLE IX

ALLOY NO. 6811-15 9 Cr, 8 Ni, 1 Mn, 0.4 C, bal. Fe

TENSILE PROPERTIES

Test Temperatures	RT			-78°C			-196°C			100°C		
Thermo-Mechanical Treatment	Y.S. 10^3 Psi	U.T.S. 10^3 Psi	Elong. %	Y.S. 10^3 Psi	U.T.S. 10^3 Psi	Elong. %	Y.S. 10^3 Psi	U.T.S. 10^3 Psi	Elong. %	Y.S. 10^3 Psi	U.T.S. 10^3 Psi	Elong. %
80%, RT	289	--	0.4	260	-	1.5	266*	-	0	281*	-	0
80%, 100°C	226	251	23.3	188	325	18.6	200	204	4.7	227*	-	0
80%, 250°C	203	286	25.8	158	336	16.8	187	224	7.2	236	-	1.9
80%, 450°C	177	293	24.8	126	335	15.3	129	186	5.4	217	-	1.9
60%, 450°C	175	255	29.6	101	312	12.2	112	152	4.1	-	-	-
40%, 450°C	158	172	14.9	113	216	8.9	86	109	2.3	-	-	-
20%, 450°C	97	118	13.3	91	170	9.5	65	146	3.0	108	112	3.4

* Fracture strength

TABLE X

ALLOY NO. 689-18 9 Cr, 8 Ni, 1 Mn, 0.5 C, bal. Fe

TENSILE PROPERTIES

Test Temperatures	RT			-78°C			-196°C			100°C		
Thermo-Mechanical Treatment	Y.S. 10^3 Psi	U.T.S. 10^3 Psi	Elong. %	Y.S. 10^3 Psi	U.T.S. 10^3 Psi	Elong. %	Y.S. 10^3 Psi	U.T.S. 10^3 Psi	Elong. %	Y.S. 10^3 Psi	U.T.S. 10^3 Psi	Elong %
80%, RT	278	-	3.4	260	286	15.8	248 *	-	0	258	-	1.0
80%, 100°C	255	-	5.0	250	299	19.0	271	-	1.0	252	-	1.5
80%, 250°C	254	-	3.0	225	325	20.4	271 *	-	0	234	-	1.0
80%, 450°C	220	231	7.0	206	330	20.0	202	-	1.0	218	222	1.5
60%, 450°C	204	215	14.3	200	280	18.0	193	-	1.5	201	-	1.5
40%, 450°C	154	175	12.0	159	189	14.6	176	-	1.0	158	163	4.0
20%, 450°C	115	142	17.0	125	156	16.3	142 *	-	0	109	114	3.0

* Fracture strength

TABLE XI

ALLOY NO. 692-8 9 Cr, 8 Ni, 3 Mn, 0.2 C, bal. Fe

TENSILE PROPERTIES

Test Temperatures	RT			-78°C			-196°C			100°C		
Thermo-Mechanical Treatment	Y.S. 10^3 Psi	U.T.S. 10^3 Psi	Elong. %	Y.S. 10^3 Psi	U.T.S. 10^3 Psi	Elong. %	Y.S. 10^3 Psi	U.T.S. 10^3 Psi	Elong. %	Y.S. 10^3 Psi	U.T.S. 10^3 Psi	Elong %
80%, RT	324	-	0.4	330	-	0.4	369**	-	0	-	-	-
80%, 100°C	208	232	31.4	172	277	19.7	202	300	11.7	-	-	-
80%, 250°C	172	230	30.6	142	273	19.6	177	201	8.4	-	-	-
80%, 450°C	174	234	27.1	138	282	17.1	154	330	12.8	183	192	1.6
60%, 450°C	135	226	26.5	119	272	17.2	133	(266)*	(10.8)*	-	-	-
40%, 450°C	130	201	26.8	100	(260)*	(15.9)*	107	(235)*	(10.8)*	-	-	-
20%, 450°C	101	176	31.2	72	(227)*	(13.0)*	77	160	8.9	-	-	-

*Specimens broke at hole

**Fracture strength

TABLE XII

ALLOY NO. 6812-11 9 Cr, 8 Ni, 3 Mn, 0.3 C, bal. Fe

TENSILE PROPERTIES

Test Temperatures	RT			-78°C			-196°C			100°C		
Thermo-Mechanical Treatment	Y.S. 10^3 Psi	U.T.S. 10^3 Psi	Elong. %	Y.S. 10^3 Psi	U.T.S. 10^3 Psi	Elong. %	Y.S. 10^3 Psi	U.T.S. 10^3 Psi	Elong. %	Y.S. 10^3 Psi	U.T.S. 10^3 Psi	Elong %
80%, RT	273	-	2.8	254	300	22.2	287	-	1.6	-	-	-
80%, 100°C	224	-	7.3	215	285	28.6	234	-	7.0	-	-	-
80%, 250°C	217	-	14.5	206	283	24.2	222	222	9.4	-	-	-
80%, 450°C	206	219	34.8	185	300	23.5	203	206	8.7	195	201	2.9
60%, 450°C	178	189	26.5	166	283	25.9	182	195	9.4	-	-	-
40%, 450°C	133	152	19.7	138	261	25.1	151	-	2.9	-	-	-
20%, 450°C	94	120	25.0	96	172	17.2	116	119	7.9	-	-	-

TABLE XIII

ALLOY NO. 692-6 9 Cr, 8 Ni, 3 Mn, 0.4 C, bal. Fe

TENSILE PROPERTIES

Test Temperatures	RT			-78°C			-196°C			100°C		
Thermo-Mechanical Treatment	Y.S. 10^3 Psi	U.T.S. 10^3 Psi	Elong. %	Y.S. 10^3 Psi	U.T.S. 10^3 Psi	Elong. %	Y.S. 10^3 Psi	U.T.S. 10^3 Psi	Elong. %	Y.S. 10^3 Psi	U.T.S. 10^3 Psi	Elong %
80%, RT	253	-	2.6	249	-	5.1	288	-	0.7	-	-	-
80%, 100°C	230	-	3.0	231	284	32.1	252	-	1.3	-	-	-
80%, 250°C	229	-	3.7	211	280	24.0	244	-	0.8	-	-	-
80%, 450°C	225	-	10.9	211	303	24.0	227	-	0.4	217	225	1.4
60%, 450°C	195	196	4.2	177	251	19.5	198	-	0.9	-	-	-
40%, 450°C	143	159	10.9	148	196	17.5	167	-	1.3	-	-	-
20%, 450°C	99	121	13.5	111	158	19.8	135	138	1.5	-	-	-

TABLE XIV

ALLOY NO. 686-22 9 Cr, 8 Ni, 3 Mn, 0.5 C, bal. Fe

TENSILE PROPERTIES

Test Temperatures	RT			-78°C			-196°C			100°C		
Thermo-Mechanical Treatment	Y.S. 10^3 Psi	U.T.S. 10^3 Psi	Elong. %	Y.S. 10^3 Psi	U.T.S. 10^3 Psi	Elong. %	Y.S. 10^3 Psi	U.T.S. 10^3 Psi	Elong. %	Y.S. 10^3 Psi	U.T.S. 10^3 Psi	Elong %
80%, RT	252	-	1.3	263	-	411	296*	-	0	236	-	0.4
80%, 100°C	254	-	1.8	248	266	22900	290*	-	0	225	228	1.1
80%, 250°C	249	-	2.4	252	279	31.0	266	-	0.5	219	229	1.5
80%, 450°C	236	-	2.1	229	276	21.6	252**	-	0.2	212	219	0.4
60%, 450°C	209	-	2.4	213	252	28.4	246*	-	0	187	192	0.6
40%, 450°C	152	166	5.5	159	176	10.7	202*	-	0	144	151	1.5
20%, 450°C	112	126	10.2	122	138	6.7	156**	-	0.2	108	117	4.4

* Fracture strength

** Fracture strength = yield strength

TABLE XV

ALLOY NO. 689-19 9 Cr, 8 Mi, 4 Mn, 0.5 C, bal. Fe

TENSILE PROPERTIES

Test Temperatures	RT			-78°C			-196°C			100°C		
Thermo-Mechanical Treatment	Y.S. 10^3 Psi	U.T.S. 10^3 Psi	Elong. %	Y.S. 10^3 Psi	U.T.S. 10^3 Psi	Elong. %	Y.S. 10^3 Psi	U.T.S. 10^3 Psi	Elong. %	Y.S. 10^3 Psi	U.T.S. 10^3 Psi	Elong %
80%, RT	257	-	2.3	284	-	3.5	320	-	1.6	242	-	2.3
80%, 100°C	249	-	4.7	260	-	5.5	314	-	1.6	-	-	-
80%, 250°C	245	-	4.2	272	-	6.7	314	-	2.3	227	-	2.2
80%, 450°C	273	-	2.7	265	270	39.55	320	-	1.0	242	-	3.4
60%, 450°C	229	-	4.6	246	-	4.3	-	--	-	-	-	-
40%, 450°C	170	177	8.0	182	193	6.8	-	-	-	-	-	-
20%, 450°C	129	145	24.2	138	165	23.0	178	185	2.7	-	-	-
80%, 550°C	250	-	2.0	254*	-	0	272*	-	0	234	-	3.0

* Fracture strength

TABLE XVI

ALLOY NO. 692-9 9 Cr, 8 Ni 1 Mn, 0.2 C, bal Fe

TENSILE PROPERTIES

(Special Tests)

Test Temperatures	RT			RT (Prestrained at -78°C)					-78°C		
Thermo-Mechanical Treatment	Y.S. 10^3 Psi	U.T.S. 10^3 Psi	Elong. %	Y.S. at -78°C 10^3 Psi	Strain at -78°C %	Y.S. at RT 10^3 Psi	U.T.S. at RT 10^3 Psi	Total Elong. %	Y.S. 10^3 Psi	U.T.S. 10^3 Psi	Elong %
80%, 250°C	256	275	12.9	231	0.4	260	277	5.6	211	300	9.3
40%, 450°C	194	240	13.5	151	0.4	204	246	11.7	140	271	8.3
20%, 450°C	180	216	18.3	132	1.5	178	214	15.4	126	261	11.4

Table XVII. Chemical composition of the alloys

Alloy No.	wt.% Cr	wt.% Ni	wt.% Mn	wt.% C	wt.% Fe
692-9	9	8 (7.6)	1	0.2 (0.212)	Balance
692-7	9	8	1	0.3 (0.29)	Balance
6811-15	9 (10.1)	8 (7.6)	1	0.4 (0.432)	Balance
689-18	9 (10.3)	8	1	0.5 (0.535)	Balance
6811-14	9 (10.1)	8 (7.6)	2	0 (0.008)	Balance
6811-13	9 (10.1)	8 (7.6)	2 (2.2)	0.1 (0.173)	Balance
6811-12	9 (10.7)	8 (7.7)	2	0.2 (0.285)	Balance
689-15	9 (9.8)	8	2	0.3 (0.325)	Balance
689-16	9 (10.2)	8	2	0.4 (0.354)	Balance
686-21	9 (9.2)	8 (7.8)	2 (2.3)	0.5 (0.507)	Balance
692-8	9	8	3	0.2 (0.249)	Balance
6812-11	9 (10.1)	8 (7.7)	3	0.3 (0.34)	Balance
692-6	9	8	3 (3.4)	0.4 (0.422)	Balance
686-22	9	8 (7.8)	3 (3.2)	0.5 (0.519)	Balance
689-19	9 (10)	8	4	0.5 (0.512)	Balance

( ) value as analyzed; only listed when deviating from desired value. Accuracy of C-analysis is not known.

FIGURE CAPTIONS

Fig. 1 Dimensions of 0.050 in. thick tensile specimen.

Fig. 2 Stress strain curves of alloys with varying C contents at given Mn contents after 80% reduction in thickness at 450°C.

(a) Room temperature tests of 1% Mn alloys.

(b) Room temperature tests of 2% Mn alloys.

(c) Room temperature tests of 3% Mn alloys.

(d) Dry ice tests of 1% Mn alloys.

(e) Dry ice tests of 2% Mn alloys.

(f) Dry ice tests of 3% Mn alloys.

Fig. 3 Yield strength vs. C content curves of 1% Mn alloys after 80% reduction in thickness at 450°C obtained at different test temperatures.

(a) Room temperature and 100°C test values.

(b) Dry ice and 100°C test values.

(c) Dry ice and room temperature test values.

(d) Differences in yield strength between 100°C and room temperature tests, 100°C and dry ice tests, and room temperature and dry ice tests as a function of C content.

Fig. 4 Yield strength vs C content curves of 2% Mn alloys after 80% reduction in thickness at 450°C obtained at different test temperatures.

(a) Room temperature and 100°C test values.

(b) Dry ice and 100°C test values.

(c) Dry ice and room temperature test values.

(d) Differences in yield strength between 100°C and room temperature tests, 100°C and dry ice tests, and room

temperature and dry ice tests as a function of C content.

Fig. 5 Yield strength vs C content curves of 3% Mn alloys after 80% reduction in thickness at 450°C obtained at different test temperatures.

(a) Room temperature and 100°C test values.

(b) Dry ice and 100°C test values.

(c) Dry ice and room temperature test values.

(d) Differences in yield strength between 100°C and room temperature tests, 100°C and dry ice tests, and room temperature and dry ice tests as a function of C content.

Fig. 6 (a) Luder's strain vs carbon content at -78°C in 3% Mn alloys after 80% reduction in thickness at 450°C.

(b) Luder's strain vs Mn content at -78°C in 0.4% C alloys after 80% reduction in thickness at 450°C.

Fig. 7 Stress strain curves of alloys with varying Mn contents at given C contents after 80% reduction in thickness at 450°C.

(a) Room temperature tests of 0.2% C alloys.

(b) Room temperature tests of 0.4% C alloys.

(c) Room temperature tests of 0.5% C alloys.

(d) Dry ice tests of 0.2% C alloys.

(e) Dry ice tests of 0.4% C alloys.

(f) Dry ice tests of 0.5% C alloys.

Fig. 8 Room temperature stress strain curves of 2% Mn alloys at given C contents after reductions in thickness of 20, 40, 60, and 80% at 450°C.

(a) 0.0% C alloy

(b) 0.1% C alloy

(c) 0.2% C alloy

(d) 0.3% C alloy

(e) 0.4% C alloy

(f) 0.5% C alloy

Fig. 9 Yield strength at room temperature vs reduction in thickness at 450°C for a 2% Mn, 0.5% C alloy.

Fig. 10 Differences in room temperature yield strength between specimens with 80 and 20% reduction in thickness at 450°C as a function of carbon content for alloys containing 1, 2 and 3% Mn.

Fig. 11 Dry ice stress strain curves of 2% Mn alloys at given C contents after reductions in thickness of 20, 40, 60, and 80% at 450°C.

(a) 0.0% C alloy

(b) 0.1% C alloy

(c) 0.2% C alloy

(d) 0.3% C alloy

(e) 0.4% C alloy

(f) 0.5% C alloy

Fig. 12 Room temperature stress strain curves of 1% Mn alloys at given C contents after reductions in thickness of 20, 40, 60 and 80% at 450°C.

(a) 0.2% C alloy

(b) 0.3% C alloy

(c) 0.4% C alloy

(d) 0.5% C alloy

Fig. 13 Dry ice stress strain curves of 1% Mn alloys at given C contents after reductions in thickness of 20, 40, 60 and 80% at 450°C.

(a) 0.2% C alloy

(b) 0.3% C alloy (no x when specimen fractured at hole)

(c) 0.4% C alloy

(d) 0.5% C alloy

Fig. 14 Room temperature stress strain curves of 3% Mn alloys at given C contents after reduction in thickness of 20, 40, 60 and 80% at 450°C.

(a) 0.2% C alloy

(b) 0.3% C alloy

(c) 0.4% C alloy

(d) 0.5% C alloy

Fig. 15 Dry ice stress strain curves of 3% Mn alloys at given C contents after reductions in thickness of 20, 40,60 and 80% at 450°C.

(a) 0.2% C alloy (no x when specimen fractured at hole)

(b) 0.3% C alloy

(c) 0.4% C alloy

(d) 0.5% C alloy

Fig. 16 Room temperature stress strain curves of 2% Mn alloys at given C contents after 80% reduction in thickness at RT, 100, 250, and 450°C.

(a) 0.0% C alloy

(b) 0.1% C alloy

(c) 0.2% C alloy

(d) 0.3% C alloy

(e) 0.4% C alloy

(f) 0.5% C alloy

Fig. 17 Room temperature yield strength vs C content curves of alloys with varying Mn contents after 80% reduction in thickness at room temperature and 450°C, respectively.

(a) 1% Mn alloy

(b) 2% Mn alloy

(c) 3% Mn alloy

(d) Differences in room temperature yield strength between specimens reduced 80% at room temperature and 450°C, respectively, as a function of C content for alloys containing 1, 2 and 3% Mn.

Fig. 18 Dry ice stress strain curves of 2% Mn alloys at given C contents after 80% reduction in thickness at RT, 100°, 250°, and 450°C.

(a) 0.0% C alloy

(b) 0.1% C alloy

(c) 0.2% C alloy

(d) 0.3% C alloy

(e) 0.4% C alloy

(f) 0.5% C alloy

Fig. 19 Room temperature stress strain curves of 1% Mn alloys at given C contents after 80% reduction in thickness at RT, 100°, 250°, and 450°C.

(a) 0.2% C alloy

(b) 0.3% C alloy

(c) 0.4% C alloy

(d) 0.5% C alloy

Fig. 20 Dry ice stress strain curves of 1% Mn alloys at given C contents after 80% reduction in thickness at RT, 100°, 250°, and 450°C.

(a) 0.2% C alloy (no x when specimen fractured at hole)

(b) 0.3% C alloy (no x when specimen fractured at hole)

(c) 0.4% C alloy

(d) 0.5% C alloy

Fig. 21 Room temperature stress strain curves of 3% Mn alloys at given C contents after 80% reduction in thickness at RT, 100°, 250°, and 450°C.

(a) 0.2% C alloy

(b) 0.3% C alloy

(c) 0.4% C alloy

(d) 0.5% C alloy

Fig. 22 Dry ice stress strain curves of 3% Mn alloys at given C contents after 80% reduction in thickness at RT, 100°, 250°, and 450°C.

(a) 0.2% C alloy

(b) 0.3% C alloy

(c) 0.4% C alloy

(d) 0.5% C alloy

Fig. 23 Yield strength vs test temperature curves of 2% Mn alloys with varying C contents for all thermo-mechanical treatments applied.

(a) 0.2% C alloy (80%, 24°C data are fracture strength values)

(b) 0.3% C alloy (80%, 24°C data are fracture strength values)

(c) 0.4% C alloy (80%, 24°C data are fracture strength values)

(d) 0.5% C alloy (all -196°C data are fracture strength values)

Fig. 24 Differences in saturation magnetization between -78°C and RT, and between -196°C and RT vs temperature for 2% Mn alloys with C contents varying from 0.2 to 0.5%. The specimens were reduced 20% at 450°C.

Fig. 25 (a,b,c) Yield strength vs test temperature curves of 0.2% C alloys with varying Mn contents for all thermo-mechanical treatments applied, except 80%, RT.

(a) 1% Mn alloy

(b) 2% Mn alloy

(c) 3% Mn alloy (0.5% C alloy at -196°C: yield strength = fracture strength)

Fig. 25 d Differents in saturation magnetization between -78°C and RT, and between -196°C and RT vs temperature for 0.2% C alloys with Mn contents varying from 1 to 3%. The specimens were reduced 20% at 450°C.

Fig. 26 Yield strength vs test temperature curves of alloys with varying C contents at given Mn contents after 20% reduction in thickness at 450°C.

(a) 1% Mn alloys

(b) 2% Mn alloys

(c) 3% Mn alloys

Fig. 27 Yield strength vs test temperature curves of alloys with varying Mn contents at given C contents after 20% reduction in thickness at 450°C.

(a) 0.2% C alloys

(b) 0.4% C alloys

Fig. 28 Optical micrographs of specimens of alloy No. 6811-13 (2% Mn, 0.1% C) after 60% reduction in thickness at 450°C (rolling time 40 min).

(a) No additional tempering; ×250

(b) Tempered for 80 minutes at 450°C; ×250

Fig. 29 Optical micrographs of polished specimen of alloy No. 6811-15 (1% Mn, 0.4% C) with 80% reduction in thickness at 250°C after formation of stress induced martensite.

(a) Martensite band formed on quenching a loaded specimen from RT to -78°C. Tensile axis is indicated by arrows; ×40.

(b,c) Surface upheavals as they appear on the unetched specimen surface, ×125.

Fig. 30 Microstructures of specimens of alloy No. 689-15 (2% Mn, 0.3% C) with varying reductions in thickness at 450°C.

(a) 20% reduction in thickness; ×70.

(b) 40% reduction in thickness; ×70.

(c) 60% reduction in thickness; ×70.

(d) 80% reduction in thickness; ×70.

The rolling directions are indicated by arrows.

Fig. 31 Microstructures of specimens of alloy No. 689-15(2% Mn, 0.3% C) with 80% reduction in thickness at different temperatures.

(a) Rolling temperature: 450°C; ×70

(b) Rolling temperature: 250°C; ×70

(c) Rolling temperature: 100°C; ×70

(d) Rolling temperature: 24°C; ×70

The rolling directions are indicated by arrows.

Fig. 32 Micrograph of a specimen of alloy No. 689-15 (2% Mn, 0.3% C) with 80% reduction in thickness at RT showing deformation markings in an austenitic grain that is surrounded by martensite; ×650.

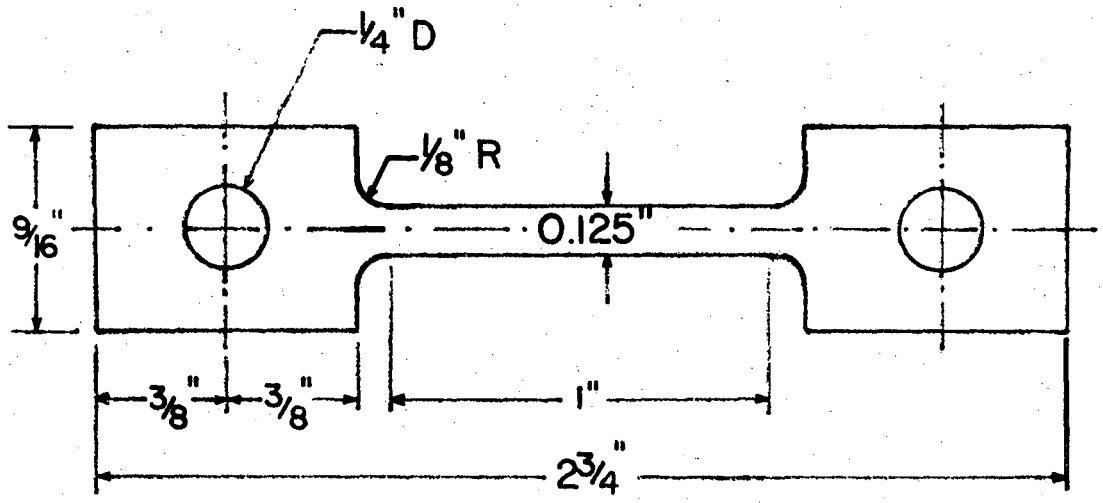

TENSILE SPECIMEN

SCALE: 2:1

XBL 698-1155

Fig. 1

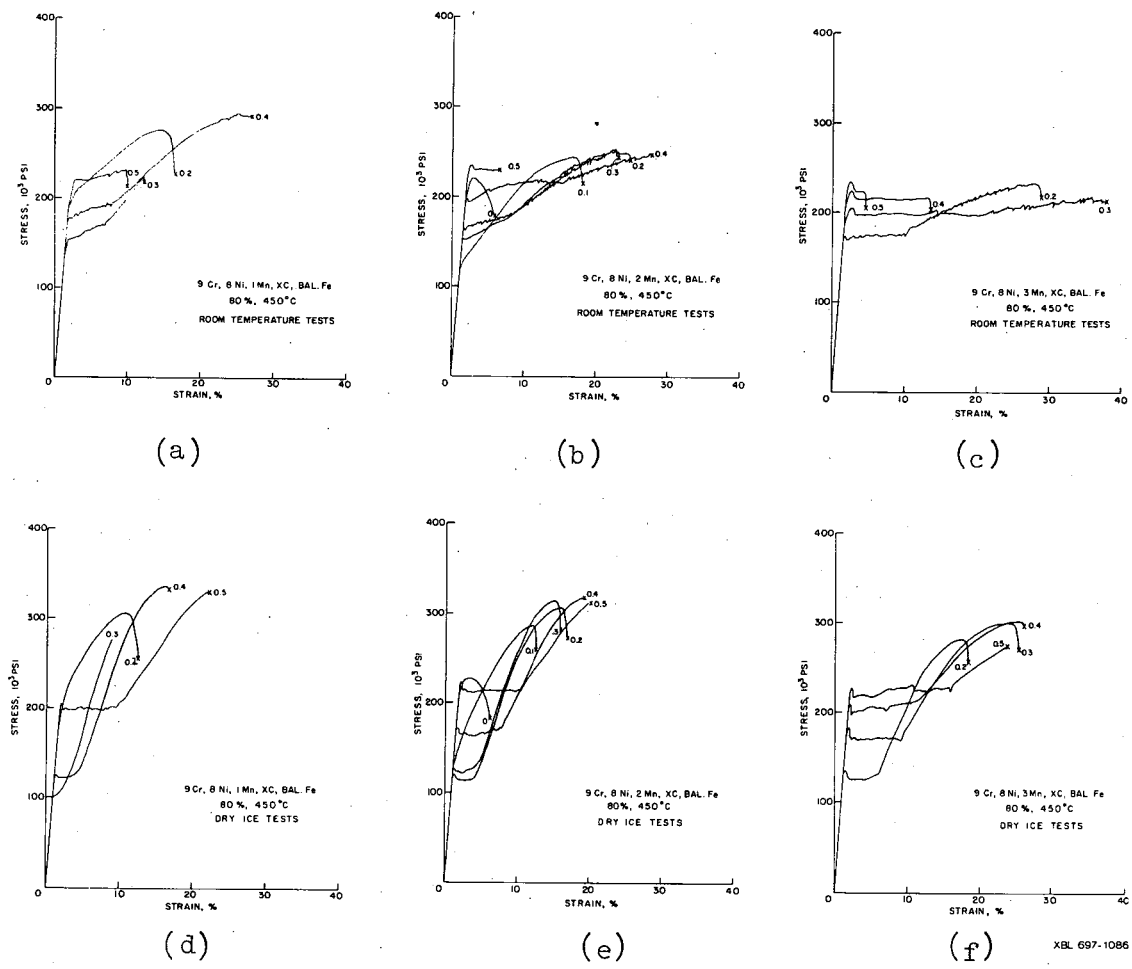
STRESS, 10^3 PSI
STRAIN, %
9 Cr, 8 Ni, 1 Mn, XC, BAL. Fe
80 %, 450°C
ROOM TEMPERATURE TESTS
(a)
9 Cr, 8 Ni, 2 Mn, XC, BAL. Fe
80 %, 450°C
ROOM TEMPERATURE TESTS
(b)
9 Cr, 8 Ni, 3 Mn, XC, BAL. Fe
80 %, 450°C
ROOM TEMPERATURE TESTS
(c)
9 Cr, 8 Ni, 1 Mn, XC, BAL. Fe
80 %, 450°C
DRY ICE TESTS
(d)
9 Cr, 8 Ni, 2 Mn, XC, BAL. Fe
80 %, 450°C
DRY ICE TESTS
(e)
9 Cr, 8 Ni, 3 Mn, XC, BAL. Fe
80 %, 450°C
DRY ICE TESTS
(f)
XBL 697-1086

Fig. 2

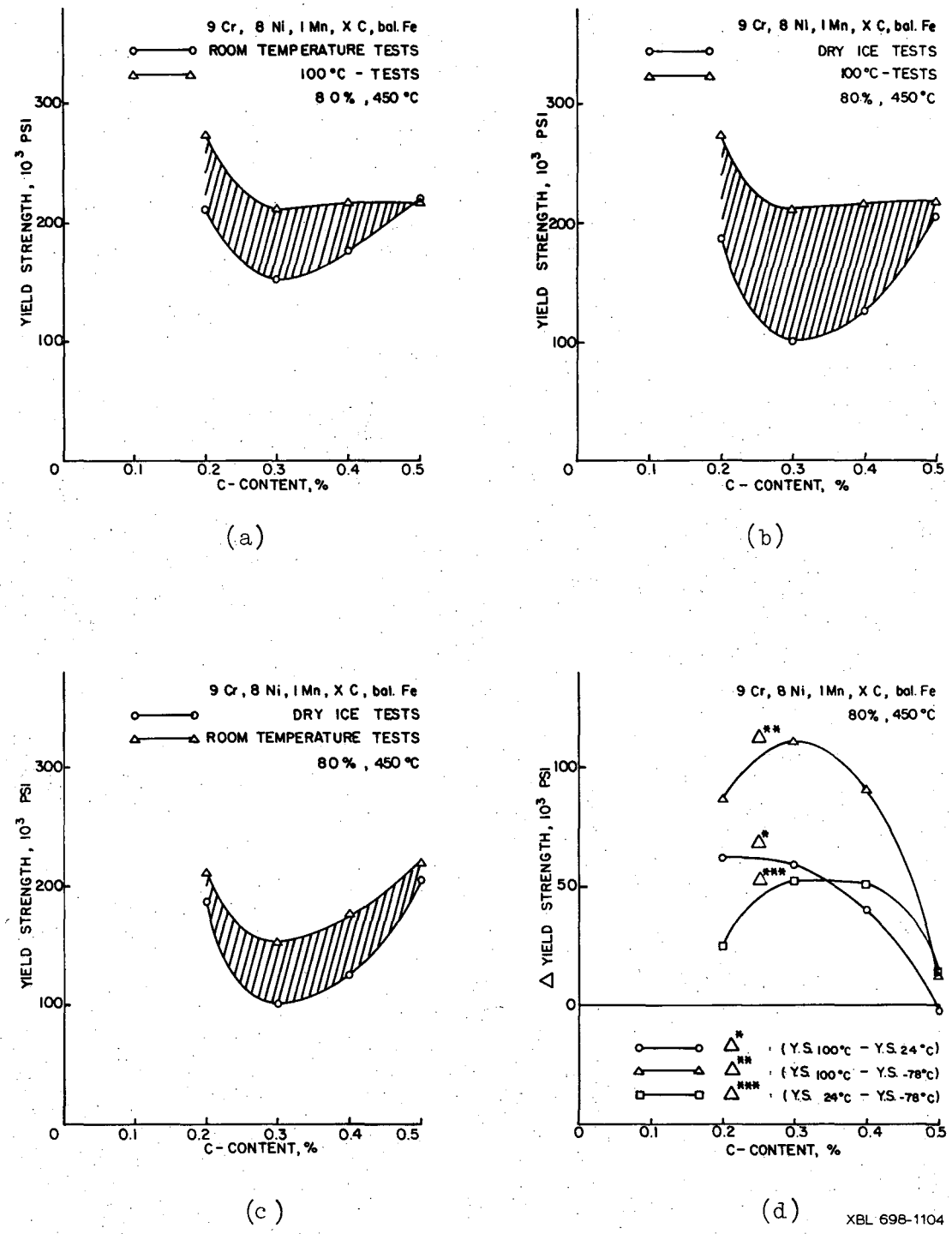
9 Cr, 8 Ni, 1 Mn, X C, bal. Fe
ROOM TEMPERATURE TESTS
100 °C - TESTS
80 %, 450 °C
YIELD STRENGTH, 10^3 PSI
C - CONTENT, %
(a)
9 Cr, 8 Ni, 1 Mn, X C, bal. Fe
DRY ICE TESTS
100 °C - TESTS
80 %, 450 °C
YIELD STRENGTH, 10^3 PSI
C - CONTENT, %
(b)
9 Cr, 8 Ni, 1 Mn, X C, bal. Fe
DRY ICE TESTS
ROOM TEMPERATURE TESTS
80 %, 450 °C
YIELD STRENGTH, 10^3 PSI
C - CONTENT, %
(c)
9 Cr, 8 Ni, 1 Mn, X C, bal. Fe
80 %, 450 °C
Δ YIELD STRENGTH, 10^3 PSI
Δ* : (Y.S. 100°C - Y.S. 24°C)
Δ** : (Y.S. 100°C - Y.S. -78°C)
Δ*** : (Y.S. 24°C - Y.S. -78°C)
C - CONTENT, %
(d)
XBL 698-1104

Fig. 3

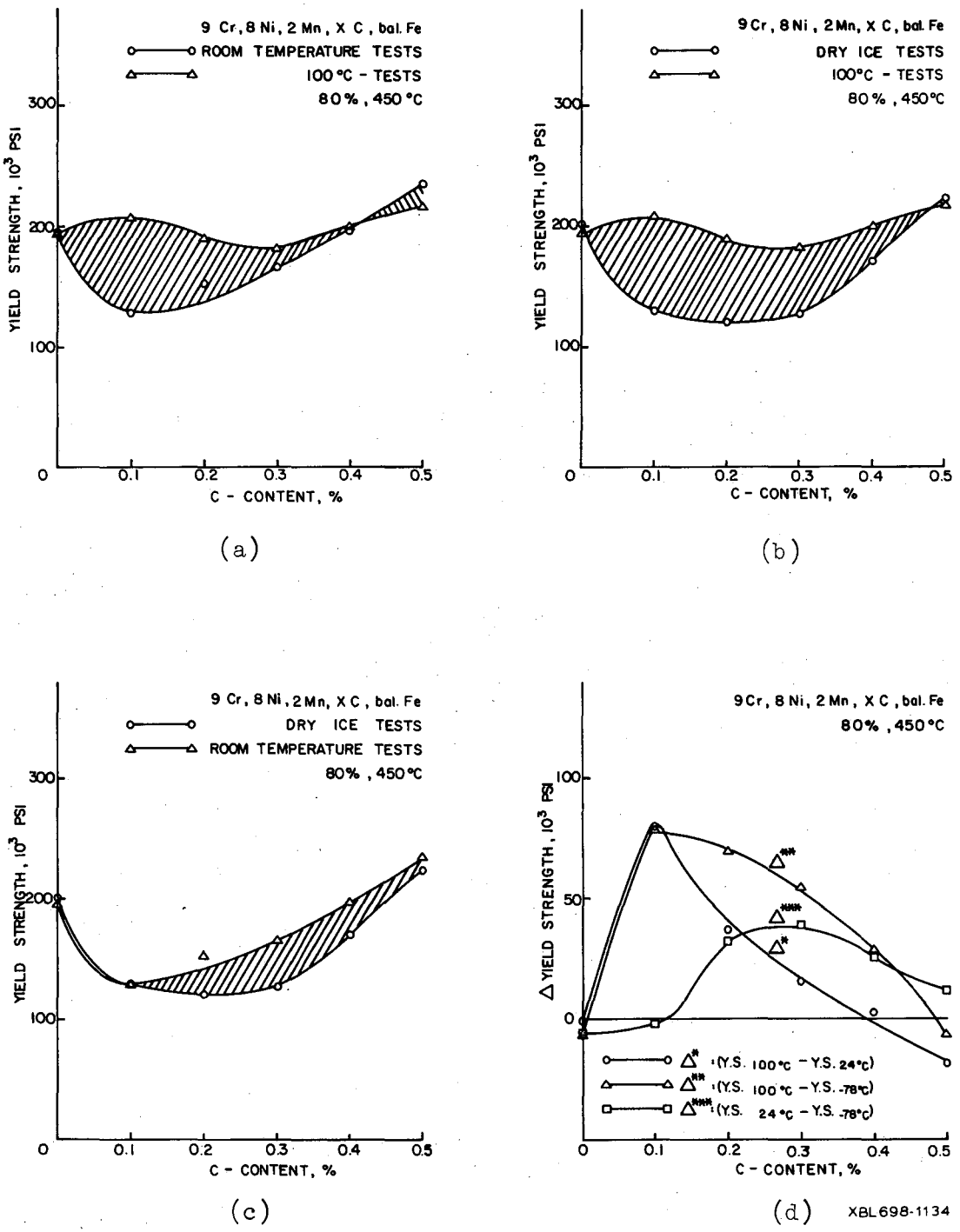
9 Cr, 8 Ni, 2 Mn, X C, bal. Fe
ROOM TEMPERATURE TESTS
100 °C - TESTS
80 %, 450 °C
YIELD STRENGTH, 10^3 PSI
C - CONTENT, %
(a)
9 Cr, 8 Ni, 2 Mn, X C, bal. Fe
DRY ICE TESTS
100 °C - TESTS
80 %, 450 °C
YIELD STRENGTH, 10^3 PSI
C - CONTENT, %
(b)
9 Cr, 8 Ni, 2 Mn, X C, bal. Fe
DRY ICE TESTS
ROOM TEMPERATURE TESTS
80 %, 450 °C
YIELD STRENGTH, 10^3 PSI
C - CONTENT, %
(c)
9 Cr, 8 Ni, 2 Mn, X C, bal. Fe
80 %, 450 °C
Δ YIELD STRENGTH, 10^3 PSI
Δ* (Y.S. 100 °C - Y.S. 24 °C)
Δ** (Y.S. 100 °C - Y.S. -78 °C)
Δ*** (Y.S. 24 °C - Y.S. -78 °C)
C - CONTENT, %
(d)
XBL698-1134

Fig. 4

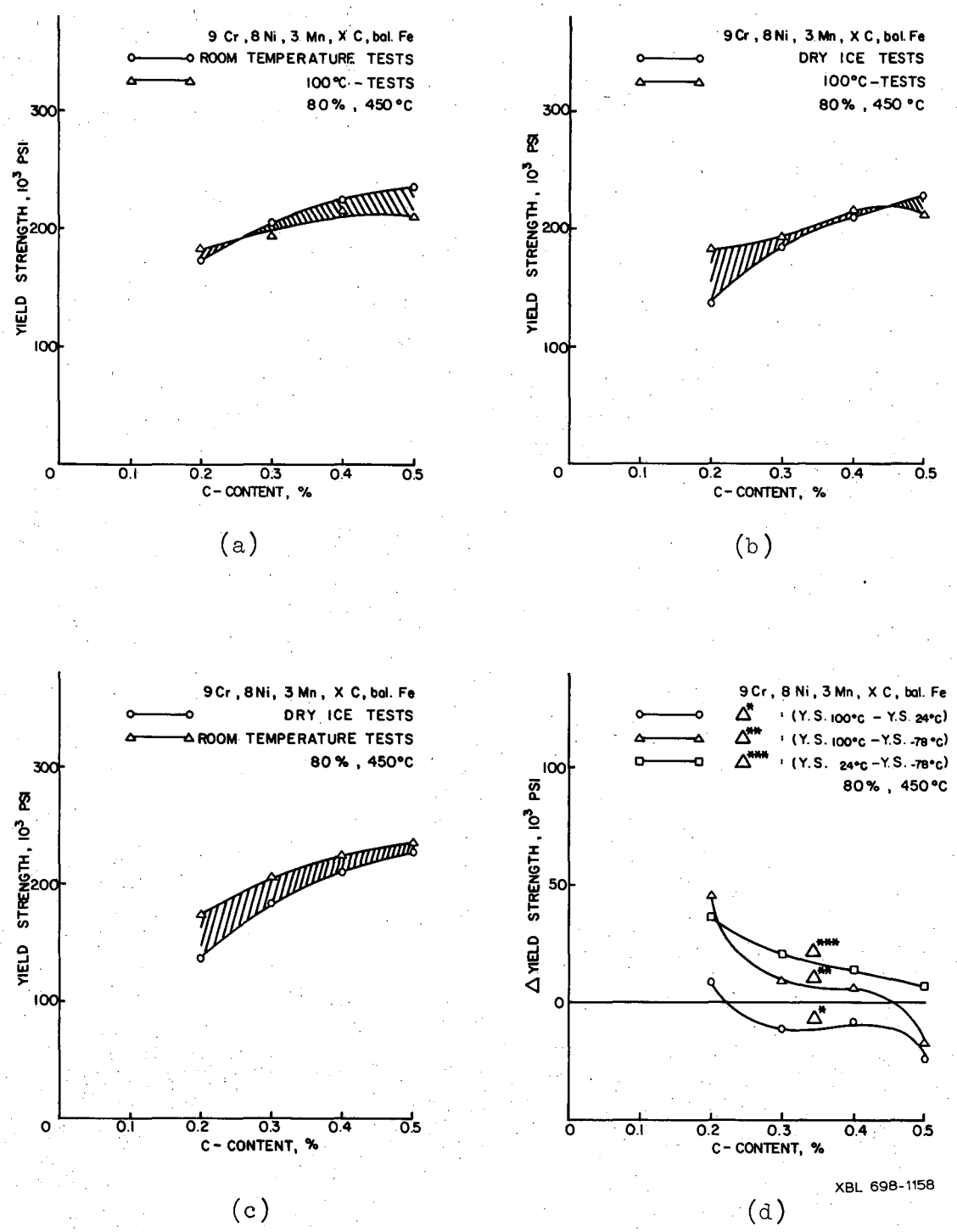
9 Cr, 8 Ni, 3 Mn, X C, bal. Fe
ROOM TEMPERATURE TESTS
100°C - TESTS
80%, 450°C
YIELD STRENGTH, 10^3 PSI
C - CONTENT, %
(a)
9 Cr, 8 Ni, 3 Mn, X C, bal. Fe
DRY ICE TESTS
100°C - TESTS
80%, 450°C
YIELD STRENGTH, 10^3 PSI
C - CONTENT, %
(b)
9 Cr, 8 Ni, 3 Mn, X C, bal. Fe
DRY ICE TESTS
ROOM TEMPERATURE TESTS
80%, 450°C
YIELD STRENGTH, 10^3 PSI
C - CONTENT, %
(c)
9 Cr, 8 Ni, 3 Mn, X C, bal. Fe
Δ* : (Y.S. 100°C - Y.S. 24°C)
Δ** : (Y.S. 100°C - Y.S. -78°C)
Δ*** : (Y.S. 24°C - Y.S. -78°C)
80%, 450°C
Δ YIELD STRENGTH, 10^3 PSI
C - CONTENT, %
XBL 698-1158
(d)

Fig. 5

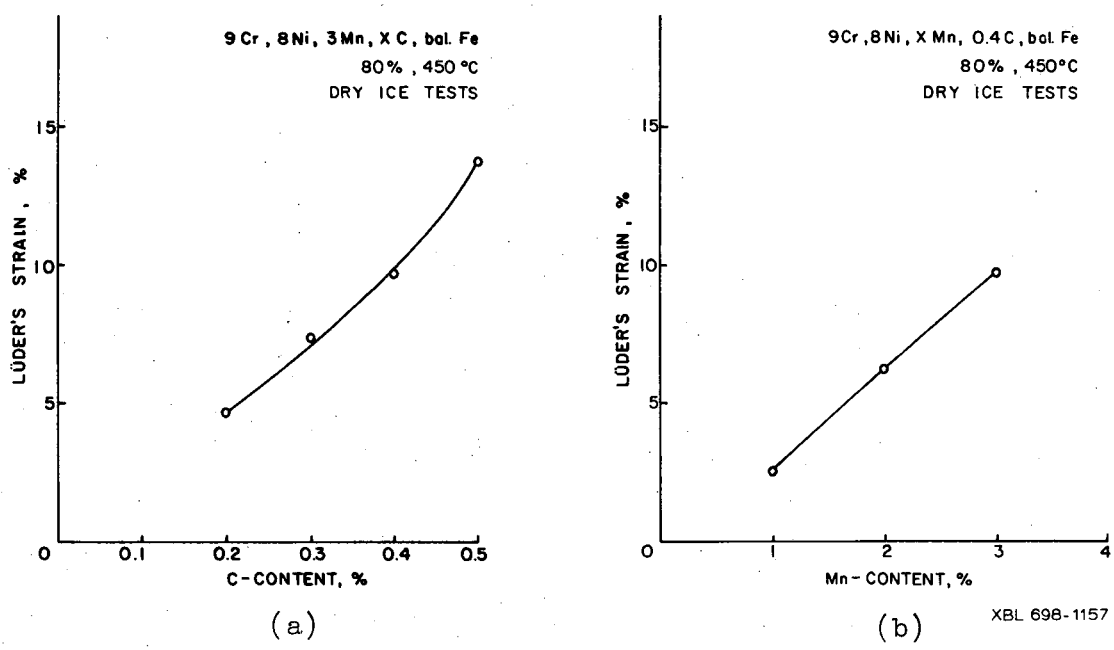
9 Cr, 8 Ni, 3 Mn, X C, bal. Fe
80%, 450 °C
DRY ICE TESTS
LÜDER'S STRAIN, %
C-CONTENT, %
0
0.1
0.2
0.3
0.4
0.5
5
10
15
(a)
9Cr, 8Ni, X Mn, 0.4 C, bal. Fe
80%, 450°C
DRY ICE TESTS
LÜDER'S STRAIN, %
Mn-CONTENT, %
0
1
2
3
4
5
10
15
(b)
XBL 698-1157

Fig. 6

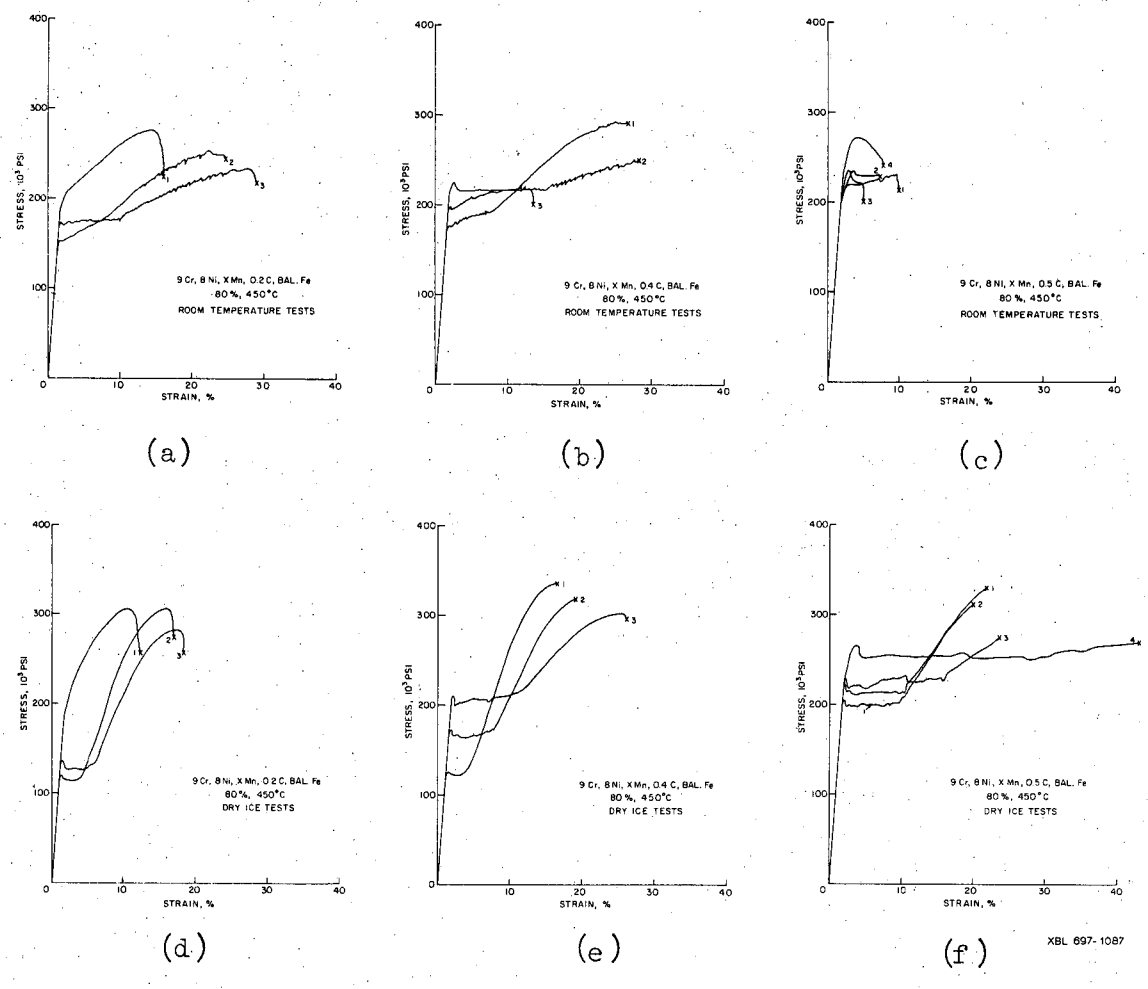
STRESS, 10^3 PSI
STRAIN, %
9 Cr, 8 Ni, X Mn, 0.2 C, BAL. Fe
80 %, 450°C
ROOM TEMPERATURE TESTS
(a)
9 Cr, 8 Ni, X Mn, 0.4 C, BAL. Fe
80 %, 450°C
ROOM TEMPERATURE TESTS
(b)
9 Cr, 8 Ni, X Mn, 0.5 C, BAL. Fe
80 %, 450°C
ROOM TEMPERATURE TESTS
(c)
9 Cr, 8 Ni, X Mn, 0.2 C, BAL. Fe
80 %, 450°C
DRY ICE TESTS
(d)
9 Cr, 8 Ni, X Mn, 0.4 C, BAL. Fe
80 %, 450°C
DRY ICE TESTS
(e)
9 Cr, 8 Ni, X Mn, 0.5 C, BAL. Fe
80 %, 450°C
DRY ICE TESTS
(f)
XBL 697-1087

Fig. 7

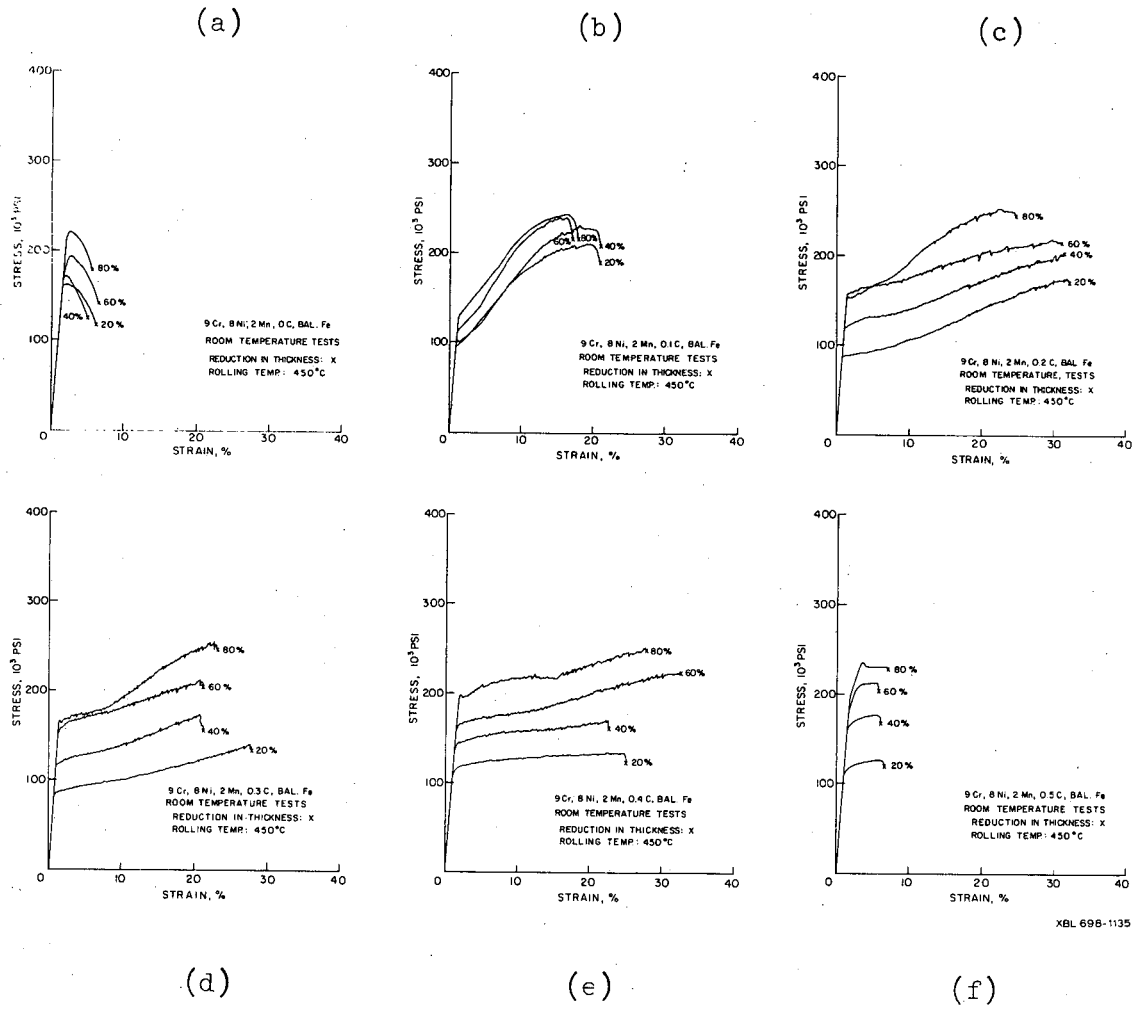
(a)
(b)
(c)
(d)
(e)
(f)
STRESS, 10^3 PSI
STRAIN, %
9 Cr, 8 Ni, 2 Mn, 0 C, BAL. Fe
ROOM TEMPERATURE TESTS
REDUCTION IN THICKNESS: X
ROLLING TEMP: 450°C
9 Cr, 8 Ni, 2 Mn, 0.1 C, BAL. Fe
9 Cr, 8 Ni, 2 Mn, 0.2 C, BAL. Fe
9 Cr, 8 Ni, 2 Mn, 0.3 C, BAL. Fe
9 Cr, 8 Ni, 2 Mn, 0.4 C, BAL. Fe
9 Cr, 8 Ni, 2 Mn, 0.5 C, BAL. Fe
80%
60%
40%
20%
XBL 698-1135

Fig. 8

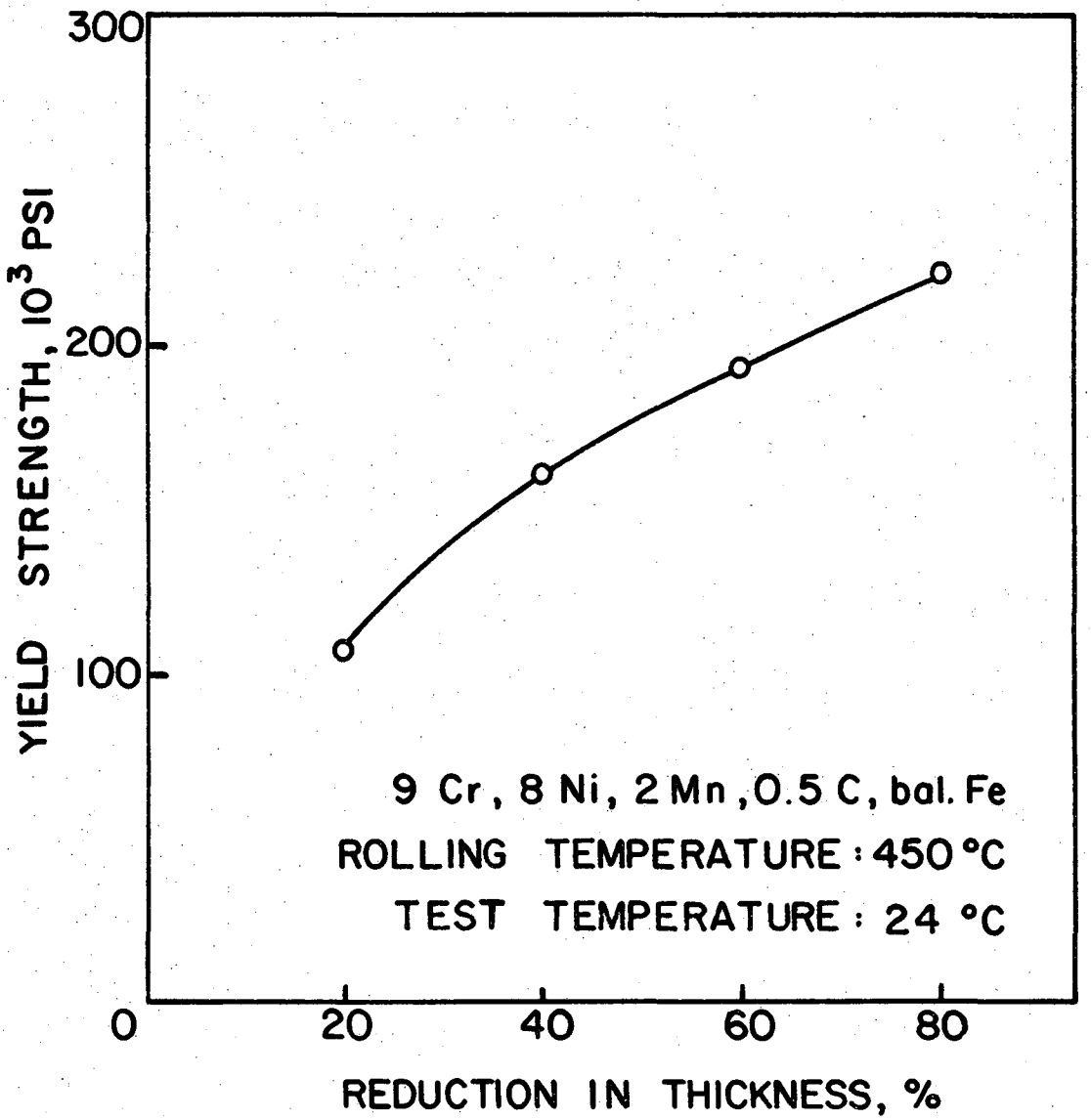

XBL 698-1133

Fig. 9

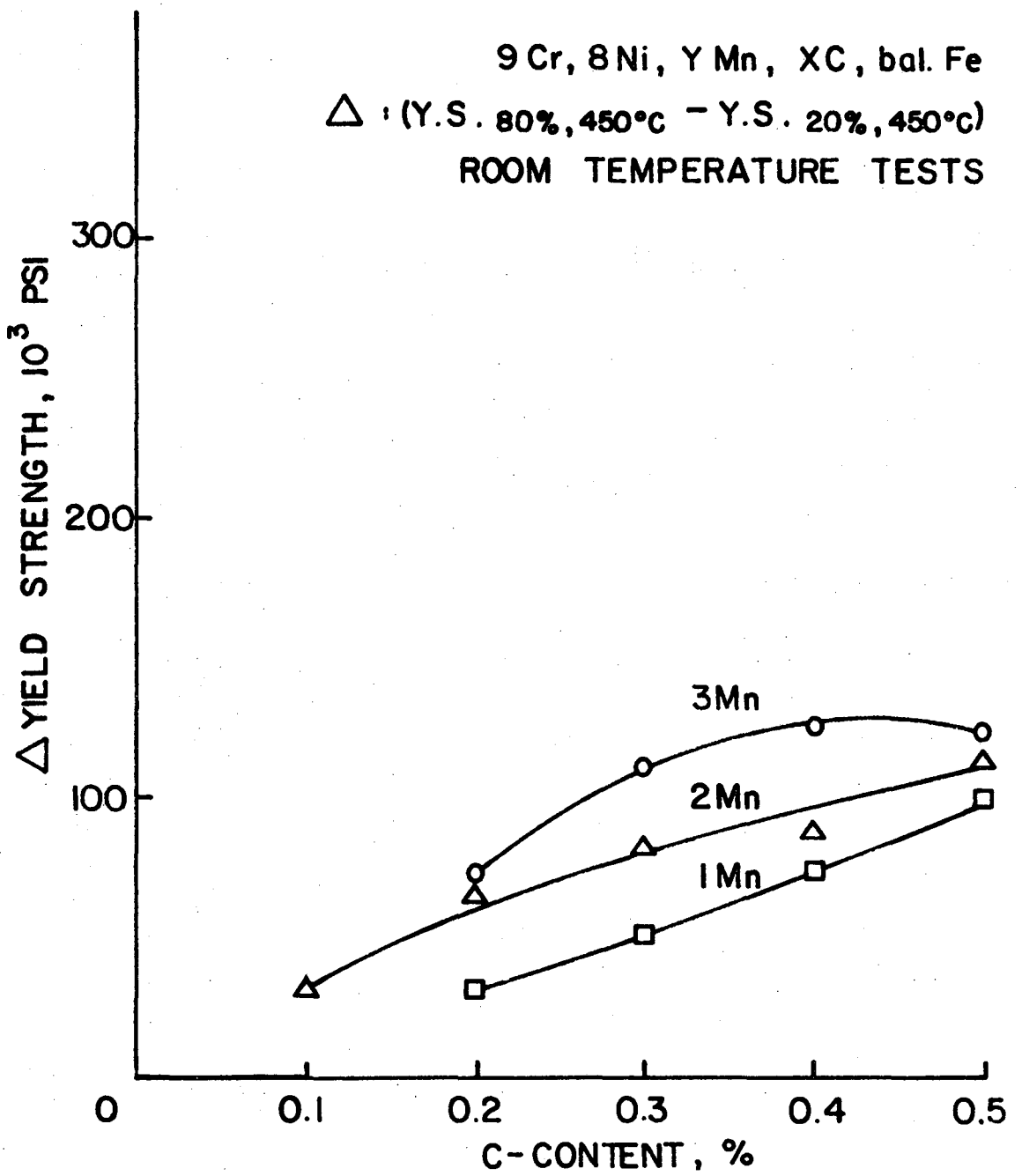

XBL 698-1156

Fig. 10

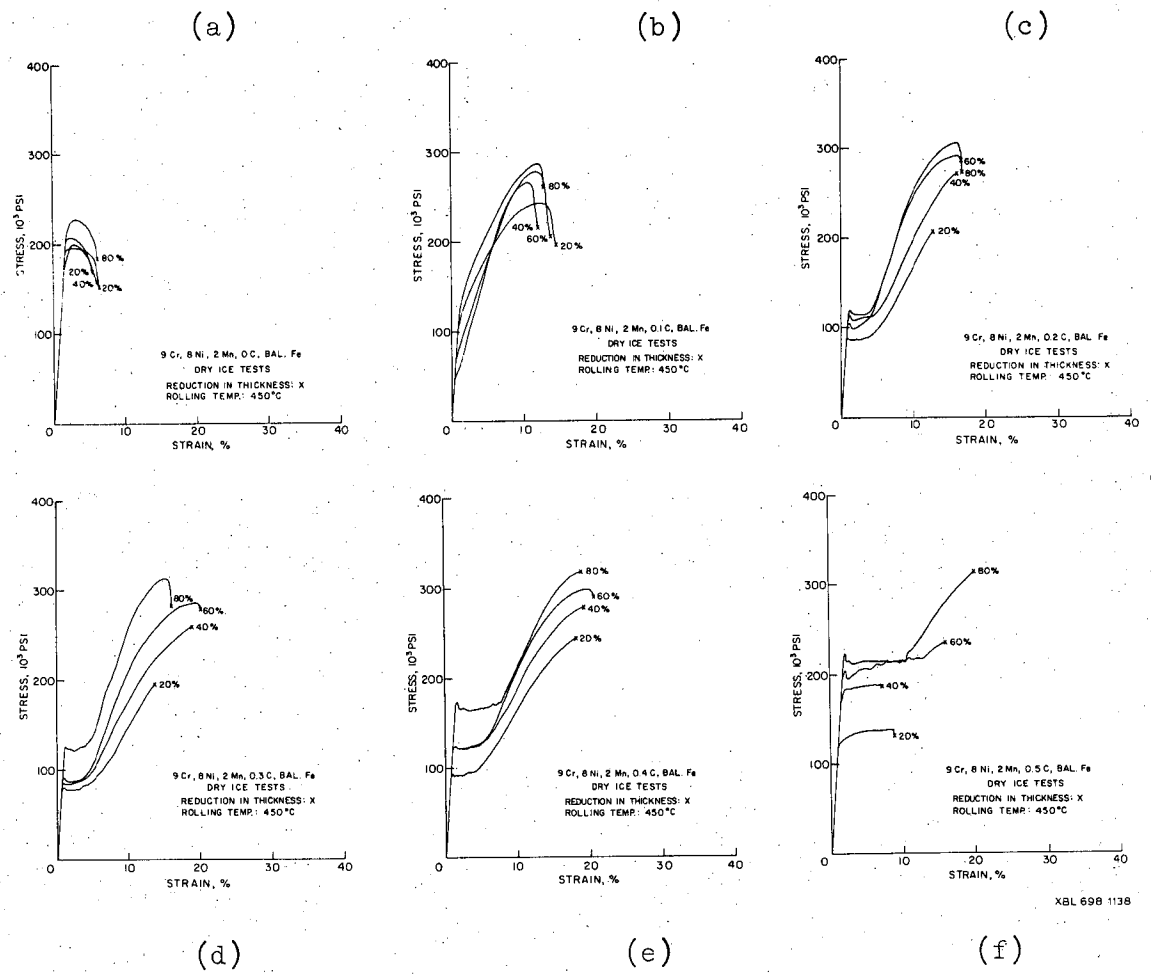
(a)
(b)
(c)
(d)
(e)
(f)
STRESS, 10^3 PSI
STRAIN, %
9 Cr, 8 Ni, 2 Mn, 0 C, BAL. Fe
DRY ICE TESTS
REDUCTION IN THICKNESS: X
ROLLING TEMP.: 450°C
9 Cr, 8 Ni, 2 Mn, 0.1 C, BAL. Fe
9 Cr, 8 Ni, 2 Mn, 0.2 C, BAL. Fe
9 Cr, 8 Ni, 2 Mn, 0.3 C, BAL. Fe
9 Cr, 8 Ni, 2 Mn, 0.4 C, BAL. Fe
9 Cr, 8 Ni, 2 Mn, 0.5 C, BAL. Fe
XBL 698 1138

Fig. 11

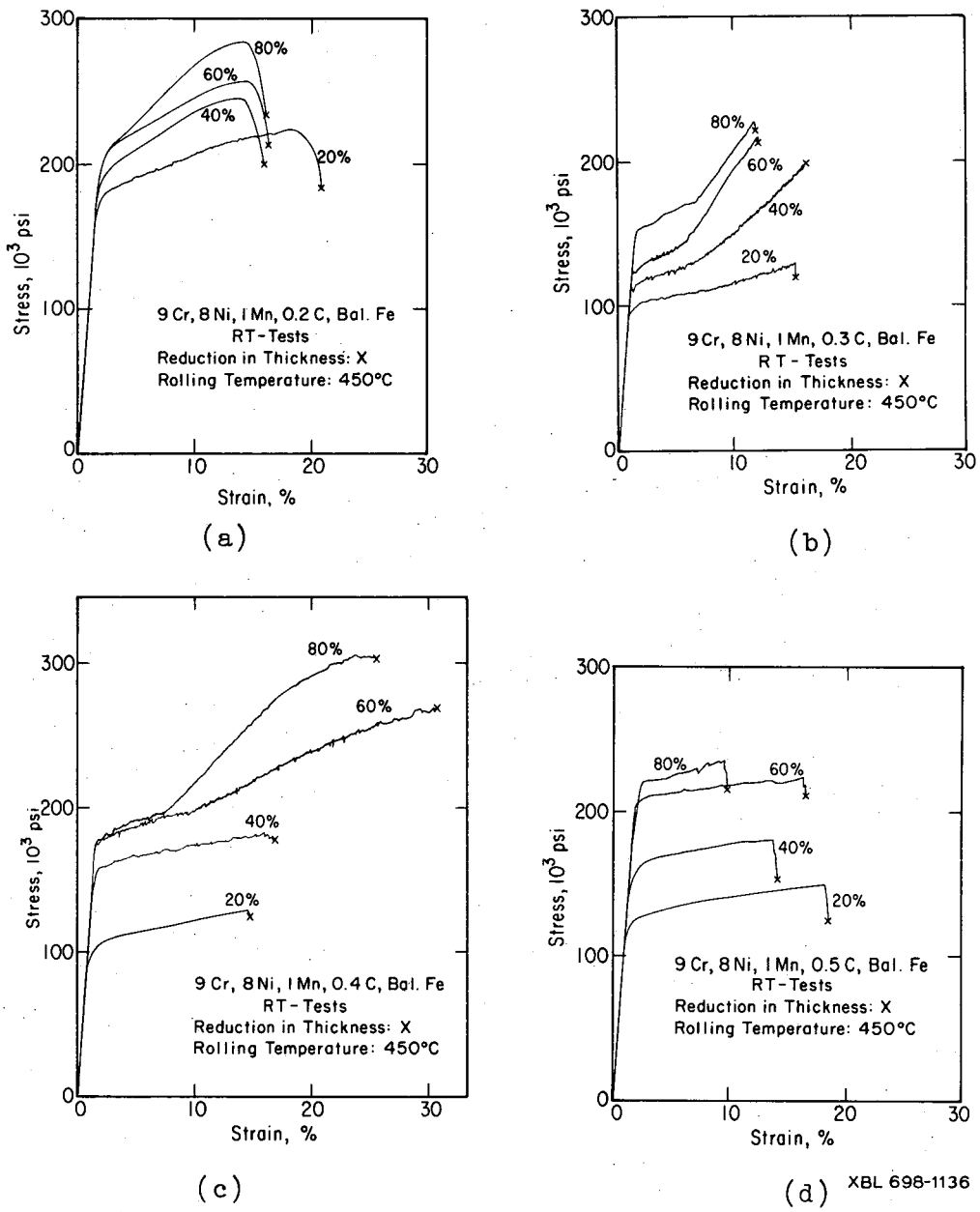
300
200
100
0
Stress, 10^3 psi
0
10
20
30
Strain, %
80%
60%
40%
20%
9 Cr, 8 Ni, 1 Mn, 0.2 C, Bal. Fe
RT-Tests
Reduction in Thickness: X
Rolling Temperature: 450°C
(a)
9 Cr, 8 Ni, 1 Mn, 0.3 C, Bal. Fe
RT-Tests
Reduction in Thickness: X
Rolling Temperature: 450°C
(b)
9 Cr, 8 Ni, 1 Mn, 0.4 C, Bal. Fe
RT-Tests
Reduction in Thickness: X
Rolling Temperature: 450°C
(c)
9 Cr, 8 Ni, 1 Mn, 0.5 C, Bal. Fe
RT-Tests
Reduction in Thickness: X
Rolling Temperature: 450°C
(d)
XBL 698-1136

Fig. 12

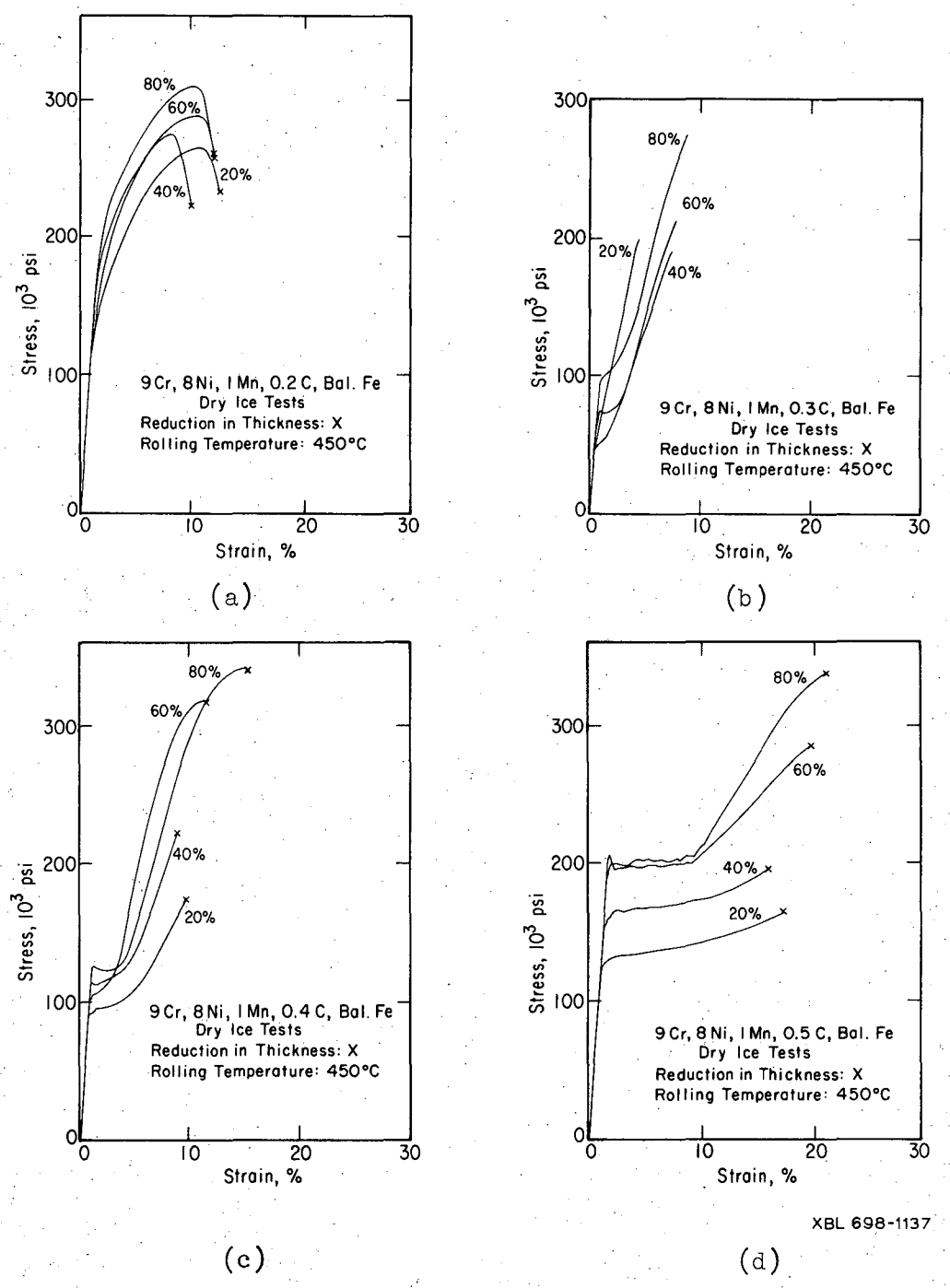
80%
60%
40%
20%
9 Cr, 8 Ni, 1 Mn, 0.2 C, Bal. Fe
Dry Ice Tests
Reduction in Thickness: X
Rolling Temperature: 450°C
Stress, 10^3 psi
Strain, %
(a)
80%
60%
20%
40%
9 Cr, 8 Ni, 1 Mn, 0.3 C, Bal. Fe
Dry Ice Tests
Reduction in Thickness: X
Rolling Temperature: 450°C
Stress, 10^3 psi
Strain, %
(b)
80%
60%
40%
20%
9 Cr, 8 Ni, 1 Mn, 0.4 C, Bal. Fe
Dry Ice Tests
Reduction in Thickness: X
Rolling Temperature: 450°C
Stress, 10^3 psi
Strain, %
(c)
80%
60%
40%
20%
9 Cr, 8 Ni, 1 Mn, 0.5 C, Bal. Fe
Dry Ice Tests
Reduction in Thickness: X
Rolling Temperature: 450°C
Stress, 10^3 psi
Strain, %
(d)
XBL 698-1137

Fig. 13

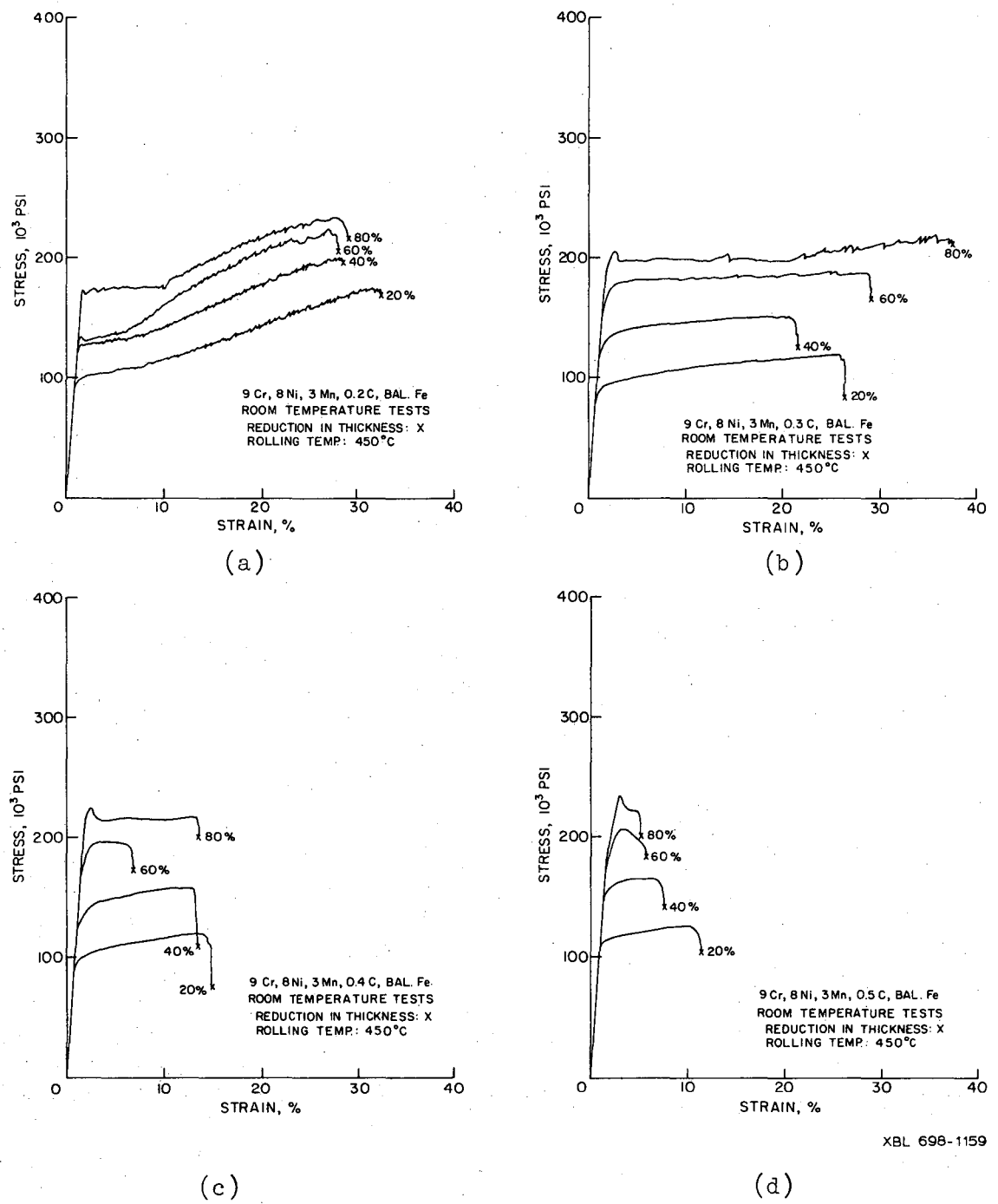
STRESS, 10^3 PSI
STRAIN, %
80%
60%
40%
20%
9 Cr, 8 Ni, 3 Mn, 0.2 C, BAL. Fe
ROOM TEMPERATURE TESTS
REDUCTION IN THICKNESS: X
ROLLING TEMP: 450°C
(a)
9 Cr, 8 Ni, 3 Mn, 0.3 C, BAL. Fe
ROOM TEMPERATURE TESTS
REDUCTION IN THICKNESS: X
ROLLING TEMP: 450°C
(b)
9 Cr, 8 Ni, 3 Mn, 0.4 C, BAL. Fe
ROOM TEMPERATURE TESTS
REDUCTION IN THICKNESS: X
ROLLING TEMP: 450°C
(c)
9 Cr, 8 Ni, 3 Mn, 0.5 C, BAL. Fe
ROOM TEMPERATURE TESTS
REDUCTION IN THICKNESS: X
ROLLING TEMP: 450°C
(d)
XBL 698-1159

Fig. 14

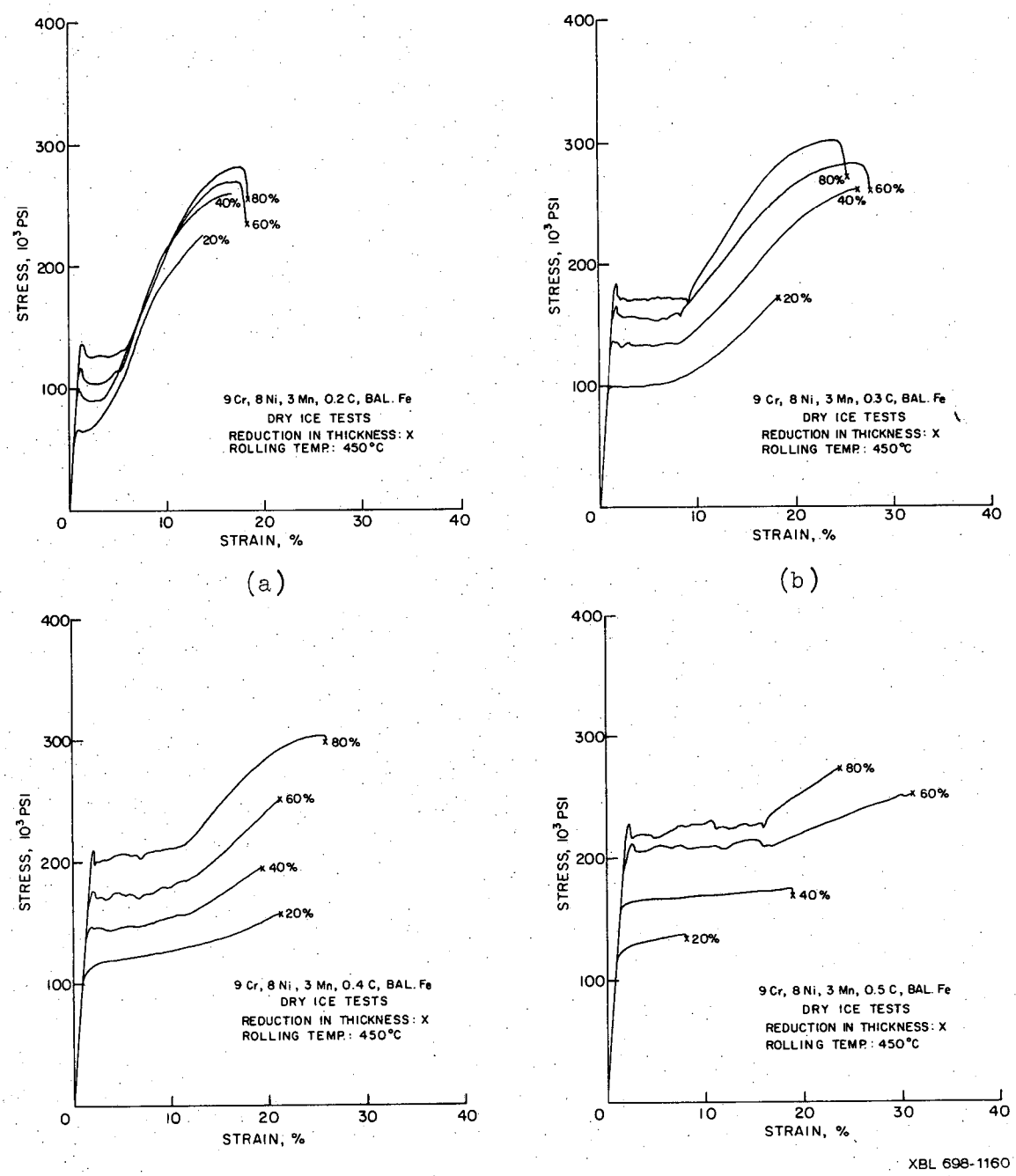
STRESS, 10^3 PSI
STRAIN, %
9 Cr, 8 Ni, 3 Mn, 0.2 C, BAL. Fe
DRY ICE TESTS
REDUCTION IN THICKNESS: X
ROLLING TEMP.: 450°C
80%
60%
40%
20%
(a)
9 Cr, 8 Ni, 3 Mn, 0.3 C, BAL. Fe
DRY ICE TESTS
REDUCTION IN THICKNESS: X
ROLLING TEMP.: 450°C
(b)
9 Cr, 8 Ni, 3 Mn, 0.4 C, BAL. Fe
DRY ICE TESTS
REDUCTION IN THICKNESS: X
ROLLING TEMP.: 450°C
(c)
9 Cr, 8 Ni, 3 Mn, 0.5 C, BAL. Fe
DRY ICE TESTS
REDUCTION IN THICKNESS: X
ROLLING TEMP.: 450°C
(d)
XBL 698-1160

Fig. 15

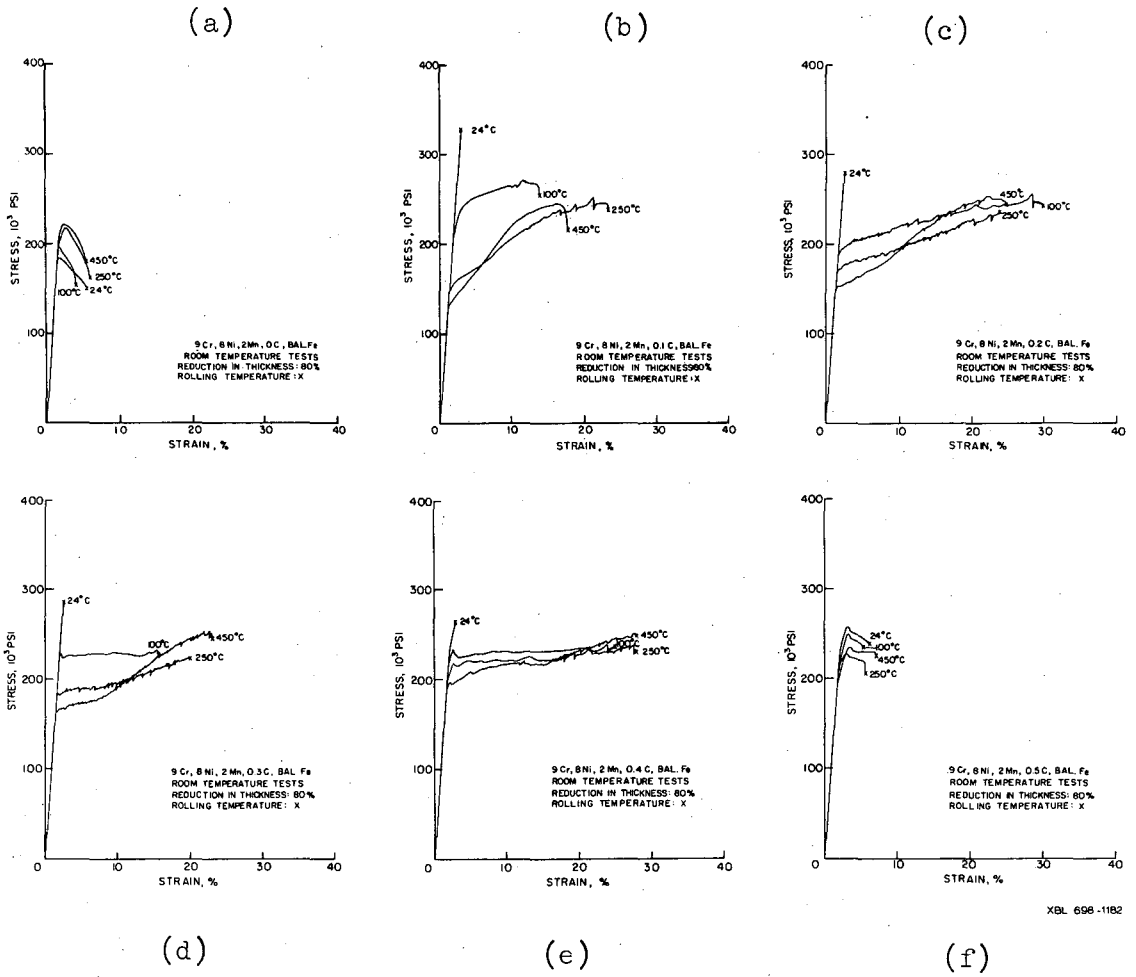
(a)
(b)
(c)
(d)
(e)
(f)
STRESS, 10^3 PSI
STRAIN, %
9 Cr, 8 Ni, 2 Mn, 0 C, BAL. Fe
ROOM TEMPERATURE TESTS
REDUCTION IN THICKNESS: 80%
ROLLING TEMPERATURE: X
9 Cr, 8 Ni, 2 Mn, 0.1 C, BAL. Fe
ROOM TEMPERATURE TESTS
REDUCTION IN THICKNESS 80%
ROLLING TEMPERATURE: X
9 Cr, 8 Ni, 2 Mn, 0.2 C, BAL. Fe
ROOM TEMPERATURE TESTS
REDUCTION IN THICKNESS: 80%
ROLLING TEMPERATURE: X
9 Cr, 8 Ni, 2 Mn, 0.3 C, BAL. Fe
ROOM TEMPERATURE TESTS
REDUCTION IN THICKNESS: 80%
ROLLING TEMPERATURE: X
9 Cr, 8 Ni, 2 Mn, 0.4 C, BAL. Fe
ROOM TEMPERATURE TESTS
REDUCTION IN THICKNESS: 80%
ROLLING TEMPERATURE: X
9 Cr, 8 Ni, 2 Mn, 0.5 C, BAL. Fe
ROOM TEMPERATURE TESTS
REDUCTION IN THICKNESS: 80%
ROLLING TEMPERATURE: X
XBL 698-1182

Fig. 16

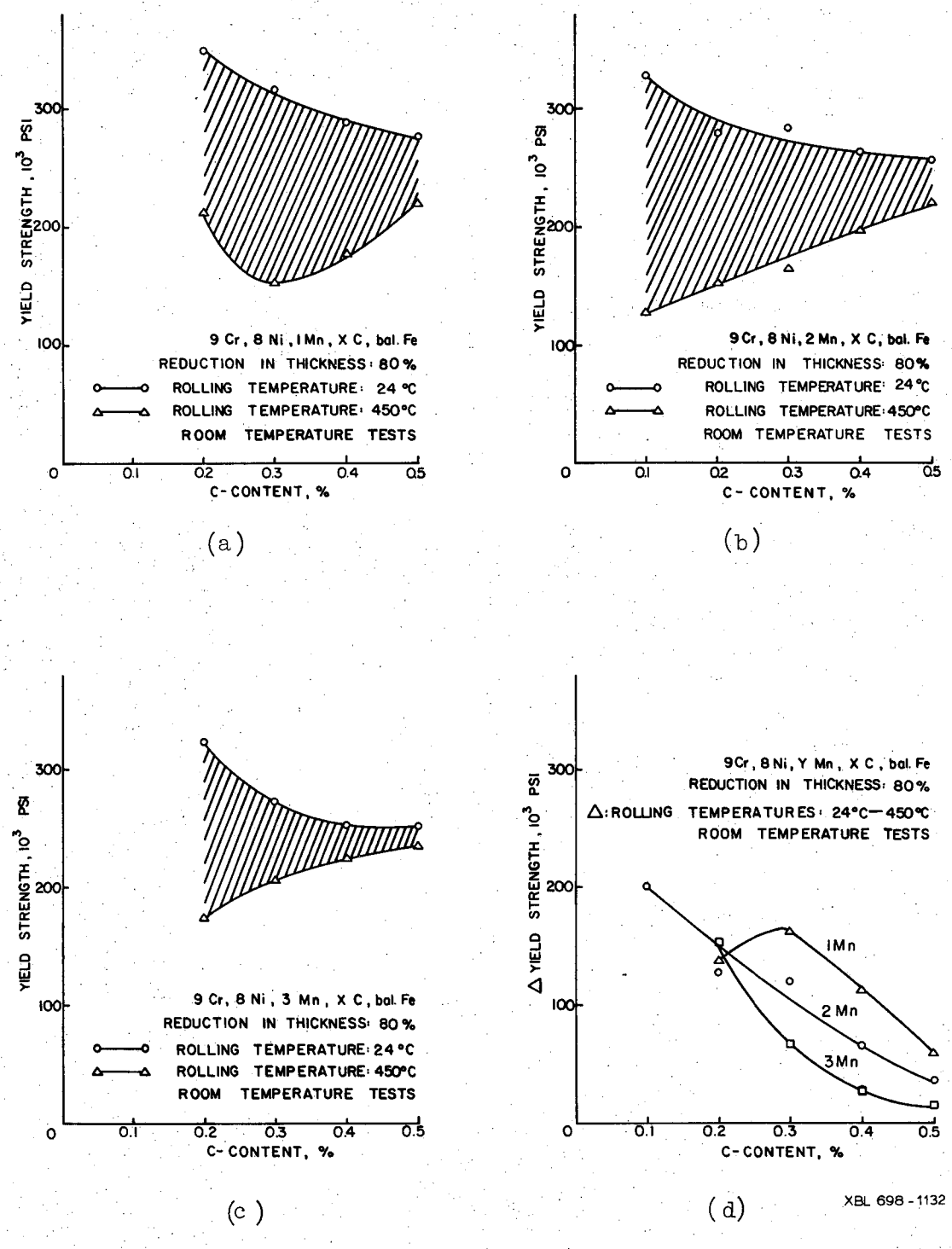
YIELD STRENGTH, 10^3 PSI
C-CONTENT, %
9 Cr, 8 Ni, 1 Mn, X C, bal. Fe
REDUCTION IN THICKNESS: 80%
ROLLING TEMPERATURE: 24 °C
ROLLING TEMPERATURE: 450°C
ROOM TEMPERATURE TESTS
(a)
9 Cr, 8 Ni, 2 Mn, X C, bal. Fe
REDUCTION IN THICKNESS: 80%
ROLLING TEMPERATURE: 24 °C
ROLLING TEMPERATURE: 450°C
ROOM TEMPERATURE TESTS
(b)
9 Cr, 8 Ni, 3 Mn, X C, bal. Fe
REDUCTION IN THICKNESS: 80%
ROLLING TEMPERATURE: 24 °C
ROLLING TEMPERATURE: 450°C
ROOM TEMPERATURE TESTS
(c)
Δ YIELD STRENGTH, 10^3 PSI
9 Cr, 8 Ni, Y Mn, X C, bal. Fe
REDUCTION IN THICKNESS: 80%
Δ: ROLLING TEMPERATURES: 24°C—450°C
ROOM TEMPERATURE TESTS
1 Mn
2 Mn
3 Mn
(d)
XBL 698-1132

Fig. 17

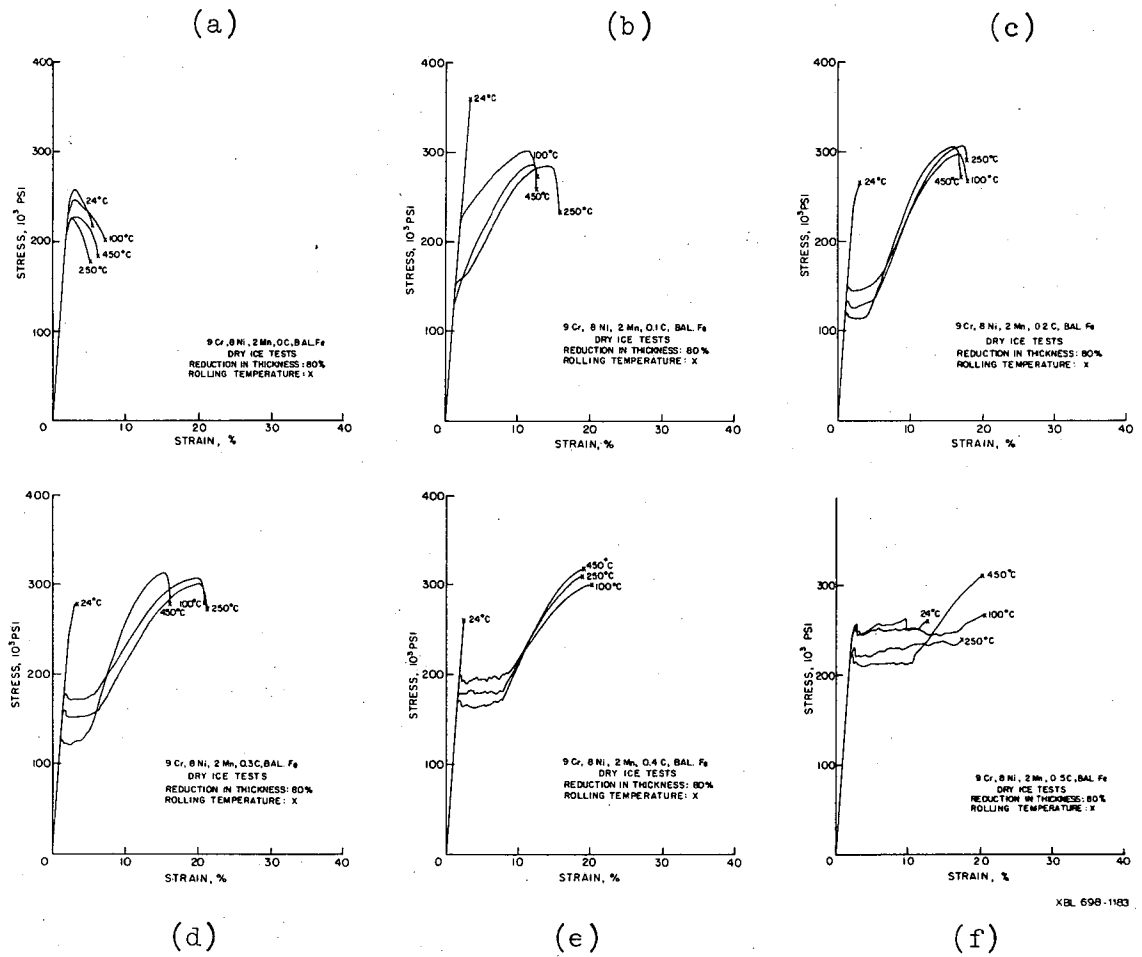
(a)
(b)
(c)
(d)
(e)
(f)
STRESS, 10^3 PSI
STRAIN, %
24°C
100°C
450°C
250°C
9 Cr, 8 Ni, 2 Mn, 0C, BAL Fe
DRY ICE TESTS
REDUCTION IN THICKNESS: 80%
ROLLING TEMPERATURE: X
9 Cr, 8 Ni, 2 Mn, 0.1 C, BAL. Fe
9 Cr, 8 Ni, 2 Mn, 0.2 C, BAL Fe
9 Cr, 8 Ni, 2 Mn, 0.3C, BAL. Fe
9 Cr, 8 Ni, 2 Mn, 0.4 C, BAL. Fe
9 Cr, 8 Ni, 2 Mn, 0.5C, BAL Fe
XBL 698-1183

Fig. 18

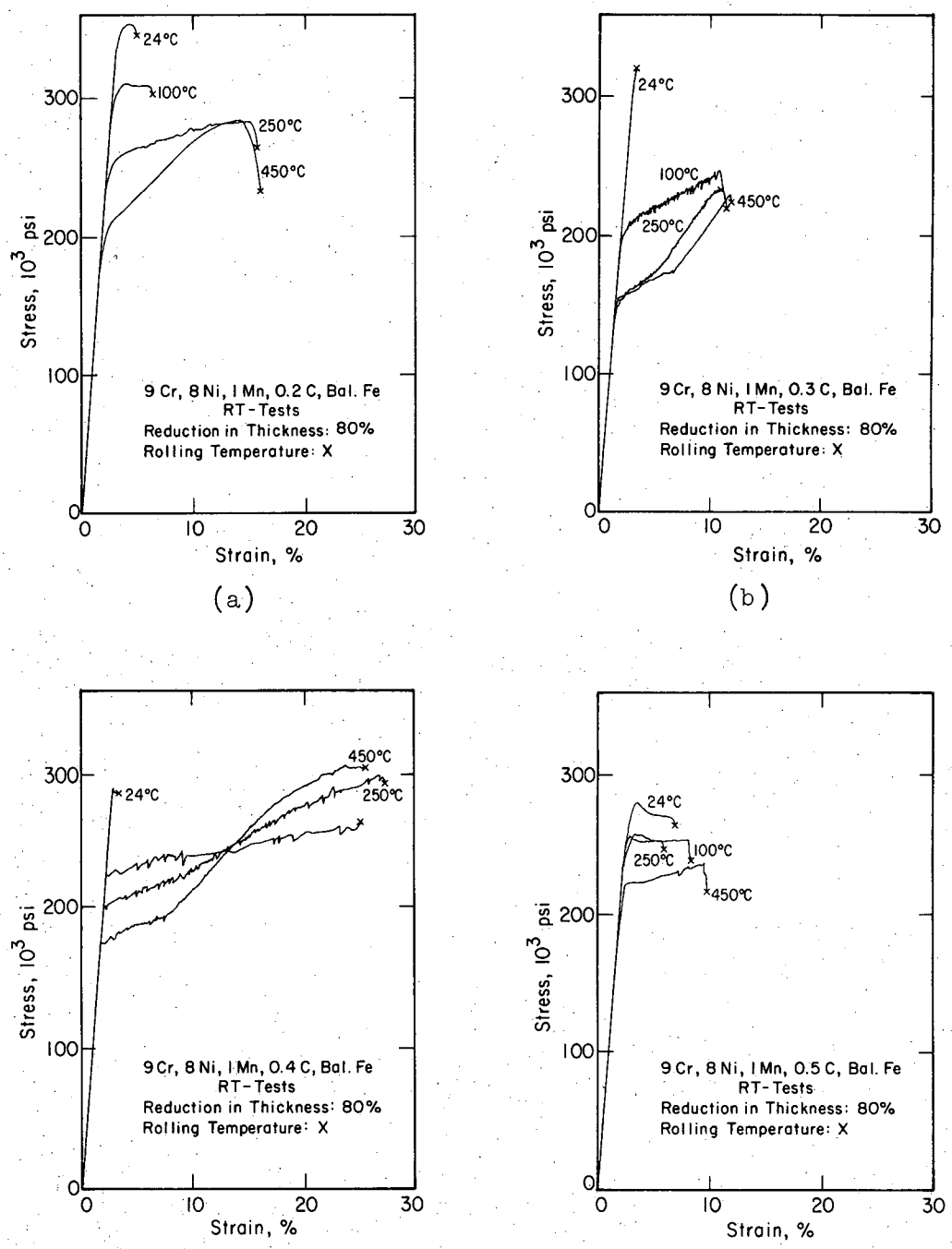
24°C
100°C
250°C
450°C
9 Cr, 8 Ni, 1 Mn, 0.2 C, Bal. Fe
RT-Tests
Reduction in Thickness: 80%
Rolling Temperature: X
Stress, 10^3 psi
Strain, %
(a)
24°C
100°C
250°C
450°C
9 Cr, 8 Ni, 1 Mn, 0.3 C, Bal. Fe
RT-Tests
Reduction in Thickness: 80%
Rolling Temperature: X
Stress, 10^3 psi
Strain, %
(b)
24°C
450°C
250°C
9 Cr, 8 Ni, 1 Mn, 0.4 C, Bal. Fe
RT-Tests
Reduction in Thickness: 80%
Rolling Temperature: X
Stress, 10^3 psi
Strain, %
(c)
24°C
250°C
100°C
450°C
9 Cr, 8 Ni, 1 Mn, 0.5 C, Bal. Fe
RT-Tests
Reduction in Thickness: 80%
Rolling Temperature: X
Stress, 10^3 psi
Strain, %
(d)
XBL 698-1177

Fig. 19

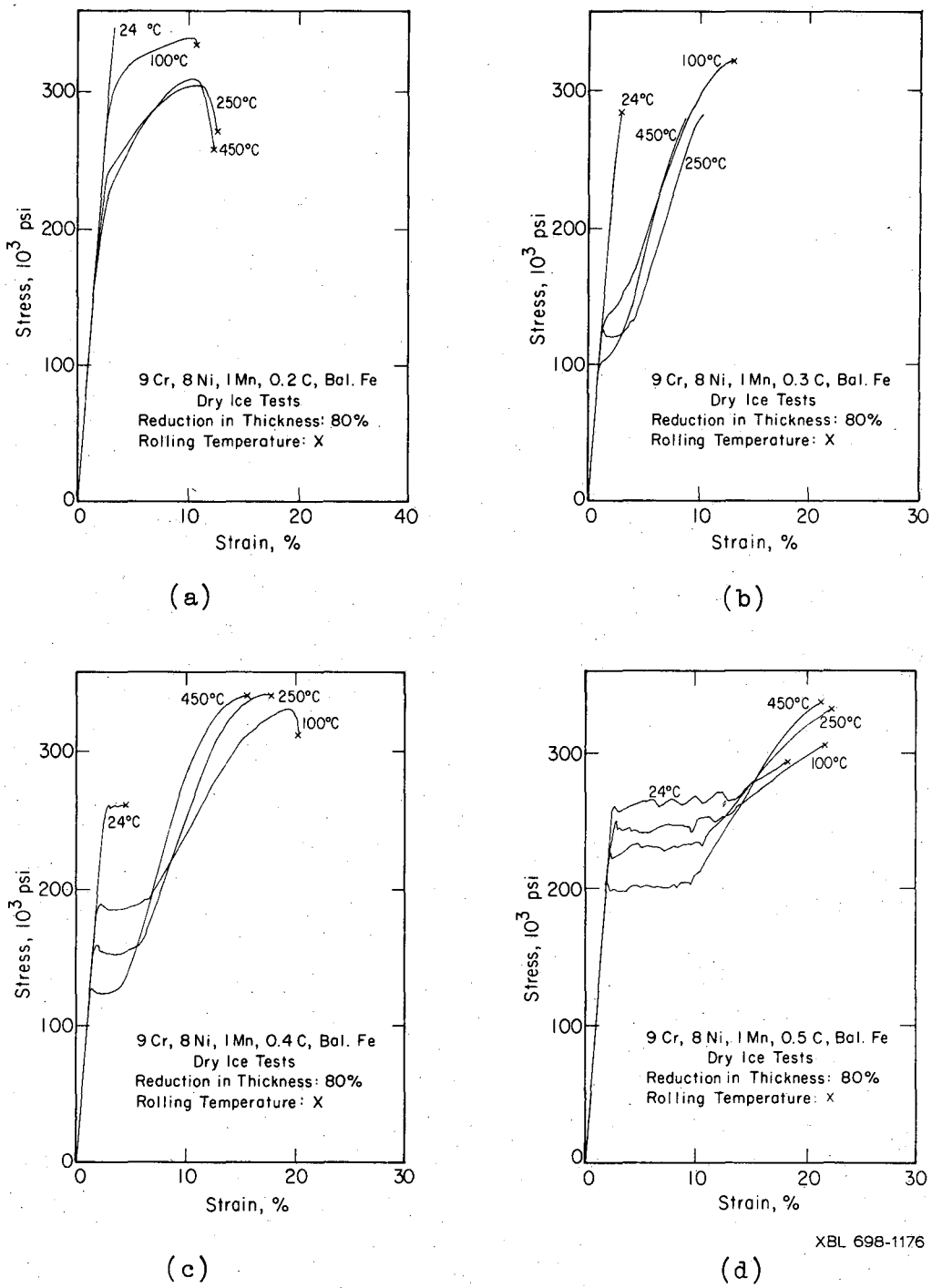
24 °C
100°C
250°C
450°C
Stress, 10^3 psi
Strain, %
9 Cr, 8 Ni, 1 Mn, 0.2 C, Bal. Fe
Dry Ice Tests
Reduction in Thickness: 80%
Rolling Temperature: X
(a)
100°C
24°C
450°C
250°C
9 Cr, 8 Ni, 1 Mn, 0.3 C, Bal. Fe
Dry Ice Tests
Reduction in Thickness: 80%
Rolling Temperature: X
(b)
450°C
250°C
100°C
24°C
9 Cr, 8 Ni, 1 Mn, 0.4 C, Bal. Fe
Dry Ice Tests
Reduction in Thickness: 80%
Rolling Temperature: X
(c)
450°C
250°C
100°C
24°C
9 Cr, 8 Ni, 1 Mn, 0.5 C, Bal. Fe
Dry Ice Tests
Reduction in Thickness: 80%
Rolling Temperature: X
(d)
XBL 698-1176

Fig. 20

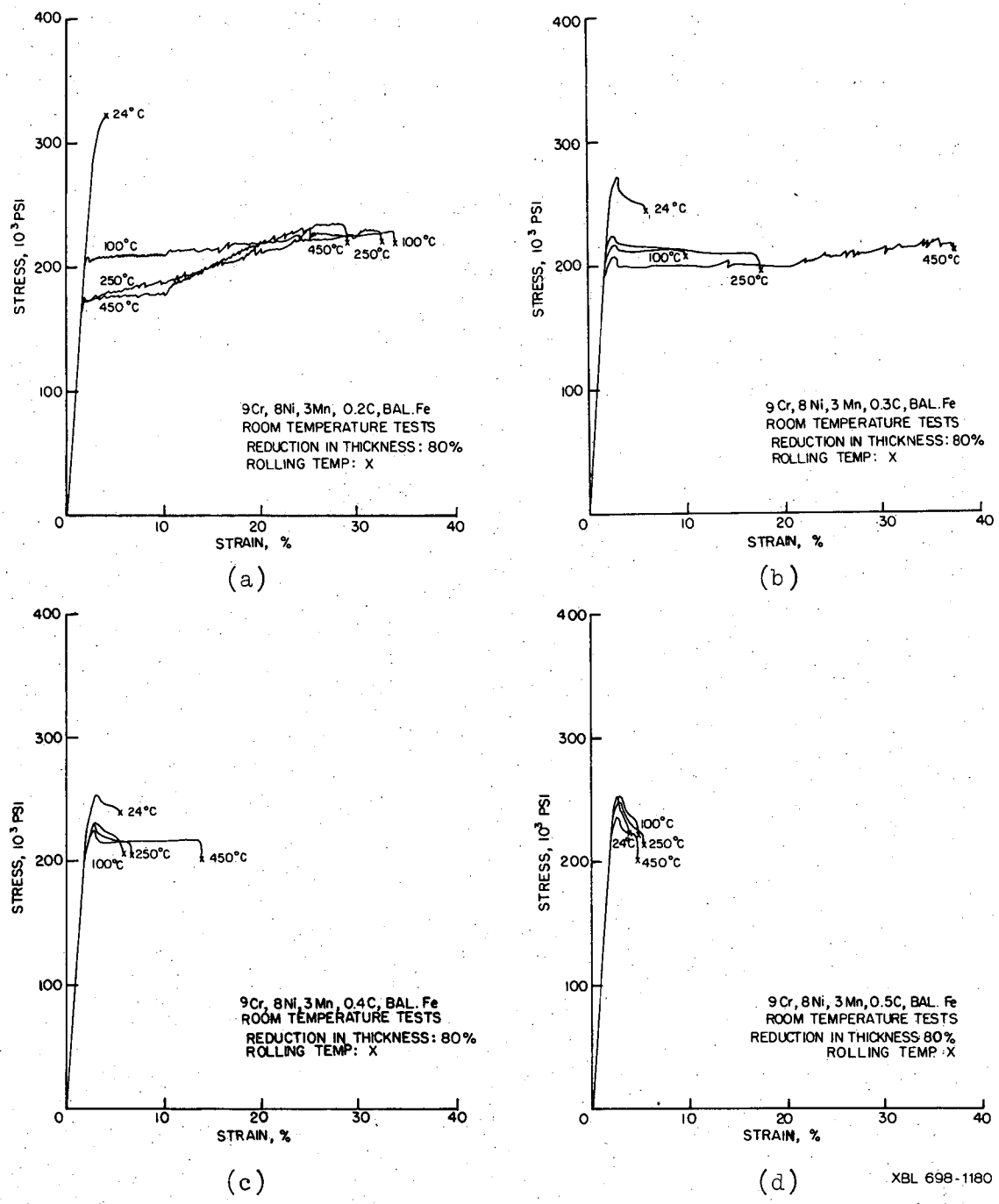
STRESS, 10^3 PSI
STRAIN, %
24°C
100°C
250°C
450°C
9Cr, 8Ni, 3Mn, 0.2C, BAL. Fe
ROOM TEMPERATURE TESTS
REDUCTION IN THICKNESS: 80%
ROLLING TEMP: X
(a)
9Cr, 8Ni, 3Mn, 0.3C, BAL. Fe
ROOM TEMPERATURE TESTS
REDUCTION IN THICKNESS: 80%
ROLLING TEMP: X
(b)
9Cr, 8Ni, 3Mn, 0.4C, BAL. Fe
ROOM TEMPERATURE TESTS
REDUCTION IN THICKNESS: 80%
ROLLING TEMP: X
(c)
9Cr, 8Ni, 3Mn, 0.5C, BAL. Fe
ROOM TEMPERATURE TESTS
REDUCTION IN THICKNESS 80%
ROLLING TEMP X
(d)
XBL 698-1180

Fig. 21

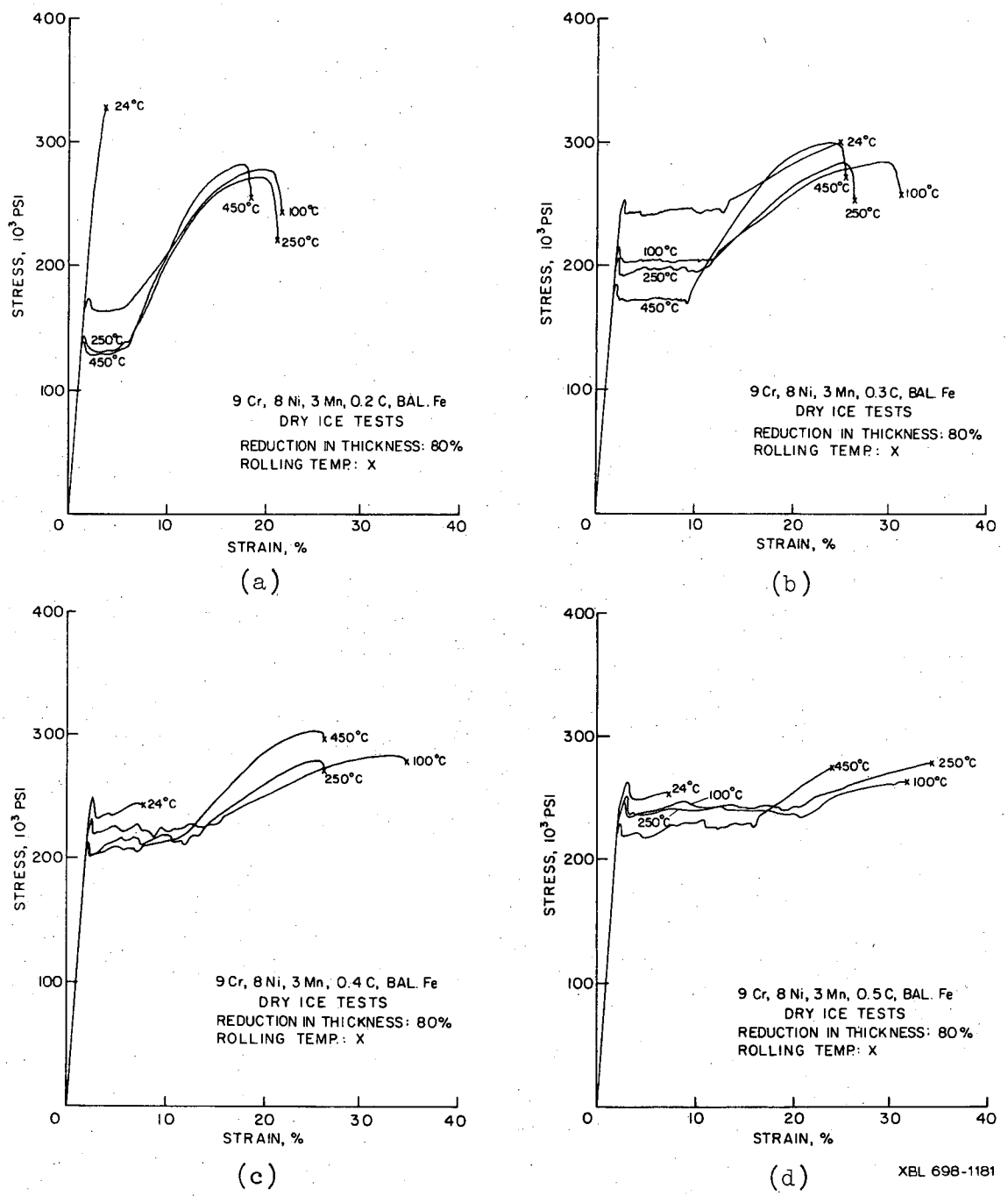
STRESS, 10^3 PSI
STRAIN, %
24°C
450°C
100°C
250°C
9 Cr, 8 Ni, 3 Mn, 0.2 C, BAL. Fe
DRY ICE TESTS
REDUCTION IN THICKNESS: 80%
ROLLING TEMP.: X
(a)
9 Cr, 8 Ni, 3 Mn, 0.3 C, BAL. Fe
DRY ICE TESTS
REDUCTION IN THICKNESS: 80%
ROLLING TEMP.: X
(b)
9 Cr, 8 Ni, 3 Mn, 0.4 C, BAL. Fe
DRY ICE TESTS
REDUCTION IN THICKNESS: 80%
ROLLING TEMP.: X
(c)
9 Cr, 8 Ni, 3 Mn, 0.5 C, BAL. Fe
DRY ICE TESTS
REDUCTION IN THICKNESS: 80%
ROLLING TEMP.: X
(d)
XBL 698-1181

Fig. 22

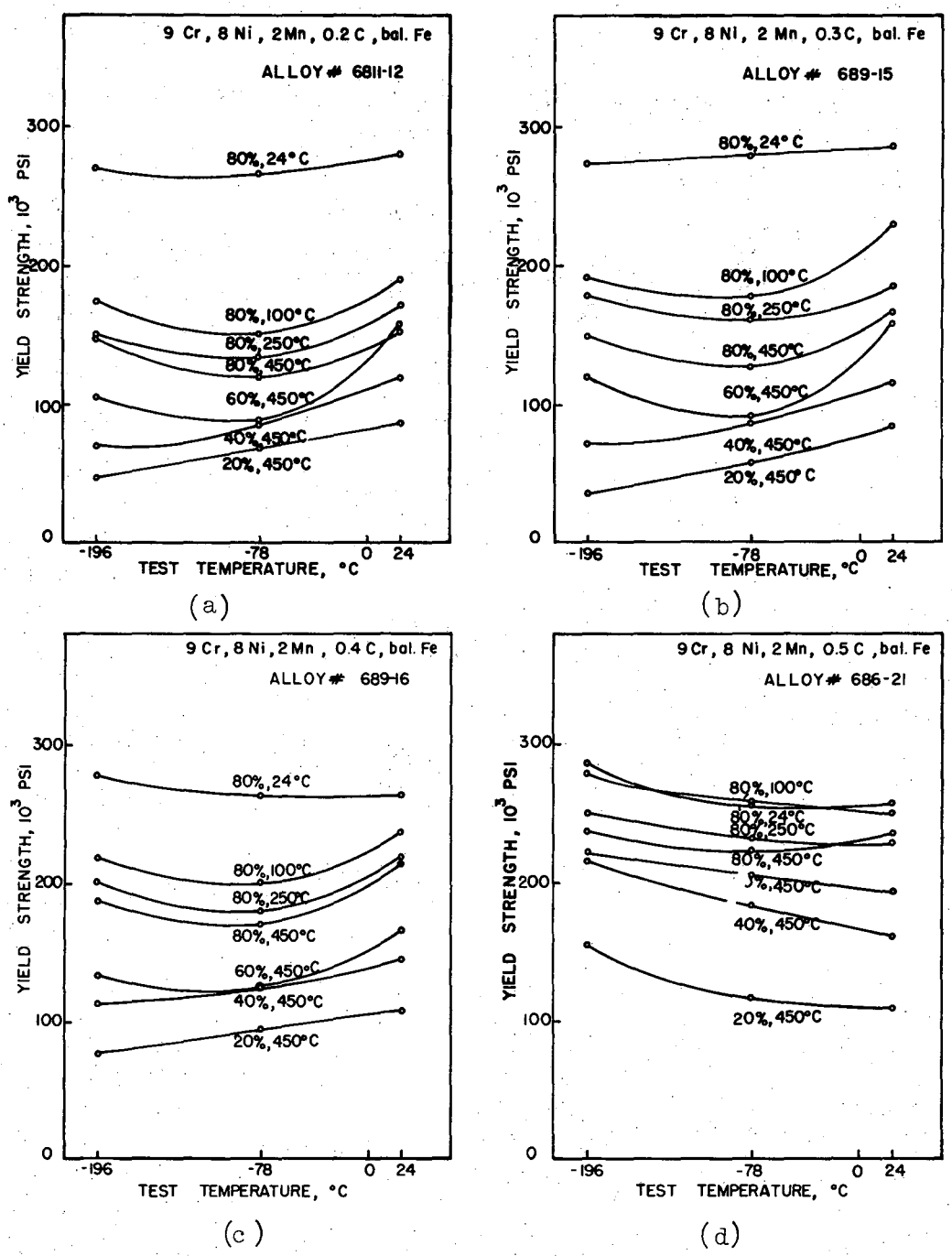

XBL 698-1097

Fig. 23

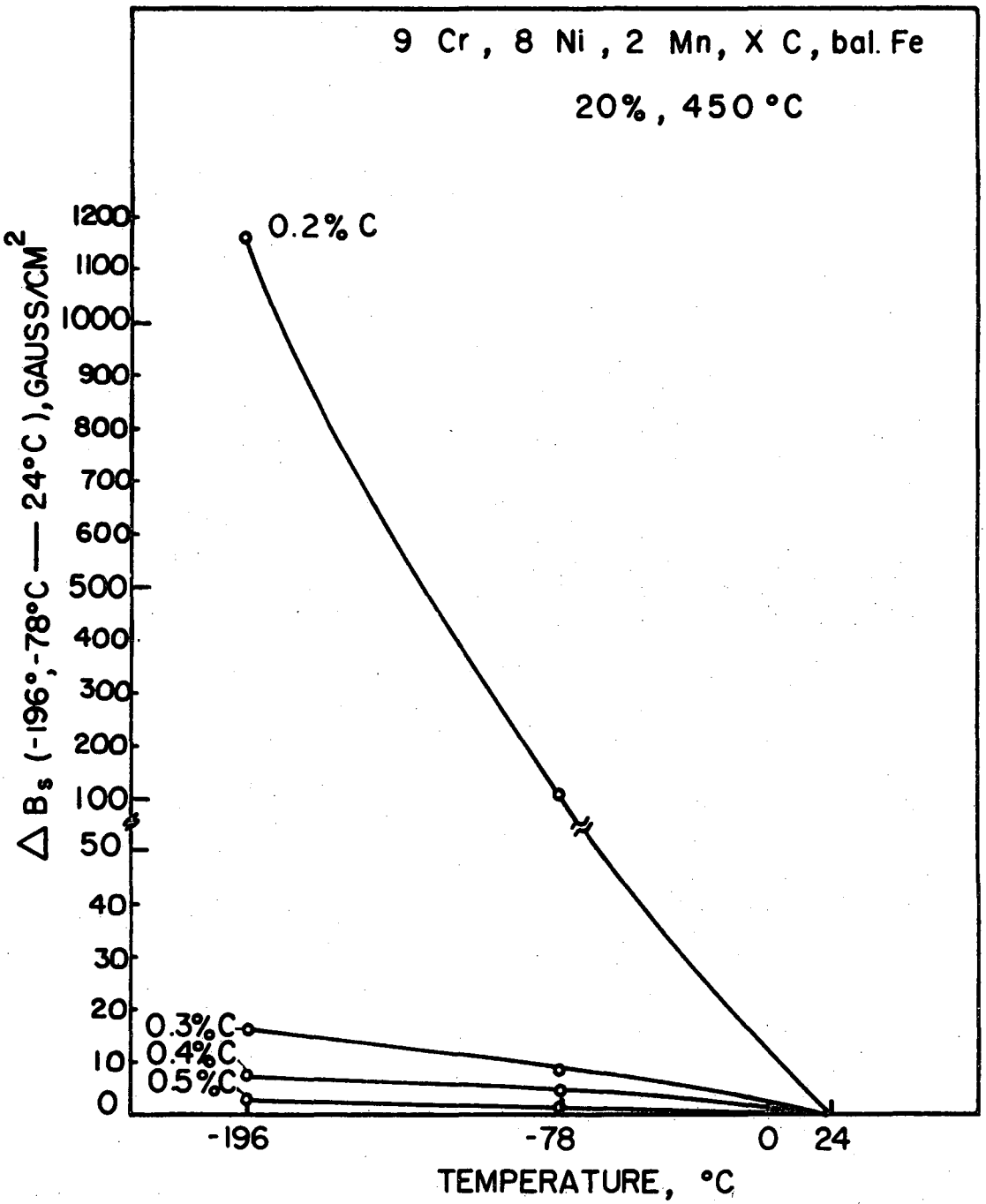

XBL 698-1093

Fig. 24

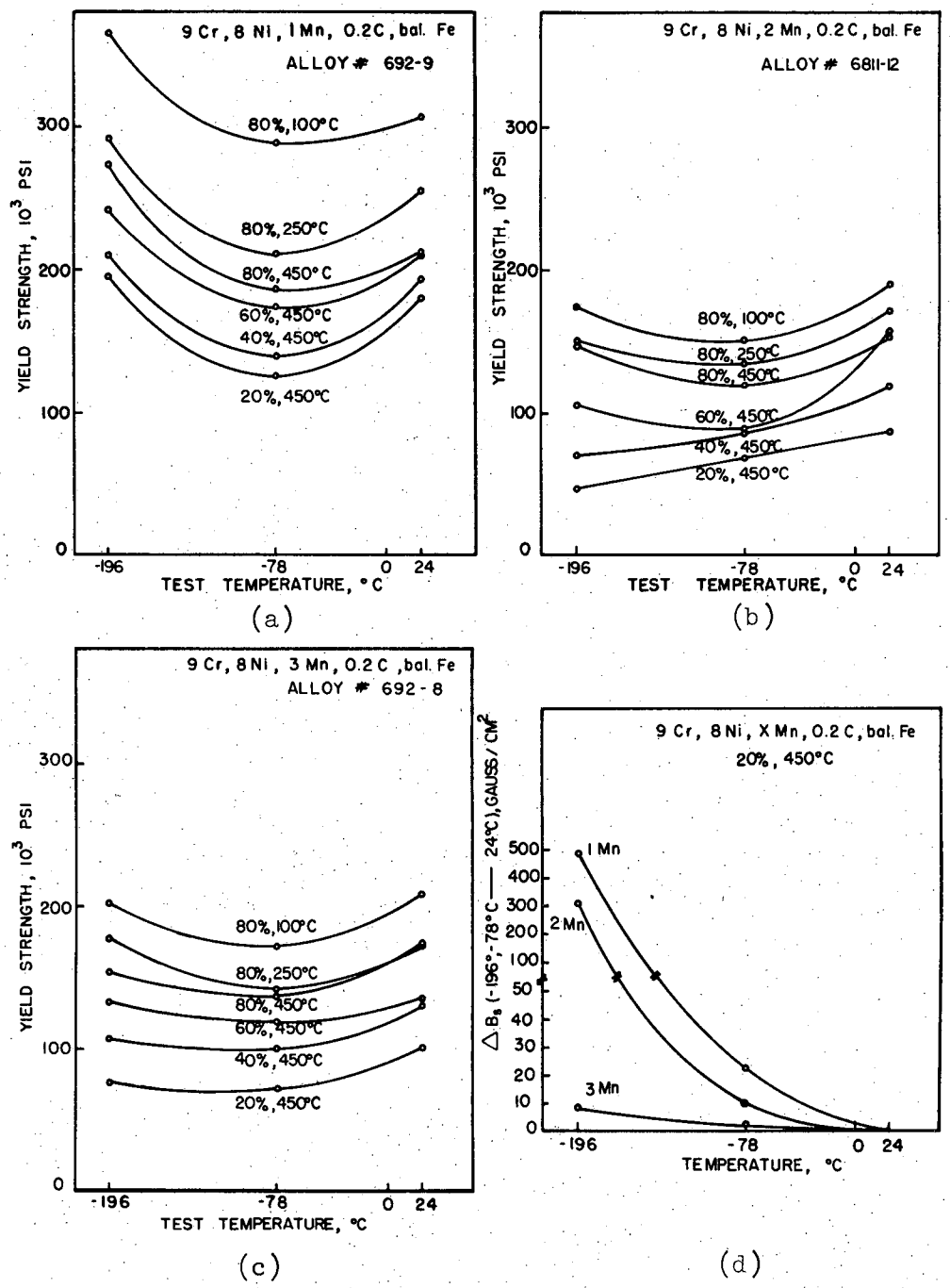

XBL 698-1096

Fig. 25

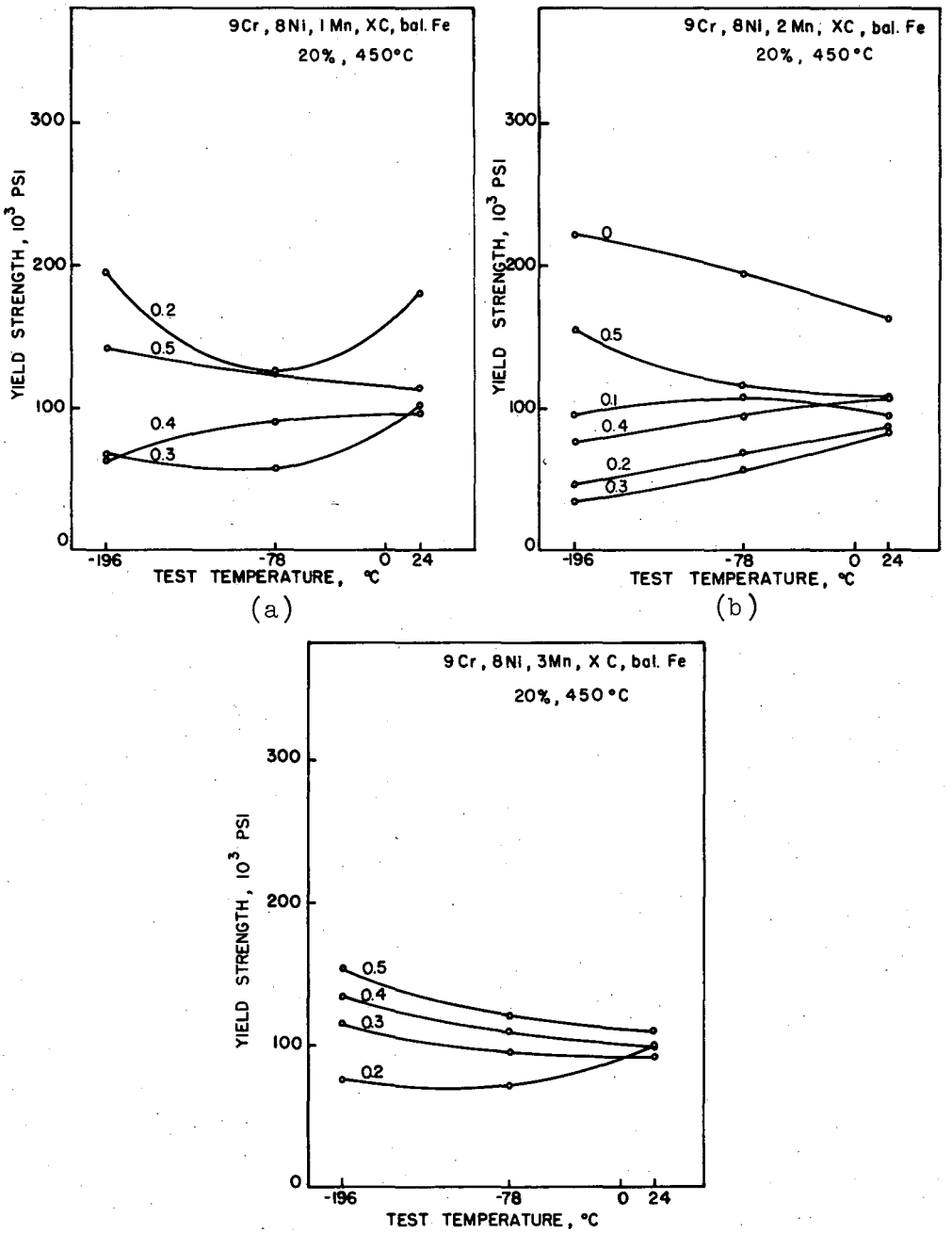

XBL 698-1094

Fig. 26

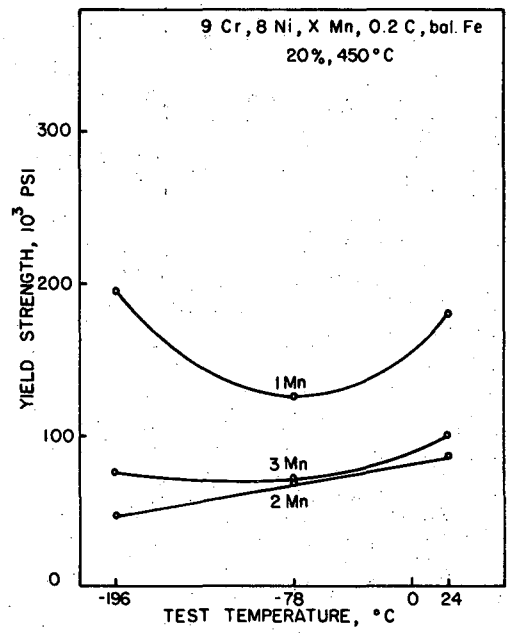

(a)

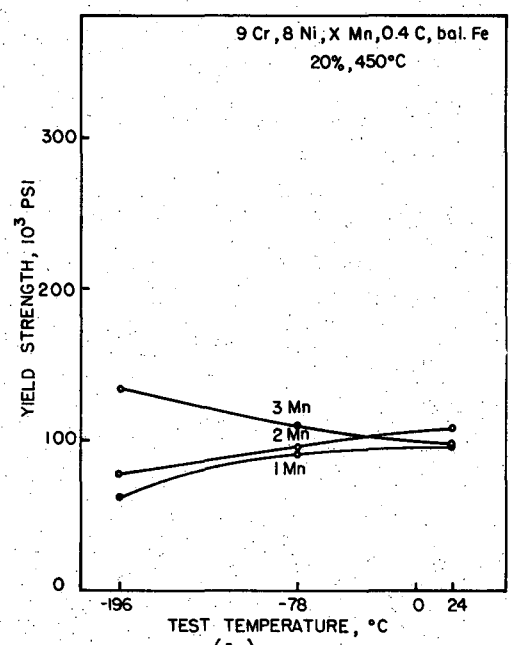

(b)

XBL 698-1095

Fig. 27

(a)

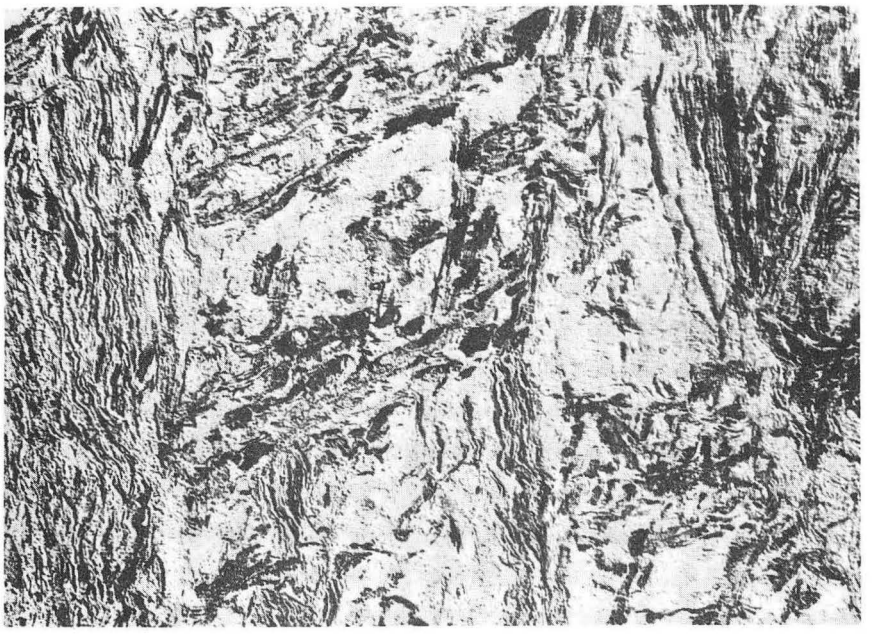

(b)

XBB 698-5049

Fig. 28

(a)

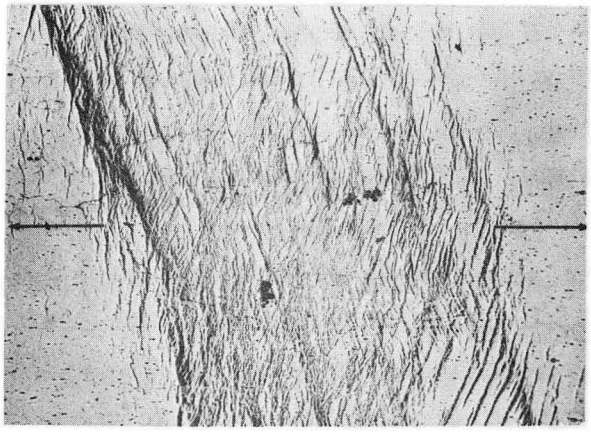

(b)

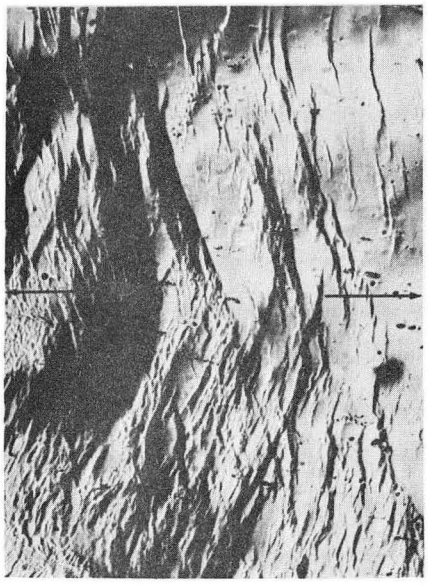

(c)

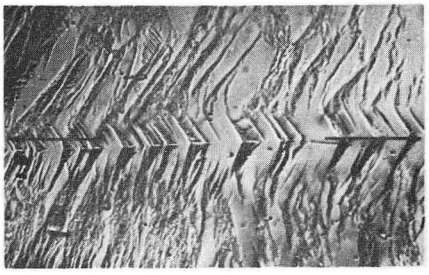

XBB 698-5044

Fig. 29

(a)

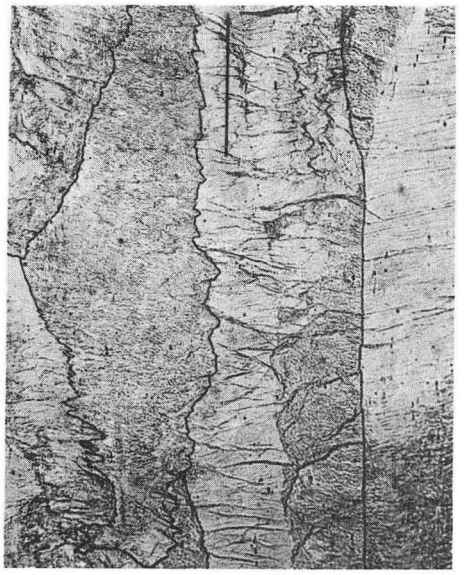

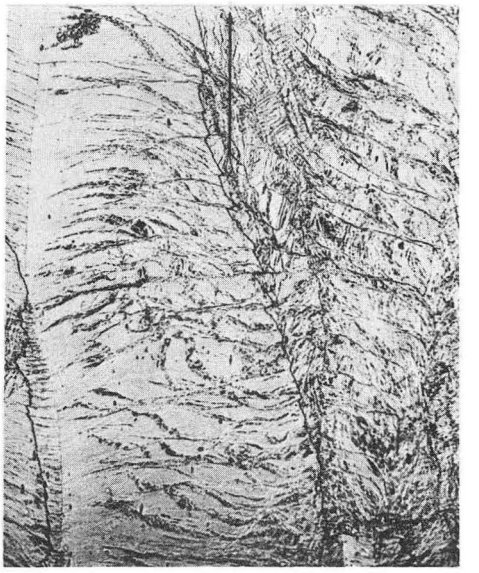

(b)

(c)

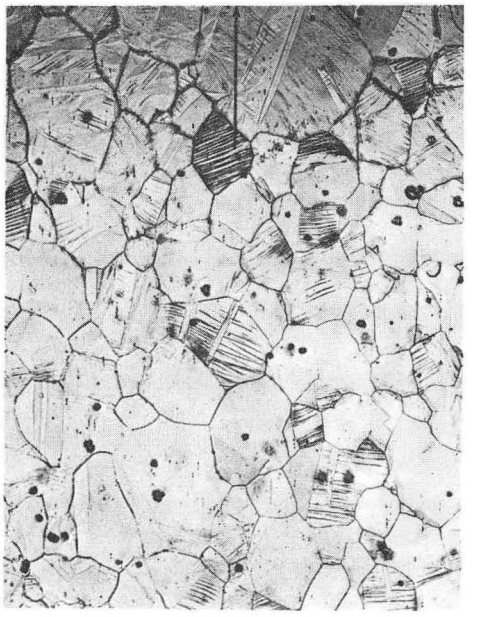

(d)

XBB 698-5047

Fig. 30

(a)

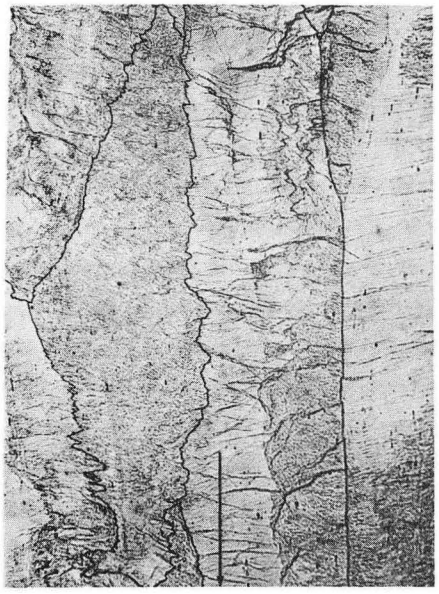

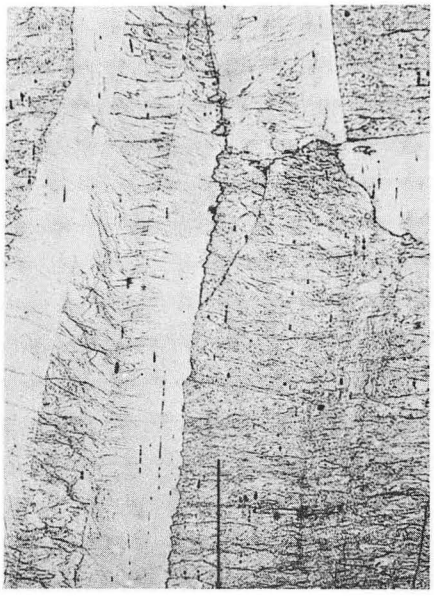

(b)

(c)

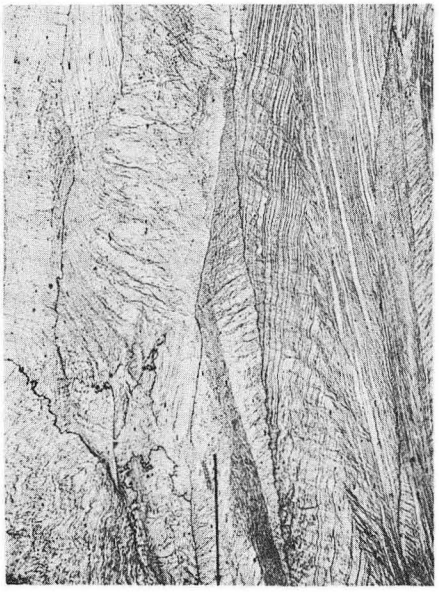

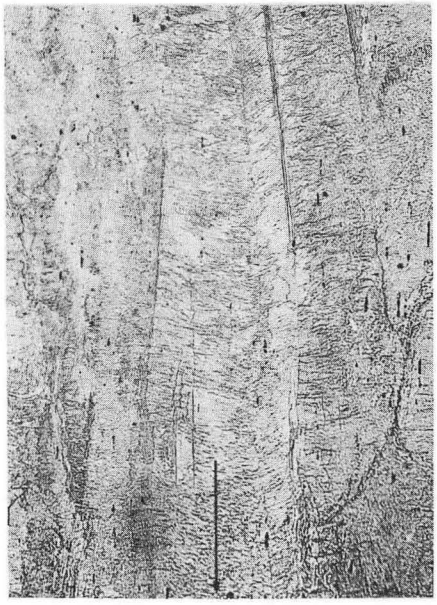

(d)

XBB 698-5048

Fig. 31

XBB 698-5045

Fig. 32

LEGAL NOTICE

This report was prepared as an account of Government sponsored work. Neither the United States, nor the Commission, nor any person acting on behalf of the Commission:

A. Makes any warranty or representation, expressed or implied, with respect to the accuracy, completeness, or usefulness of the information contained in this report, or that the use of any information, apparatus, method, or process disclosed in this report may not infringe privately owned rights; or

B. Assumes any liabilities with respect to the use of, or for damages resulting from the use of any information, apparatus, method, or process disclosed in this report.

As used in the above, "person acting on behalf of the Commission" includes any employee or contractor of the Commission, or employee of such contractor, to the extent that such employee or contractor of the Commission, or employee of such contractor prepares, disseminates, or provides access to, any information pursuant to his employment or contract with the Commission, or his employment with such contractor.

TECHNICAL INFORMATION DIVISION
LAWRENCE RADIATION LABORATORY
UNIVERSITY OF CALIFORNIA
BERKELEY, CALIFORNIA 94720